Bioorganic Chemistry 107 (2021) 104569

Contents lists available at ScienceDirect

Bioorganic Chemistry

journal homepage: www.elsevier.com/locate/bioorg

Design, synthesis and *in silico* insights of new 7,8-disubstituted-1,3-dimethyl-1*H*-purine-2,6(3*H*,7*H*)-dione derivatives with potent anticancer and multi-kinase inhibitory activities

Abdalla R. Mohamed [a,*], Ahmed M. El Kerdawy [b,c], Riham F. George [b,*], Hanan H. Georgey [b,d], Nagwa M. Abdel Gawad [b]

[a] Pharmaceutical Chemistry Department, Faculty of Pharmacy, Egyptian Russian University, Badr City, Cairo 11829, Egypt
[b] Pharmaceutical Chemistry Department, Faculty of Pharmacy, Cairo University, Cairo 11562, Egypt
[c] Department of Pharmaceutical Chemistry, Faculty of Pharmacy, New Giza University, New Giza, km 22 Cairo–Alexandria Desert Road, Cairo, Egypt
[d] Department of Pharmaceutical Chemistry, Faculty of Pharmacy, Heliopolis University for Sustainable Development, Cairo 11777, Egypt

ARTICLE INFO

Keywords:
Anticancer
Xanthine
Multi-kinase targeting
B-Raf
PI3K

ABSTRACT

Aiming to obtain an efficient anti-proliferative activity, structure- and ligand-based drug design approaches were expanded and utilized to design and refine a small compound library. Subsequently, thirty-two 7,8-disubstituted-1,3-dimethyl-1*H*-purine-2,6(3*H*,7*H*)-dione derivatives were selected for synthesis based on the characteristic pharmacophoric features required for PI3K and B-Raf oncogenes inhibition. All the synthesized compounds were evaluated for their *in vitro* anticancer activity. Compounds **17** and **22c** displayed an acceptable potent activity according to the DTP-NCI and were further evaluated in the NCI five doses assay. To validate our design, compounds with the highest mean growth inhibition percent were screened against the target PI3Kα and B-Raf_{V600E} to confirm their multi-kinase activity. The tested compounds showed promising multi-kinase activity. Compounds **17** and **22c** anticancer effectiveness and multi-kinase activity against PI3Kα and B-Raf_{V600E} were consolidated by the inhibition of B-Raf_{WT}, EGFR and VEGFR-2 with IC_{50} in the sub-micromolar range. Further investigations on the most potent compounds **17** and **22c** were carried out by studying their safety on normal cell line, *in silico* profiling and predicted ADME characteristics.

1. Introduction

Cancer is one of the leading causes of death worldwide accounting for estimated deaths of 9.6 million in 2018 [1]. Discovering new anticancer agents remains a critical challenge to overcome many tumor- and drug-related obstacles such as side effects, systemic toxicity, and drug resistance [2]. A general phenomenon in tumor formation is the stepwise accumulation of genetic information changes (mutations) [3]. Several receptor tyrosine kinase (RTK) inhibitors were approved by the FDA for treating several malignancies. However, due to many resistance mechanisms, numerous RTK inhibitors are facing acquired resistance and deficiency in durable efficacy [4,5]. For instance, it was reported that hyperactivation of PI3K/AKT/mTOR signaling is often associated with resistance to EGFR mediated endocrine chemotherapy, and other forms of targeted therapy [6].

PI3K family, a lipid kinase family, is responsible for the phosphorylation of phosphatidylinositol 4,5-bisphosphate to phosphatidylinositol 3,4,5-trisphosphate initiating a wide range of RTKs- and Ras-associated signal transduction cascades activating the oncogene Akt and subsequently a huge number of downstream signaling events including mammalian target of rapamycin (mTOR) activation [7]. PI3K/Akt/mTOR pathway regulates fundamental cellular functions including transcription, translation, proliferation, growth and survival. The cascade was found to be dysregulated almost in all human cancers [8]. Activation of tyrosine kinase growth factor receptors or oncogenes upstream, loss or inactivation of the tumor suppressor PTEN (phosphatase and tensin homolog deleted on chromosome 10), mutation and/or amplification of PI3Ks themselves are accounting for PI3K pathway dysregulation in a wide spectrum of human cancers [9].

The crystal structures of PI3Kγ co-crystalized with several diverse PI3K inhibitors show common binding interactions at the ATP binding site and the affinity pocket. These involve a hydrogen bond acceptor

* Corresponding authors.
E-mail addresses: abdallaharafa@eru.edu.eg (A.R. Mohamed), riham.eskandar@pharma.cu.edu.eg (R.F. George).

https://doi.org/10.1016/j.bioorg.2020.104569
Received 25 October 2020; Received in revised form 13 December 2020; Accepted 16 December 2020
Available online 30 December 2020

interaction with the hinge region Val882, and both a hydrogen-bond donor with Asp841, Asp836, Asp964 and/or a hydrogen-bond acceptor with Lys833, Tyr867 in the affinity pocket [10–15]. The collaboration of high-throughput screening (HTS) and structure-based design have led to the discovery of a large set of diverse PI3K inhibitors (e.g., compounds **I-IX**, Fig. 1A) [10–18]. Furthermore, it was found that purine ring is employed as a well-accommodated scaffold in the development of the dual pan-PI3K/mTOR inhibitor, compound VS-5584 **VI**, which was identified by using structure- and ligand-based design. Additionally, it is involved in PI3K inhibition by strengthen the hinge region interaction at the ATP binding site (Idelalisib **VII**) [15,16].

Nevertheless, the encountered limitations of PI3K inhibitors that are ranging from severe and occasionally fatal side effects to the adaptive resistance and activation of compensatory pathways, are still a great challenge to deal with [19,20]. These limitations are well reflected in the decreased number of approved PI3K inhibitors despite of the PI3K boosted functionality in malignancy. Moreover, it was reported that the inhibition of the PI3K/Akt/mTOR cascade alone does not increase apoptosis in NPA melanoma cells unless the cells are lacking B-Raf expression or were treated with B-Raf inhibitor, where, the promoted apoptosis is mediated through MEK/ERK-independent manner [21].

B-Raf functions in the linear Ras-Raf-MEK-ERK mitogen activated protein kinase (MAPK) pathway [22]. Uncontrolled cellular signaling due to oncogenic mutation in MAPK cascade members has been considered among the most common mutations in human cancers [23]. B-Raf inhibitors show general binding interaction over the gate area with Glu500 (Glu501 B-Raf$_{V600E}$) and Asp593 (Asp594 B-Raf$_{V600E}$) amino acids and in the hinge region with Cys531 (Cys532 and/or Gln530 B-Raf$_{V600E}$).

The introduction of sorafenib **X** (Nexavar, Fig. 2), the multi-kinase inhibitor (VEGFR1/2/3, CDK8 and B-Raf), was a breakthrough in the treatment of hepatocellular carcinoma, advanced/metastatic renal cell carcinoma and thyroid carcinoma [24]. However, It exhibits weak antitumor activity in cells with mutant B-Raf$_{V600E}$ and its clinical efficacy in cancers with B-Raf$_{WT}$ might be attributed to its multi-kinase inhibition profile [25], which shed the light on multi-kinase inhibitors as more efficacious alternative for drug combination [26]. The more selective compounds towards the mutant B-Raf$_{V600E}$ such as vemurafenib **XI** (Zelboraf) and dabrafenib **XII** (Tafinlar) are showing success in melanoma harboring B-Raf$_{V600E}$ (Fig. 2) [27,28]. However, they showed minimal efficacy against tumors with wild-type B-Raf (B-Raf$_{WT}$) and can accelerate the growth of Ras mutant tumors through paradoxical activation of Raf dimers. This vulnerability was manifested in the resistance of B-Raf$_{WT}$ phenotypic melanoma SK-MEL-2 cell line [29].

2. Rational design of the target compounds

Several studies reported the potential activity of 1,3-dimethyl-1*H*-purine-2,6(3*H*,7*H*)-dione derivatives (methylxanthines) on the molecular aspects of tumor cells and their growth [30–32]. The well-known methylxanthine derivatives, theophylline and caffeine, possess the capacity to inhibit not only cell proliferation, but also the metastatic behavior of melanoma cancer cells [33]. Subsequently, substitution at *N*-7 and/or C-8 of xanthine ring attracted many researchers to identify novel antitumor agents [34–37]. Generally, purine ring is the corner stone in many potent PI3K inhibitors (**VI-VIII**, Fig. 1A) and B-Raf inhibitors (**XIII** and **XIV**, Fig. 2) [38,39]. Particularly, the 1,3-dimethylxanthine derivative (**XV**, Fig. 3A) was reported to possess potent PI3Kα inhibitory activity [35]. Simultaneously, inspired by the scaffold- and structure-based drug design approaches that were introduced by Card, G. L. *et al* [40], which were extended to discover vemurafenib **XI** through compounds **XVI-XVIII** (Fig. 3B) over multi-steps of substructural motif identification for the oncogenic B-Raf inhibition coupled with engineered co-crystallography [41,42].

In the current work, a small compound library was compiled relaying on the previous approaches, using privileged structures and followed by diverse screening, as reported for efficient lead acquirement [43]. This was achieved through several substitutions at *N*-7 of the privileged 1,3-dimethyl-2,6-purine-dione scaffold. Substitution at *N*-7 with benzyl derivatives was relied on the platform of B-Raf$_{V600E}$ mutant inhibitor (**XVII**, Fig. 3B) [41,42] to afford the aimed hybrid (**XIX**, Fig. 3C). Furthermore, the presence of the amide fragment, between the aryl and *N*-7 methylene, affording the phenylacetamide derivatives, offers the hydrogen bond donor and/or acceptor required for the interaction with the target kinases. Many substitutions were explored at the phenylacetamide side chain, which allowed different electronic and lipophilic environments, rigidification and expansion of the molecular structure (Fig. 3C).

Substitutions at C-8 (X-Y, Fig. 3C) were relied on fragments from high throughput screening results such as compound **V**; the imidazo tricyclic structure with pyrimidine side chain (Fig. 1A), and also based on the crystallographic information that led to identification of a highly potent kinases inhibitors such as the sulfonamide derivative compound **XIV** (Fig. 2) [14,38,44]. Additionally, the x-ray crystal structure of sorafenib **X** bound to B-Raf$_{WT}$ that extends over the key regions (Fig. 3D) [45]. Subsequently, further interactions at the affinity pocket and the hinge region of PI3K were provided, and further interactions at the gate area of B-Raf were explored. Diversity of moieties at *N*-7 and C-8 investigates binding interaction at both targets regions together with 2/6-carbonyl oxygen or *N*-9 of purine (Compiled library segments, Molecular docking Supplementary Materials).

Because the construction of the compiled library was based on the characteristics of two distinct targets (PI3K and B-Raf), two consecutive filtration steps were applied, one step for each target. First filtration step was based on the interpretation of the molecular docking data (binding pattern and binding score) of the library members on PI3Kγ (PDB ID: 4GB9). An add-on pharmacophore filter was used on hinge region Val882 and affinity pocket Lys833 during performing this docking filtration step. 3D pharmacophore models are usually combined with docking to reduce the number of candidate compounds for fairly complex scoring calculations [34]. A second filtration step was achieved using molecular docking in B-Raf$_{WT}$ (PDB ID: 1UWH).

Compound selection from the promising set (survived the filtration steps) was carried out such that to cover the different library segments to be able to produce a fruitful SAR study. Noteworthy, some compounds were chosen from the compiled library despite of their poor predicted docking results to maintain the structural diversity in the chosen set of compounds to obtain a comprehensive SAR results (Fig. 4). (For further details see Molecular modeling section)

3. Results and discussion

3.1. Chemistry

The adopted synthetic pathways of the new 7,8-disubstituted-1,3-dimethyl-1*H*-purine-2,6(3*H*,7*H*)-dione derivatives were illustrated in Schemes 1-6. In Scheme 1, compounds **1**–**8** were synthesized according to the reported methods using variety of reaction conditions [46–58] with the exception of the new compound **4**. Where, the thiazole ring cyclization was achieved through reflux of **3f** with thiourea in absolute ethanol to produce **4,** as reported by a similar reaction [59].

Scheme 2 depicted the synthetic strategies for the preparation of compounds **9**–**11**. Theophylline *N*-7 was alkylated with benzyl chloride or 4-fluorobenzyl chloride to give compounds **9a** and **9b**, respectively, via nucleophilic substitution reaction (S_N2) utilizing the previously reported conditions by our group [60]. Wherein, potassium carbonate was used as a base with a catalytic amount of potassium iodide in DMF. On the other hand, 6-(4-fluorophenyl)-4-oxo-2-thioxo-1,2,3,4-tetrahydropyrimidine-5-carbonitrile **8b** required strong basic conditions to elaborate the free thiol and deprotonate it, which subsequently undergoes nucleophilic aromatic substitution (S_NAr) of compound **9b** 4-

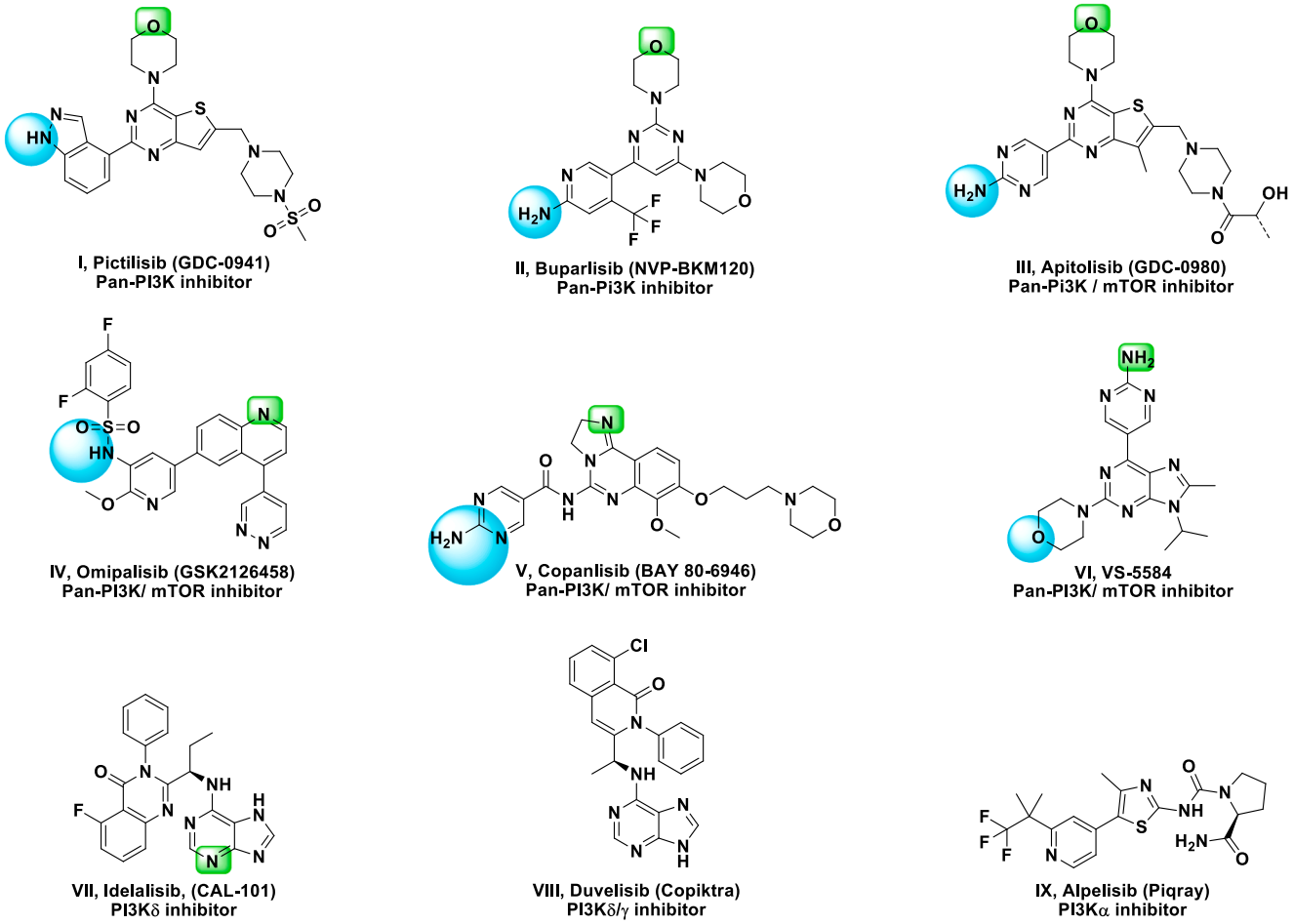

A

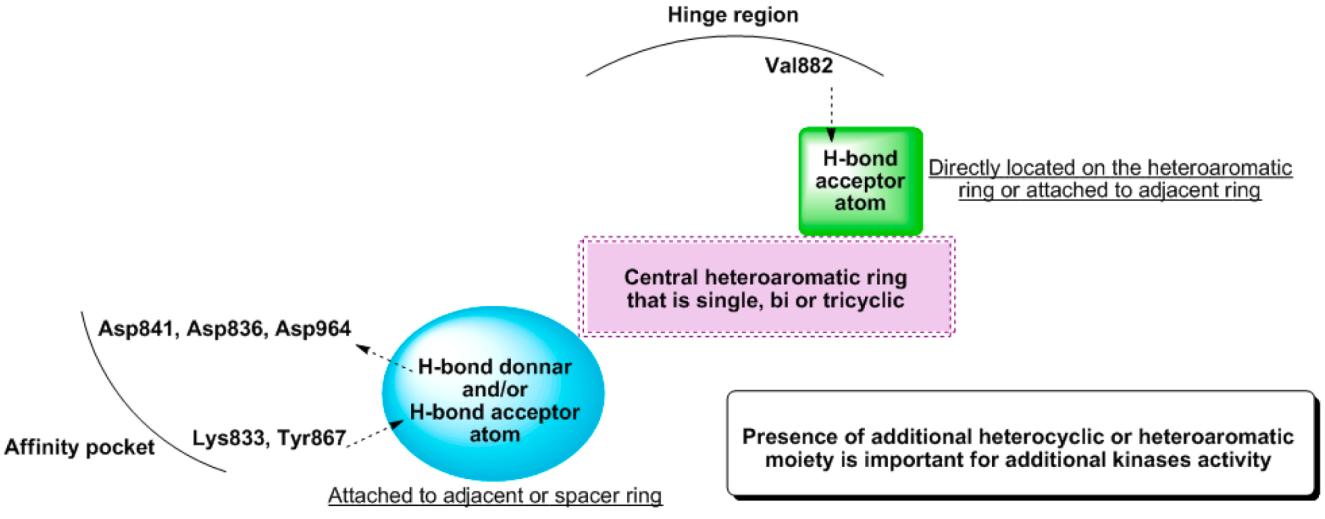

B

Fig. 1. A; Structures of representative PI3K inhibitors, with respect to PI3Kγ, atoms that make hydrogen bond interactions with the hinge region are illustrated by the green squares and those that make hydrogen bonds with the affinity pocket are illustrated with blue circles. B; Representative diagram shows the general features of PI3K inhibitor's H-bond interactions on gamma isoform. (For interpretation of the references to color in this figure legend, the reader is referred to the web version of this article.)

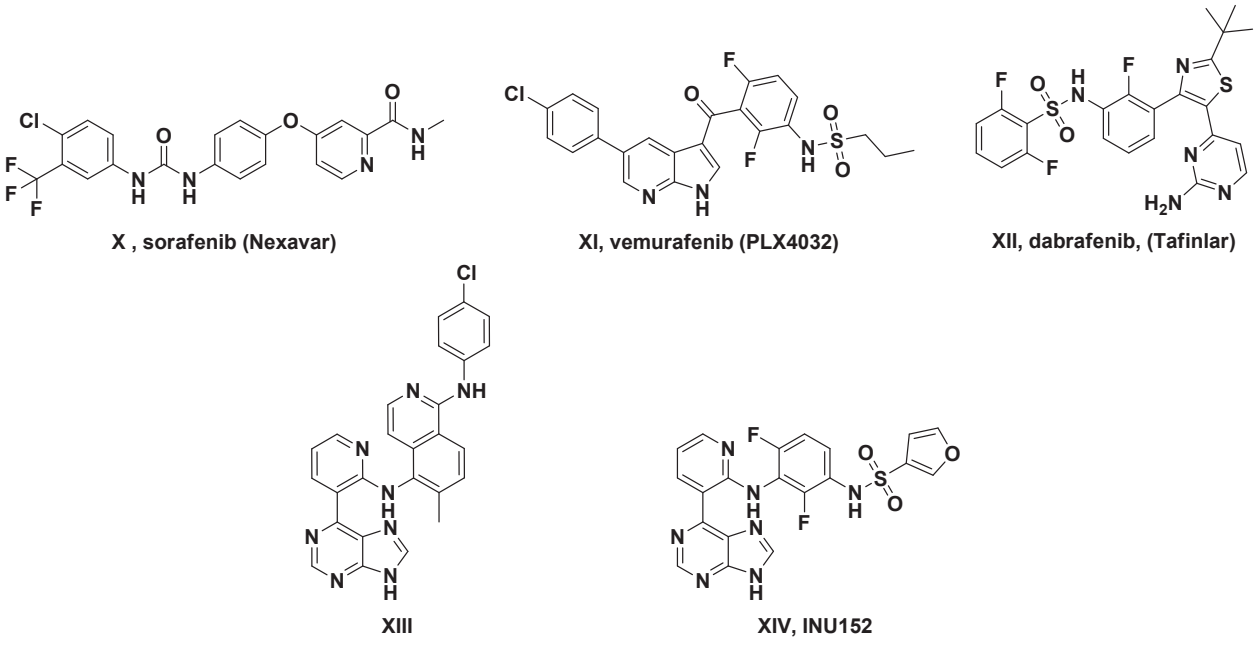

Fig. 2. Structures of representative B-Raf inhibitors.

fluorophenyl using sodium hydride in DMF at relatively high reaction temperature to give compound **10**. ^{1}H NMR spectrum of compound **10** showed the additional aromatic signals at range 7.18–8.28 ppm and NH exchangeable proton at 11.85 ppm. ^{13}C NMR spectrum also revealed the presence of a cyanide carbon at 115.9 and additional aromatic signals at the range of 117.9–165.3 ppm, additional carbonyl signal at 168.6 ppm and disappearance of C═S normally present at 175–180 ppm [61]. Compounds **9a** and **9b** were further brominated at C-8 using NBS in DMF to produce **11a** and **11b**, respectively, which were confirmed by the disappearance of C-8 purine proton signal (8.57 ppm) in their ^{1}H NMR spectra.

In general, aromatic nucleophilic substitutions of bromo at C-8 of *N*-7 substituted xanthines with different secondary amines [62], or primary aliphatic amines [63], were performed in DMF using potassium carbonate as a base. We directed our effort towards optimization of the basic condition to overcome the decreased nucleophilicity of intermediates primary amines (**2, 4, 7,** 6-aminouracil and aniline derivatives); due to aromaticity or being adjacent to π bond. At the same time, the stabilization of the produced secondary amine at C-8 could drive the reaction forward.

In Scheme 3, substitution of the bromo substituent on **11**C-8 with different intermediates primary amines was achieved. Compounds **12a** and **12b** were synthesized by substitution of the bromo substituent on **11a** and **11b** C-8 with the primary amine of (1,1-dioxo-1,2-benzothiazol-3-yl)amine **2** under basic conditions afforded by potassium carbonate and catalytic amount of 4-dimethylaminopyridine (DMAP) in DMF. ^{1}H NMR spectra showed the additional aromatic and NH signals at 7.09–8.21 ppm, and ^{13}C NMR spectra also revealed the additional aromatic signals at δ 99.7–138.9 ppm.

DMAP produced better results as a base with 4-(2-aminothiazol-5-ylamino)benzenesulfonamide **4** in DMF to afford compound **13**, which could be attributed to the suitability of the produced PKa (DMAP-PKa = 9.7) for intermediate **4** solubilization or the accessibility of DMAP to the reaction desired nucleophile [64,65]. Compound **14** was readily afforded by reaction of (*Z*)-2-(2-oxoindolin-3-ylidene)hydrazinecarbothioamide **7** with **11a** using potassium carbonate in DMF. As a more reactive nucleophile, the primary amine of 2-chloroethylamine HCl utilized a milder basic condition using triethylamine in DMF to neutralize the HCl and initiate the aromatic substitution of **11a** C-8 bromo group, which was followed by addition of potassium carbonate for termination of reaction to give **15**. Furthermore, sulfadiazine primary amine was alkylated with the chlorinated derivative (**15**) using sodium hydride in DMF to produce compound **16.** Reaction of 6-aminouracil with **11a** C-8 bromo group required an optimization of the medium pH to direct the nucleophic attach through its primary amine, thus, sodium acetate as a base in acetic acid prevented the de-protonation of uracil NHs, and produced **17**.

In the same context, Scheme 4 presented aromatic nucleophilic substitution of **11a** and **11b** C-8 bromo group with 6-aminothiouracil thiol group to produce **18a** and **18b**, respectively. The reaction was performed using DMAP as a base in DMF, which produced optimally the desired product in term of selectivity. Similarly to compound **10**, compounds **19a** and **19b** were afforded by reacting the thiol group of the appropriate 4-oxo-6-phenyl-2-thioxo-1,2,3,4-tetrahydropyrimidine-5-carbonitrile derivative **8b** and **8c**, respectively, with **11b** C-8 bromo group using sodium hydride in DMF, with manipulating the reaction temperature from 0 to 80 °C to prevent the fluoro substitution (4-fluorophenyl at *N*-7), which it seems easier. Interestingly, the reaction at C-8 needed lower reaction temperature compared to the 4-position of the benzyl moiety at *N*-7 which could be due to steric considerations.

Scheme 5 depicted the synthesis of compounds **20**–**29**. The 2-chloro-*N*-arylacetamide derivative **3c** alkylated theophylline at *N*-7 to afford compound **20** according to the same previously mentioned condition to produce compounds **9a** and **9b** [60,66]. Moreover, 8-bromotheophylline **21** was prepared according to the reported procedure from theophylline [67], and was subsequently alkylated at *N*-7 with 2-chloro-*N*-arylacetamide derivatives **3a-f** using potassium carbonate as a base in DMF at room temperature to obtain compounds **22a-f**, respectively [60,66]. Compounds **22a-f** were then used as premises to give the target compounds (**23**–**27**) by aromatic nucleophilic substitution of C-8 bromo group with amine or thiol groups of key intermediates or reagents. These reactions produced their products exploiting their previous congener's strategies, taking into consideration the presence of *N*-7 acetamide fragment. Wherein, compounds **22e** and **22f** were reacted with (1,1-dioxo-1,2-benzothiazol-3-yl)amine **2** to give **23a** and **23b**, respectively, using sodium hydride in DMF at lower reaction temperature compared to the reaction that afforded **12a,b** (utilizing potassium carbonate and DMAP). Aniline derivatives (sulfanilamide and 4-fluoroaniline) were also reacted with **22e** and **22f** under the same reaction condition to yield **24a** and **24b**, respectively. Additional stirring time at room temperature

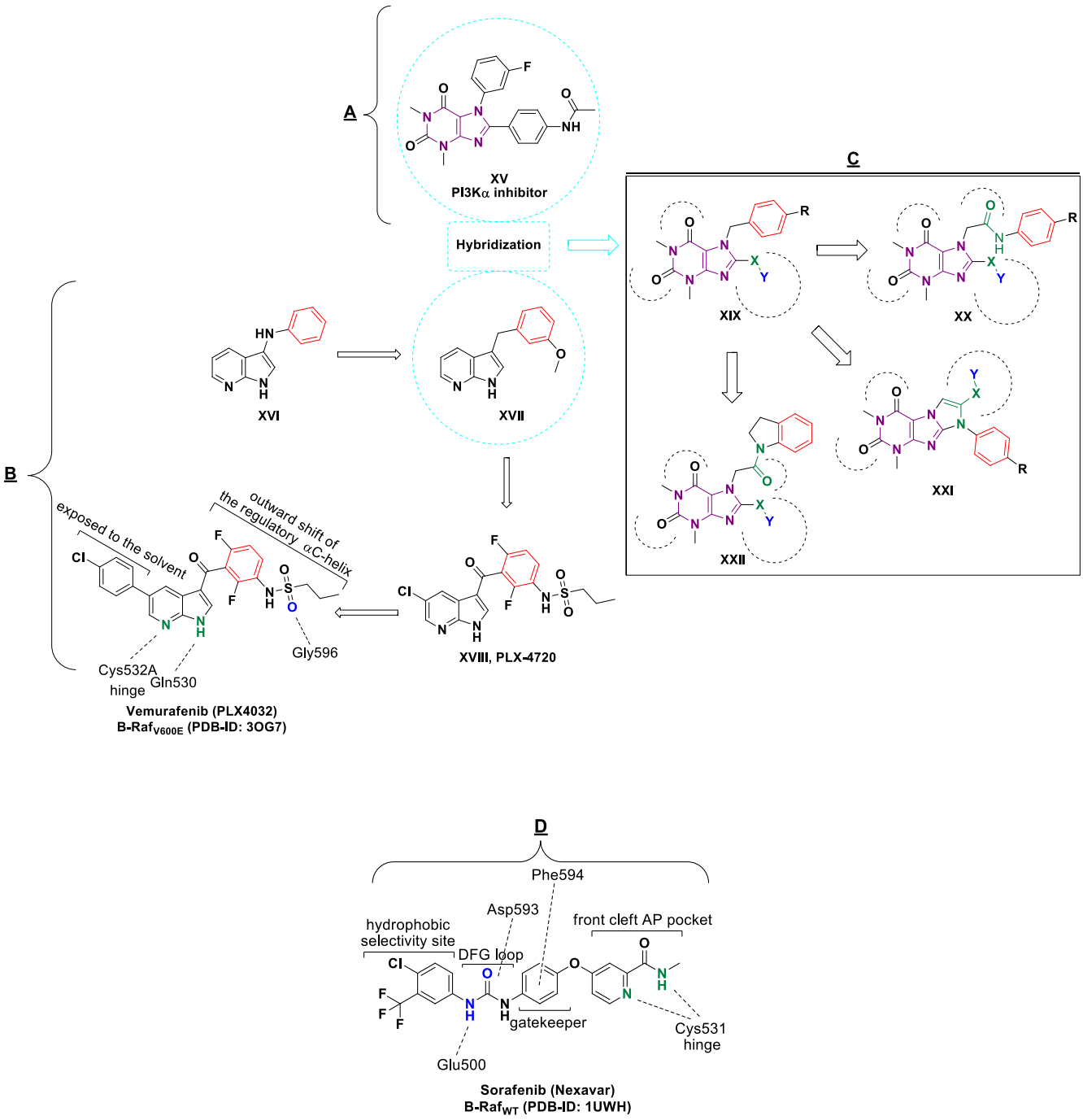

Fig. 3. Demonstration of the aimed approach. A; Compound **XV**. B; Development of vermurafenib and its binding interactions at B-Raf$_{V600E}$ (PDB: 3OG7). Sky blue illustrates the hybridization between PI3Kα inhibitor **XV** (**A**) and **XVII** (**B**). C; Chemical structures of the designed library segments (**XIX-XXII**), showing the putative sites of binding interactions (dashed circular lines) at both targets (PI3K and B-Raf). D; Binding interactions of sorafenib at the different regions of B-Raf$_{WT}$ (PDB: 1UWH). (For interpretation of the references to color in this figure legend, the reader is referred to the web version of this article.)

was required for the reaction termination without the degradation or side reaction of *N*-7 *N*-phenylacetamide group. Compounds **25** and **26** were prepared by the reaction of compound **22f** with 6-aminouracil and 6-aminothiouracil, respectively, using the same conditions that were used to afford compounds **17** and **18**. Similar to its reaction with compound **11b**, the thiol group of **8a** substituted **22e** and **22f** C-8 bromo group to give **27a** and **27b**, respectively, in a slightly better yield, using sodium hydride in DMF with modulation of the reaction temperature.

Several reports addressed the cyclization utilizing *N*-7 and C-8 of 8-bromotheophylline **21** to produce tricyclic derivatives [68–70]. The tricyclic imidazo[1,2-*f*]purine derivative **28** was afforded by the deprotonation of the acetamide NH at *N*-7 of the reported compound **22a** [60,66] what needed a careful gradual heating in DMF in the presence of a strong base such as sodium hydride. Subsequently, an intramolecular aromatic nucleophilic substitution of the C-8 bromo group was achieved and followed by a ketone to enol tautomeric shift at C-7. Therefore, compound **28** IR spectrum showed an OH band at 3383 cm^{-1}. Furthermore, its ^1H NMR spectrum revealed the disappearance of the CH_2 protons' singlet signal and the exchangeable NH signal at 5.10 and 9.00 ppm, respectively. Meanwhile, it showed the presence of a singlet signal at 9.43 ppm corresponding to the imidazole-H, and an exchangeable signal at 11.90 ppm corresponding to the OH group.

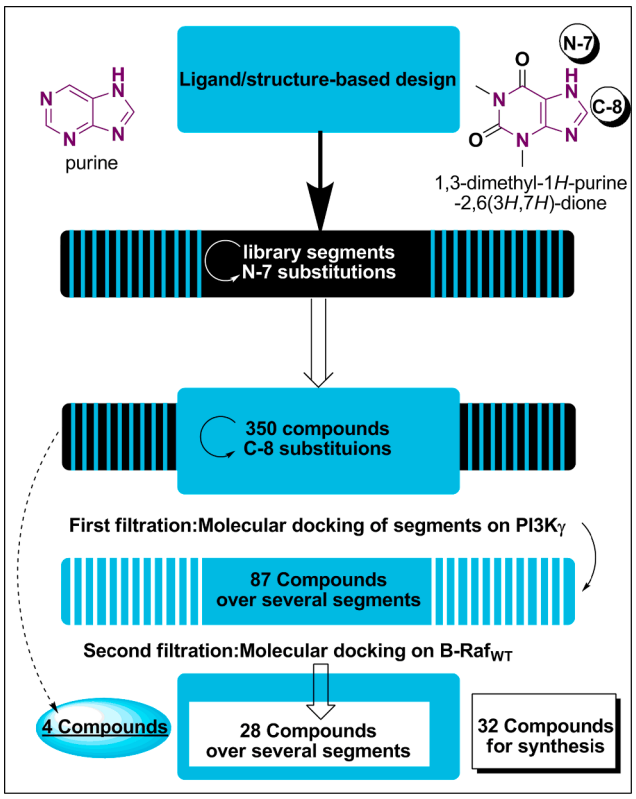

Fig. 4. Flow chart demonstrates the crucial steps that are driving to the synthesized candidates.

Furthermore, ^{13}C NMR spectrum also confirmed the disappearance of the CH_2 signal.

The *N*-phenylacetamide derivatives (**22b-e**) underwent the same reaction conditions that were used to give **28**, and subsequently reacted with compound **8a** in the same pot to produce **29a-d**, respectively. The thiol group of compound **8a** was found to be capable of replacing the *in situ* produced tertiary hydroxyl group under the basic condition of sodium hydride and DMF at relatively high temperature. This reaction could be afforded by Newman–Kwart rearrangement [71]. Similar to compound **28**, compounds **29a-d** revealed the disappearance of signals relative to CH_2 in ^{1}H NMR, ^{13}C NMR and DEPT-135 spectra (**29b**), in addition to the presence of aromatic (include the imidazole-H) and exchangeable protons corresponding to the 6-oxo-4-phenyl-1,6-dihydropyrimidine-5-carbonitrile substitution in their ^{1}H NMR spectra at ranges of 7.22–8.81 and 10.00–12.31 ppm, respectively. ^{13}C NMR spectra also showed the presence of C≡N signal (115.8–119.2 ppm), additional aromatic and C=O signals (91.3–171.5 and 156.0–168.7 ppm, respectively). Their IR spectra revealed the presence of bands at the range of 2214–2218 cm^{-1} due to C≡N group.

Otherwise, Scheme 6 outlined the *N-7* alkylation of 8-bromotheophylline **21** with 2-chloro-*N*-(naphthalen-1-yl)acetamide **5** and 2-chloro-1-(indolin-1-yl)ethanone **6** to produce **30** and **31**, respectively, using potassium carbonate in DMF (the same condition used to afford **22a-f**) [60,66]. It is worth noting that the absence of the NH (*N*-phenylacetamide) greatly enhanced the compound **31** yield (88% versus 49–70% of their acetamide derivatives). According to the previously mentioned conditions to produce compounds **23a, 23b** and **26**, (1,1-Dioxo-1,2-benzothiazol-3-yl)amine **2** and 6-aminothiouracil were substituted compound **31**C-8 bromo group by their primary amine and thiol groups, respectively, to give compounds **32** and **33**, respectively.

3.2. In vitro anticancer screening

All the newly synthesized 7,8-disubstituted-1,3-dimethyl-2,6-purinedione derivatives (thirty two compounds) were submitted and selected to be examined for their antitumor activity at the NCI Developmental Therapeutic Program (DTP), Bethesda, Maryland, USA, in accordance with the drug evaluation branch protocol [72]. NCI cytotoxic activity evaluation was followed by an investigation of the normal human diploid fibroblasts (WI-38) cell line cytotoxicity, for compounds that were selected for NCI five dose assay.

3.2.1. Growth inhibition % (in vitro single dose, 10 μM, screening)

Firstly, the novel thirty two compounds were *in vitro* screened in a primary one dose (10 μM) against NCI-panel of 60 human cancer cell lines. This panel is comprised of nine subpanels of leukemia, non-small cell lung carcinoma (NSCLC), melanoma, and colon, CNS, ovarian, renal, prostate, and breast cancers. Results are reported as mean-graph of the percent growth relative to control and presented as percentage growth inhibition (GI%, Tables 1 and 2, Supplementary Materials). Furthermore, mean GI% of each compound in all panel cell lines is presented in Fig. 5.

Investigation of the primary GI% data revealed that compound **17** exerted the highest activity among the newly synthesized 7-benzyl-1,3-dimethyl-1*H*-purine-2,6(3*H*,7*H*)-dione derivatives (**10-19a,b**) with mean GI of 41%. Compound **17** showed potent GI% and broad-spectrum activity over all NCI subpanels except leukemia. It exhibited lethality (100% GI or more) against COLO 205 and HT29 colon cancer cell lines, SNB-75 CNS cancer cell line, MDA-MB-435 and SK-MEL-2 melanoma cell lines, OVCAR-3 ovarian, A498 renal, and HS 578 T breast cancer cell lines. Replacement of the 2,6-dioxo-1,2,3,6-tetrahydropyrimidin-4-ylamino substitution at C-8 of compound **17** confined the activity mainly to renal cancer cell lines (Table 1, Supplementary Materials). This is demonstrated in compound **14** with indolin-2-one substitution at C-8 and a hydrazinecarbothioamide spacer, and compound **16** with a sulfadiazine moiety and an ethylamine spacer at the same position with mean GI of 12 and 5%, respectively.

On the other hand, replacement of *N*-7 benzyl side chain with *N*-phenylacetamide, together with a bromo substitution at C-8, which was investigated in a previous work [66], resulted in interesting findings. The 4-tolyl congener with a C-8 bromo substituent, compound **22c**, showed the highest anticancer activity in this study (mean GI of 79%). Replacement of the 4-methyl moiety with a 2,4-dichloro (**22d**) or a 4-acetyl (**22e**) substituents resulted in a rather moderate growth inhibition. Removal of bromo at C-8 of **22c** (compound **20**) revealed a complete loss of growth inhibition activities, which indicates the significance of C-8 bromo for the anti-proliferative activity.

The tricyclic imidazo[1,2-*f*]purine derivatives combined with a 6-oxo-4-phenyl-1,6-dihydropyrimidine-5-carbonitrile moiety (compounds **29a-d**) revealed a promising cytotoxic activity. The 2,4-dichloro congener **29c** showed broad and potent cytotoxic activity with mean GI of 53%, and with the highest GI% per subpanel on CCRF-CEM (leukemia; 52%), NCI-H460 (NSCLC; 86%), HCT-116 (colon cancer; 81%), SNB-75 (CNS cancer; 106%), LOX IMVI (melanoma; 67%), OVCAR-4 (ovarian cancer; 133%), UO-31 (renal cancer; 102%), DU-145 (prostate cancer; 49%), HS 578 T and T-47D (breast cancer; both are 89%) cell lines (Table 2, Supplementary Materials). This again highlights the significance of lipophilicity on SAR, together with structural conformation; **29c** mean GI% surpassed both of 2,4-dichlorophenylacetamide derivative (**22d**) and other compounds bearing 6-oxo-4-phenyl-1,6-dihydropyrimidine-5-carbonitrile moiety (**19a,b** and **27a,b**), Fig. 5.

3.2.2. In vitro five-dose assay on full NCI-60 cell line panel

The preliminary screening results revealed that compounds **17** (NSC: D – 821,302 / 1), **22c** (NSC: D – 821,290 / 1) and **29c** (NSC: D-823294 / 1) showed prominent mean GI% (Fig. 5). Compounds **17** and **22c** were selected by the NCI for further evaluation, owing to their acceptable

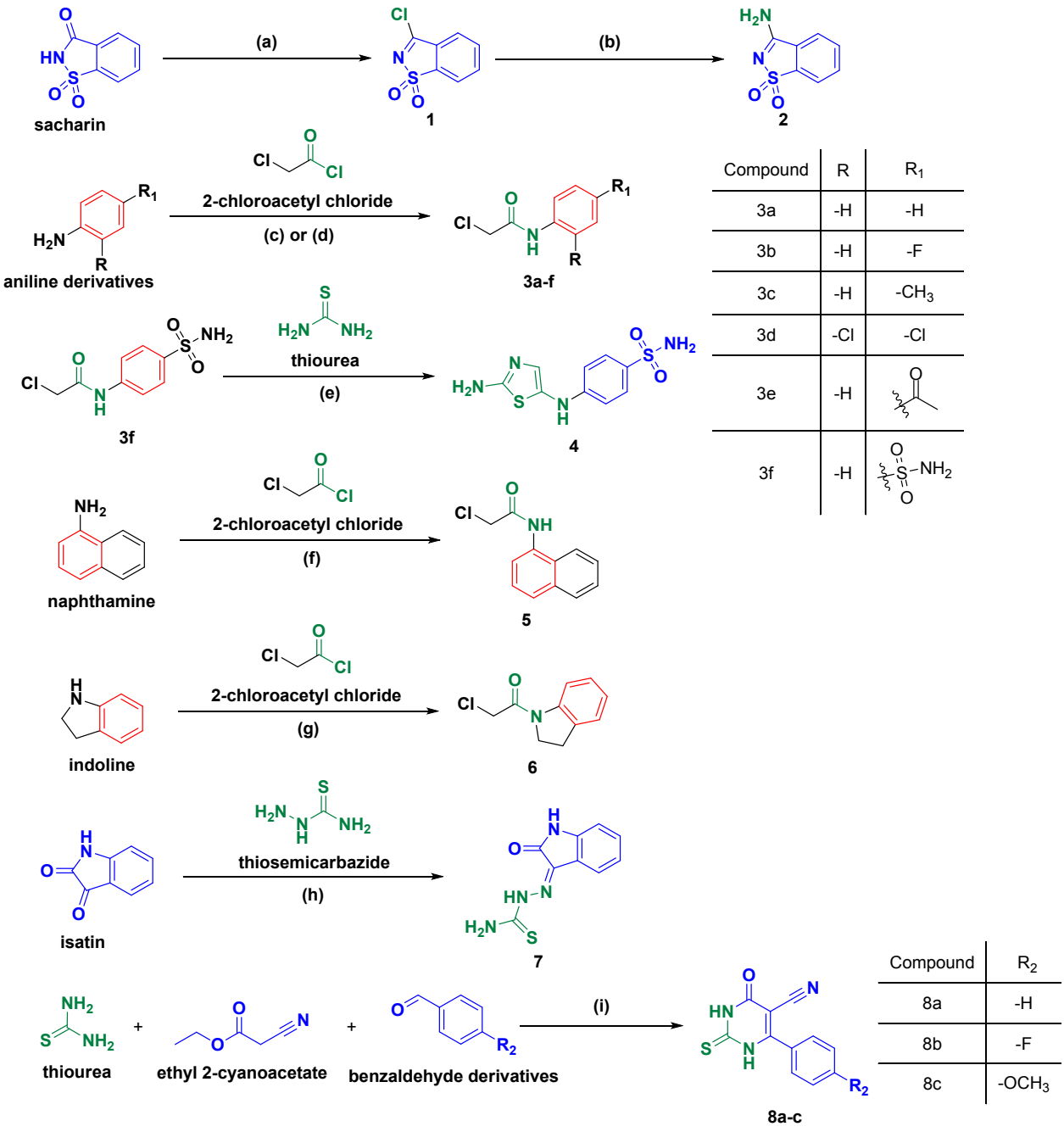

Compound	R	R_1
3a	-H	-H
3b	-H	-F
3c	-H	$-CH_3$
3d	-Cl	-Cl
3e	-H	
3f	-H	

Compound	R_2
8a	-H
8b	-F
8c	$-OCH_3$

Scheme 1. Synthesis of compounds **1**–**8**, reagents and conditions: (a) PCl_5, reflux 180 °C, 1 h; (b) ammonia, ethanol, r.t., 24 h; (c) 2 N NaOH, CH_2Cl_2, r.t.,1h (**3a-c**); (d) DMF, TEA, r.t., 24 h (**3d-f**); (e) ethanol, reflux, 12 h; (f) 2 N NaOH, CH_2Cl_2, r.t.,1h; (g) DMF, TEA, r.t., 24 h; (h) ethanol, acetic acid, reflux, 2 h; (i) K_2CO_3, ethanol, reflux, 8 h.

criteria and their anti-proliferative activities according to the Developmental Therapeutic Program (DTP), at five-dose assay (0.01–100 μM). The calculated response parameters for both compounds along with sorafenib **X** , as reference standard [73], are the GI_{50} (50% growth inhibition), TGI (total growth inhibition; total cytostatic effect) and LD_{50} (lethal dose for 50% of cells; LC_{50}) against 60 cell lines (Table 3**,** Supplementary Materials). They were determined according to the established NCI protocols [72], and the GI_{50} values were presented in Table 1.

The purinedione and pyrimidinedione hybrid, compound **17**, showed distinctive anti-proliferative activity against several cell lines from different subpanels; leukemia (RPMI-8226; GI_{50} of 15.9 μM), NSCLC (HOP-92; GI_{50} of 7.51 μM), CNS (SNB-75; GI_{50} of 12.5 μM) and renal (A498; GI_{50} of 7.97 μM) cell lines, Table 1. Moreover, it showed non-significant cytostatic activity and lethality toward all cell lines (TGI and LD_{50} > 100 μM, Supplementary materials). Meanwhile, the purinedione and tolylacetamide crossbred, compound **22c,** showed a potent growth inhibition at a single digit micromolar concentration against 43 cell lines belonging to various subpanels, Table 1.

Concerning the cytostatic and lethal (TGI and LC_{50}) effects, compound **22c** was found to be superior over sorafenib on 18 and 26 cell lines, respectively. Interestingly, OVCAR-4 ovarian cell line was 5 and 10 times more sensitive to **22c** than sorafenib, regarding TGI and LC_{50} (4.57, 9.93 μM vs 23.17, 100.00 μM of sorafenib, respectively). In addition, compound **22c** was nearly 2.5 times more cytostatic active and lethal than sorafenib (TGI = 9.59 μM and LC_{50} = 30.20 μM) on CNS (SNB-75) with TGI and LC_{50} of 3.95 and 12.10 μM, respectively (Table 3,

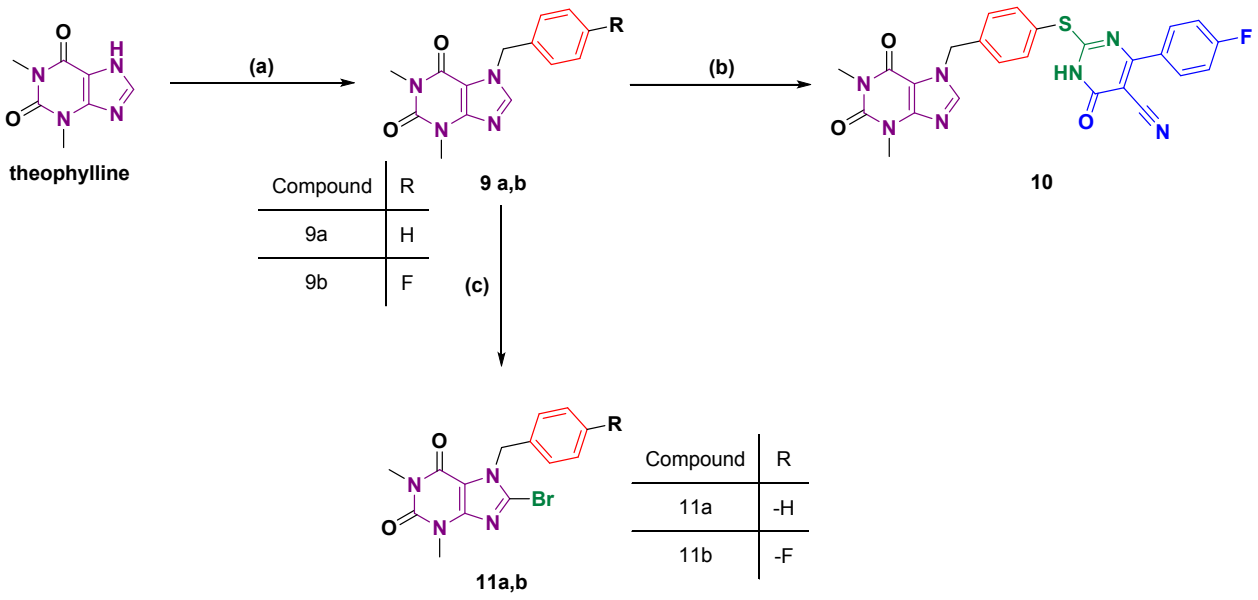

Scheme 2. Synthesis of compounds **9**–**11**, reagents and conditions: (a) benzyl chloride or 4-fluorobenzyl chloride, K_2CO_3, KI, DMF, 80 °C, 6 h; (b) **9b**, **8b**, NaH, DMF, 120 °C, 24 h; (c) NBS, DMF, 90 °C, 8 h.

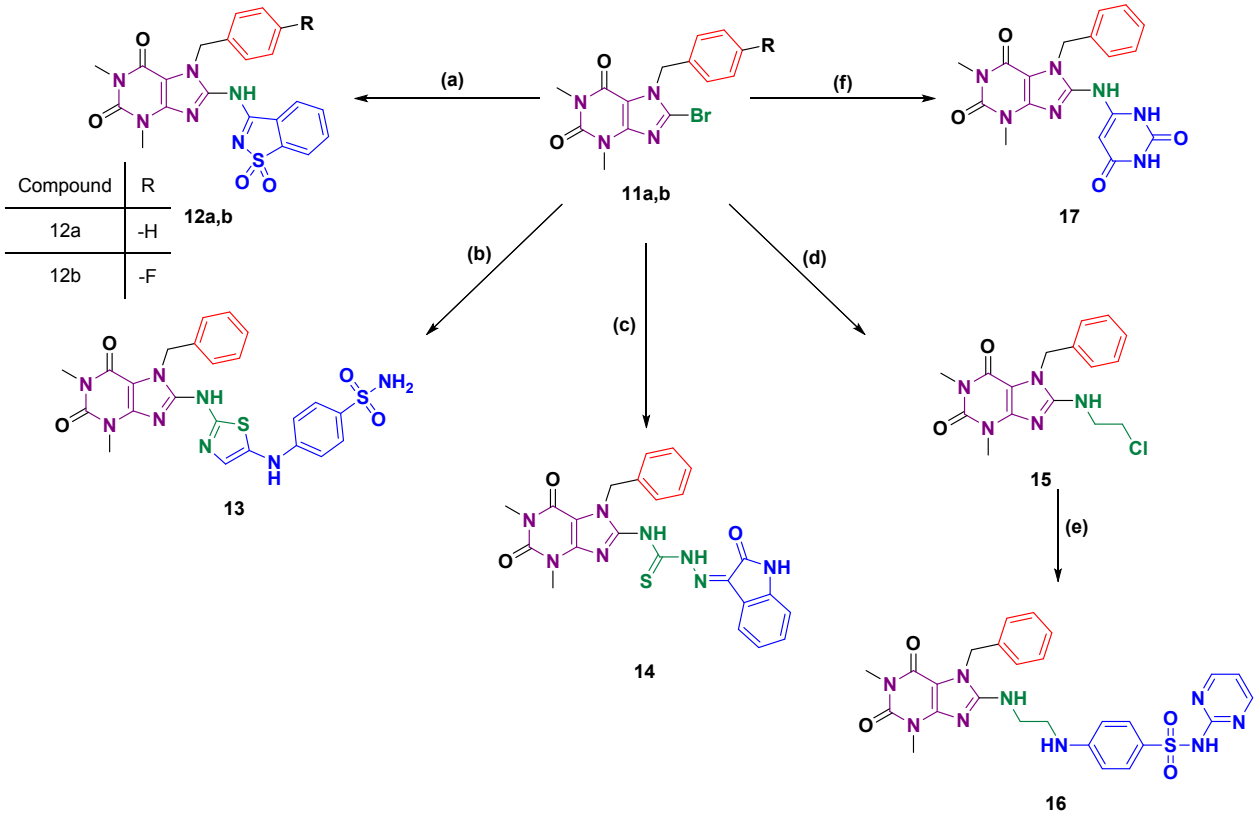

Scheme 3. Synthesis of compounds **12**–**17**, reagents and conditions: (a) **11a,b**, **2**, K_2CO_3, DMAP, DMF, 100 °C, 16 h; (b) **11a**, **4**, DMAP, DMF, reflux 80–90 °C, 6 h; (c) **11a**, **7**, K_2CO_3, DMF, 70 °C, 10 h; (d) i- **11a**, 2-chloroethylamine HCl, TEA, DMF, 50–60 °C, 2 h, ii- K_2CO_3, 70 °C, 8 h; (e) sulfadiazine, NaH, DMF, 80 °C, 12 h, (f) **11a**, 6-aminouracil, NaOAc, acetic acid, 90 °C, 16 h.

Supplementary Materials).

As indicated from selectivity index conception [74], which calculated by dividing the full panel MG-MID (μM) of compounds by their individual subpanel MG-MID (μM) which giving an average activity over individual subpanels, compound **22c** exhibited a non-selective broad spectrum anticancer activity against all tumor subpanels with respect to GI_{50} (SI = 0.32–1.98, Table 4, Supplementary Materials). Renal, ovarian, CNS and breast cancer subpanels were the most sensitive with MG-MID of 2.78, 4.27, 5.28 and 5.67 μM, respectively. The greatest activity of **22c** toward the influenced cell lines were NSCL (HOP-92, NCI-H226), CNS (SF-539, SNB-75), ovarian (OVCAR-4, SK-OV-3) and renal (A498, UO-31) with GI_{50} ranging from 1.43 to 2.15 μM. Moreover,

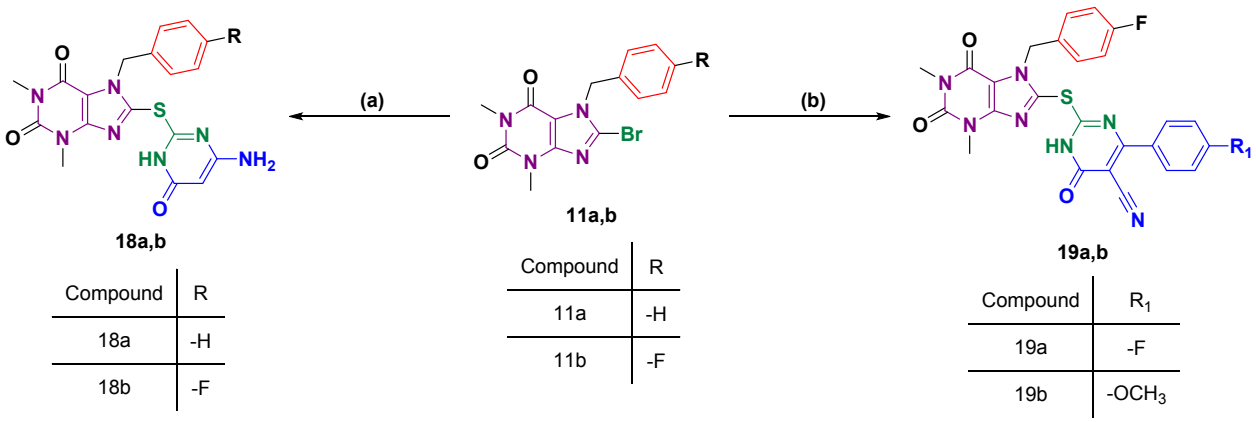

Compound	R
18a	-H
18b	-F

Compound	R
11a	-H
11b	-F

Compound	R_1
19a	-F
19b	$-OCH_3$

Scheme 4. Synthesis of compounds **18** and **19**, reagents and conditions: (a) 6-aminothiouracil, DMAP, DMF, reflux 80–90 °C, 8 h; (b) i- **11b**, **8b**,**c**, NaH, DMF, r.t., 24 h, ii- 80 °C, 10 h.

compound **22c** showed activity overcoming sorafenib (regarding GI_{50}) on ten cell lines, attributed descendingly to renal, ovarian and CNS cancer.

3.2.3. In vitro cytotoxicity toward human normal lung WI-38 cell line

It was reported that PI3K and B-Raf kinases are identified as having a key role in the pathogenesis of various forms of human cancer, including lung cancer [75,76]. Compounds **17** and **22c** were further evaluated for their cytotoxic effect against WI-38 lung cell line, as representative for normal human cells, to investigate their general safety and selectivity toward tumor cells using the MTT assay [77]. Sorafenib was used in this test as an example for a safe approved targeted chemotherapy.

Table 2 showed that both compounds **17** and **22c** demonstrated non-significant cytotoxic effect toward WI-38 cell line compared to sorafenib **X**.

3.3. Multi-kinase inhibitory activity evaluation

3.3.1. In vitro PI3Kα and B-RafV600E inhibitory activity screening

According to the anti-proliferative activity of the newly synthesized compounds, **14, 16, 17, 19a, 22c, 29a-c** and **30** override the remaining congener derivatives activity on the NCI 60 cell lines, with mean GI% ranged from 5 to 79%. To study the aimed approach regarding these candidates, *in vitro* inhibitory activity on PI3Kα and the mutant B-Raf ($B\text{-}Raf_{V600E}$) were assessed and reported in Table 3.

As seen in Table 3, all the tested compounds showed potent inhibitory activity in the nanomolar range against PI3Kα. Compound **14**, with 2-(2-oxoindolin-3-ylidene)hydrazinecarbothioamide at C-8 purine along with *N*-7 benzyl, was the most potent inhibitory on PI3Kα with IC_{50} of 8.46 nM. The increased hydrophobicity of phenylacetamide side chain at *N*-7 along with C-8 bromo substituent that were represented in compounds **30** and **22c**, accounted for their high activity (IC_{50} = 9.76 and 10.3 nM, respectively). Whereas, *N*-phenylacetamide rigidification into a tricyclic scaffold, in combination with the 6-oxo-4-phenyl-1,6-dihydropyrimidine-5-carbonitrile moiety, decreased the inhibitory activity except for the 4-tolyl congener (**29b**, IC_{50} = 10.8 nM).

On the other hand, all the tested compounds showed enhanced potency with sub-micromolar range against mutant $B\text{-}Raf_{V600E}$. Compound **16**, resembling dabrafenib **XII** [28], in inclusion of benzenesulfonamide and pyrimidine moieties, was found to be the most active in term of $B\text{-}Raf_{V600E}$ inhibition (IC_{50} = 99.6 nM). Furthermore, compounds **22c, 29a, 30** and **17** exhibited a potent $B\text{-}Raf_{V600E}$ inhibitory activity exceeding that of sorafenib **X** (IC_{50} = 129.8–199.6 nM). It is worth mentioning that compounds **22c** and **17** were found to be the most correlated over the inhibitory activity of both targets (PI3Kα and $B\text{-}Raf_{V600E}$) along with their mean GI%.

3.3.2. In vitro B-RafWT, EGFR and VEGFR-2 inhibitory activity screening

The combined results of the anti-proliferative activity and enzymatic inhibitory activity of compounds **17** and **22c**, encouraged further investigation for their *in vitro* effect on $B\text{-}Raf_{WT}$. Moreover, further evaluation of their inhibitory activity toward EGFR and VEGFR-2 was performed to study the effect of both of them on structurally related RTK (see the Molecular Docking section).

As illustrated in Table 4, compounds **17** and **22c** showed inhibitory activity exceeding that of sorafenib **X** against $B\text{-}Raf_{WT}$ (sub-micromolar range). Furthermore, their activity on EGFR and VEGFR-2 completed envisage of their multi-kinase inhibitory activity. Their broad multi-kinase activities justified their potent efficacy toward the different cancer cell lines such as NSCLC and CNS cancer.

Compound **22c** is surpassing compound **17** in cellular efficiency (Table 1) despite their comparable sub-micromolar kinases inhibitory activities (Tables 3 and 4). This could be rationalized by the superiority of compound **22c** over compound **17** concerning the optimum lipophilicity/hydrophilicity balance ($logP_{o/w}$ and TPSA values) as demonstrated by the presence of compound **22c** in the center of HIA region in the BOILED-EGG plot and by its location in the pink area of the bioavailability radar chart (Predicted ADME, Supplementary Materials).

3.4. Molecular modeling

Molecular Operating Environment (MOE 2010.10) software package was used for performing all the molecular docking studies and the 3D diagrams were generated by using UCSF Chimera software [78,79].

3.4.1. Compiled library filtration (selection stage)

The preliminary docking simulations were achieved with the aim of filtering the compiled library segments and compounds (350 compounds). Subsequently, the selected candidates for synthesis were shaped into the two desired pathways (PI3K and B-Raf). Compounds' selection was based on the previously mentioned criteria. Additionally, structural diversity was imposed to study the effect of subtle changes in chemical structure on the anti-proliferative activities.

Docking protocols were validated by self-docking of each co-crystallized ligand, then evaluation of the reproduced binding pattern and the produced RMSD values between the docking pose and the co-crystalized ligand experimental pose in each protein. These two simulations successfully reproduced the binding pattern of the co-crystalized ligand in PI3Kγ and $B\text{-}Raf_{WT}$ binding sites with energy scores of −13.38 and −15.46 kcal/mol, respectively, and with RMSD of 1.112 and 0.754 Å, respectively. In addition, the docking poses reproduced all the key interactions achieved by the co-crystallized ligands with the binding site hot spots in PI3Kγ (Val882, Lys833) and $B\text{-}Raf_{WT}$ (Glu500, Cys531 and Asp593) [44,80].

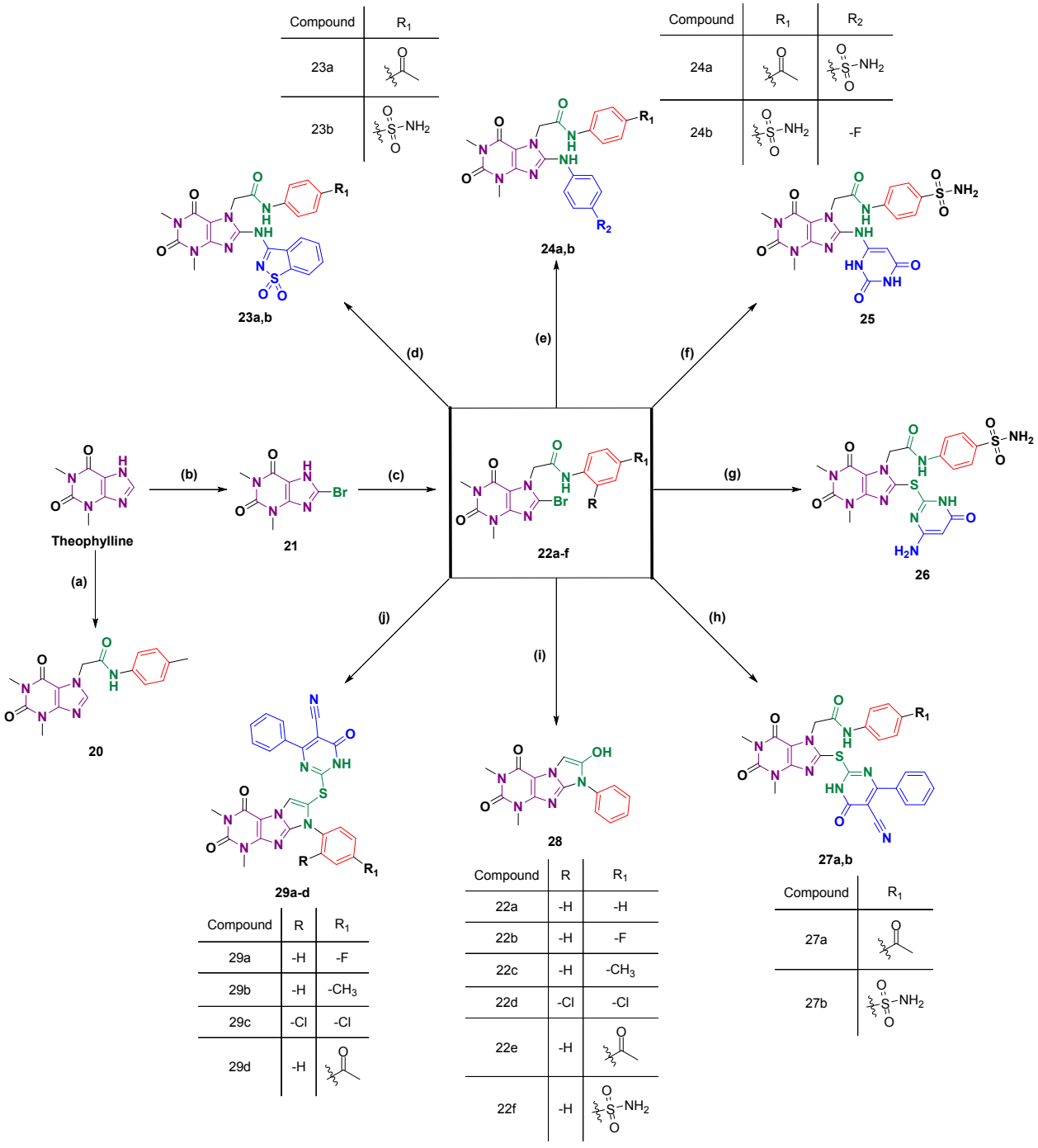

Compound	R_1
23a	
23b	

Compound	R_1	R_2
24a		
24b		-F

Compound	R	R_1
22a	-H	-H
22b	-H	-F
22c	-H	$-CH_3$
22d	-Cl	-Cl
22e	-H	
22f	-H	

Compound	R	R_1
29a	-H	-F
29b	-H	$-CH_3$
29c	-Cl	-Cl
29d	-H	

Compound	R_1
27a	
27b	

Scheme 5. Synthesis of compounds **20**–**29**, reagents and conditions: (a) **3c**, K_2CO_3, KI, 80 °C, 8 h; (b) Br_2, NaOAc, acetic acid, r.t., 24 h; (c) **3a-f**, K_2CO_3, DMF, r.t., 24 h; (d) **22e,f**, **2**, NaH, DMF, 70 °C. 12 h; (e) i- **22e,f**, sulfanilamide or 4-fluoroaniline, NaH, DMF, 70 °C, 8 h, ii- r.t., 24 h; (f) **22f**, 6-aminouracil, NaOAc, acetic acid, 90 °C, 10 h; (g) **22f**, 6-aminothiouracil, DMAP, DMF, reflux 80–90 °C, 8 h; (h) i- **22e,f, 8a**, NaH, DMF, r.t., 24 h, ii- 80 °C, 10 h; (i) **22a**, NaH, DMF, 70–90 °C, 3 h; (j) i- **22b-e**, NaH, DMF, 70–90 °C, 3 h, ii- **8a**, 90 °C, 12 h.

The first filtration step of the designed library (350 compounds) was based on satisfying the two key binding interactions on PI3Kγ (PDB ID: 4GB9) [44]. A set of 87 compounds survived this first filtration step. The second filtration step relied on binding interactions of compounds to the binding site of B-Raf_{WT} (PDB ID: 1UWH) [80], utilizing at least one key binding interaction resulting in a set of thirty two compounds.

In PI3Kγ binding site, the *N*-7 benzyl derivatives **12a,b, 13, 14, 17, 18a,b, 19b** showed a general binding pattern that is greatly imparted by H-bond interactions through purine C-8 substitutions in the front cleft (hinge region). For instance, compound **17** showed hinge region interactions utilizing the key amino acid Val882 residue through two H-bonds with the carbonyl and NH groups of the uracil ring. In addition, it shows an interaction in the affinity pocket between purine C-2 carbonyl and the key amino acid Lys833 residue. Moreover, several hydrophobic interactions directed different molecule fragments to fit properly in the binding site; purine ring (Ile963, Ile831), terminal phenyl (Met804, Met953) and uracil (Ala885, Trp812, Ile881 and Val882). (For further details see Supplementary Materials, Fig. 8)

This binding pattern was inverted upon the introduction of *N*-phenylacetamide at purine *N*-7 in compounds **20, 22c-e, 23a,b, 24b, 25,**

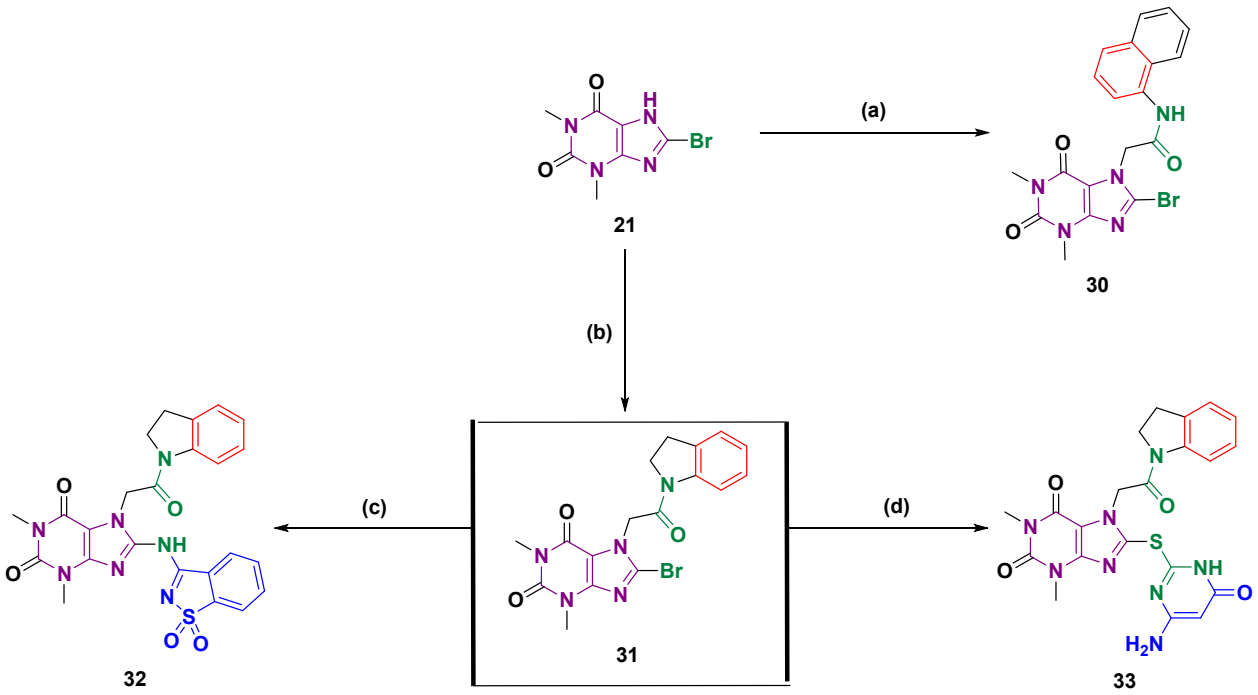

Scheme 6. Synthesis of compounds **30**–**33**, reagents and conditions: (a) **5**, K_2CO_3, DMF, r.t., 24 h; (b) **6**, K_2CO_3, DMF, r.t., 24 h; (c) **2**, NaH, DMF, 70 °C, 12 h; (d) 6-aminothiouracil, DMAP, DMF, 80–90 °C, 8 h.

27a,b and **30** such that the purine ring is fitted in the hinge region. Therefore, in the docking simulation of **22c** in PI3Kγ binding site, the carbonyl group at purine C-2 formed H-bond with the key amino acid Val882, and the acetamide moiety at *N*-7 is involved in H-bond interaction with the key amino acid Lys833. Purine ring maintained the hydrophobic interactions with Ile963 and Ile831 residues, and additionally Ile879, Trp812, Ile881 and Val882 amino acids. (For further details see Supplementary Materials, Figure 14)

1*H*-Imidazo[1,2-*f*]purine derivatives (**29a-d**) achieved a H-bond interaction with the key amino acid Lys833 utilizing purine *N*-9 (**29b,c**) or pyrimidine side chain carbonyl group (**29a,d**). Different substitutions at the directly attached phenyl ring at C-7 varied the H-bond interaction with the hinge region amino acid Val882 to be switched between C-2 purine carbonyl group (**29a**), nitrile group (**29b**) or pyrimidine carbonyl group (**29c**), and 4-acetylphenyl substitution (**29d**). Moreover, they demonstrated hydrophobic interactions with the hydrophobic side chain of the amino acids Ile879, Ile963, Ile831, Val882, Phe961, Met804, Met953, Ala885, Trp812, Leu838 and Leu1090. (For further details see Supplementary Materials, Figures 26–29)

Molecular docking in B-Raf_{WT} active site showed that for the majority of *N*-7 benzyl (**12**–**19**) and the tricyclic (**29a-d**) derivatives, C-8 and C-7 substitutions, respectively, are responsible for binding interactions with the DFG-loop amino acid Asp593 and αC helix amino acid Glu500. For instance, compound **17** is well accommodated in the gate area through two H-bond interactions with Glu500 residue by its NH at C-8 and uracil side chain NH. Moreover, the terminal phenyl and uracil rings are involved in hydrophobic interactions with Val503 and Leu513 residues. Interactions in the gate area with Glue500 and/or Asp593 were also displayed by the acetamide fragment at *N*-7, as in compound **22c** which showed H-bond donor and acceptor at both residues, respectively. Moreover, its terminal phenyl ring maintained the hydrophobic interactions with Val503, Leu504 and Leu596 residues lining the hydrophobic back pocket. Additionally, its purine ring exhibited hydrophobic interaction with Trp530, Ile462 and Val470 amino acids, in addition to π-π stacking in the gate area with Phe594 residue. (For further details see Supplementary Materials, Figures 41, 47)

3.4.2. *Molecular docking of the selected hits from the NCI-60 panel*

In order to study the binding characteristics of the best achievers on NCI-60 panel which were selected for evaluation of their multi-kinase inhibitory activity, **14, 16, 17, 19a, 22c, 29a-c** and **30,** they were docked into the crystal structure of the target kinases; PI3Kα in complex with alpelisib **IX** (NVP-BYL719, Piqray), PDB ID: 4JPS [81], and B-Raf_{V600E} in complex with compound **XIII**, PDB ID: 3IDP [38].

Molecular docking protocol was initially validated by self-docking of the co-crystalized ligands in the binding sites of PI3Kα and B-Raf_{V600E}. In PI3Kα, the docking pose reproduced the experimental binding pattern and so the key interactions achieved by the co-crystallized ligand with the binding site hot spots (Val851, Gln859) with energy score of − 11.05 kcal/mol and RMSD of 1.473 Å. In B-Raf_{V600E}, self-docking of the co-crystalized ligand in the binding site reproduced the key interactions with Glu501, Asp594 (gate area) and Cys532 (hinge region) with energy score of − 14.66 kcal/mol and RMSD of 0.31 Å. (For further details see Supplementary Materials)

Molecular docking in PI3Kα showed that the compounds bind in different patterns according to their *N*-7 and C-8 substitutions (for further details see Supplementary Materials). Except for the least active compounds, **16, 19a** and **29a** which displayed key interactions with the amino acids Val851 and/or Ser854**,** all the selected compounds showed a key binding interaction with the amino acid Gln859 (which is reported to be not conserved within the PI3K family), what imply the importance of the H-bond interaction with Gln859 for activity against PI3Kα [81].

Molecular docking simulation of the most active compound on PI3Kα **14** revealed that purine *N*-9 accepted H-bond from the key amino acid Gln859. The indolin-2-one terminal side chain displayed cation-π interaction with the positively charged side chain of Lys853 residue. Moreover, several hydrophobic interactions are achieved between the purine ring with Ile932, Met922, Ile800, Trp780 residues and *N*-7 benzyl ring with Val851 and Val850 residues. Furthermore, the thioamide spacer formed an ionic interaction with His855 residue which could rationalize the potent PI3Kα inhibitory activity of compound **14** (Fig. 6). This interaction represents a novel unique binding interaction which is different from that of conventional PI3K inhibitors and so it could be considered in designing novel potent PI3Kα inhibitors [81].

Table 1
GI_{50} (50% growth inhibition) against full NCI-60 panel cell lines for compounds **17**, **22c** and sorafenib **X**.

Cell line/Subpanel		17 GI_{50} (μM)	22c GI_{50} (μM)	Sorafenib GI_{50} (μM)
CCRF-CEM	Leukemia	>100	17.3	2.16
HL-60(TB)		>100	>100	1.61
K-562		82.5	18.5	2.84
MOLT-4		>100	27.9	2.90
RPMI-8226		15.9	3.25	1.46
SR		>100	8.96	3.05
A549/ATCC	Non-Small-Cell Lung	>100	5.61	2.93
EKVX	Cancer	56.6	10.7	2.50
HOP-62		>100	2.83	1.91
HOP-92		7.51	1.9	1.60
NCI-H226		>100	2.07	1.90
NCI-H23		>100	6.31	1.79
NCI-H322M		>100	3.68	2.81
NCI-H460		>100	3.39	2.32
NCI-H522		>100	9.27	2.14
COLO 205	Colon Cancer	>100	5.57	2.18
HCC-2998		>100	15.5	3.03
HCT-116		>100	2.43	1.74
HCT-15		>100	12.2	2.47
HT29		>100	13.8	2.19
KM12		>100	13.6	1.57
SW-620		>100	13.5	2.75
SF-268	CNS Cancer	>100	8.31	2.52
SF-295		>100	9.84	1.64
SF-539		>100	1.94	1.63
SNB-19		>100	7.92	3.43
SNB-75		12.5	**1.43**	2.96
U251		>100	2.26	2.10
LOX IMVI	Melanoma	>100	6.27	1.64
MALME-3 M		>100	2.33	2.15
M14		>100	5.98	2.16
MDA-MB-435		>100	9.32	1.77
SK-MEL-2		>100	13.4	1.83
SK-MEL-28		>100	11.4	2.64
SK-MEL-5		48	2.31	1.53
UACC-257		>100	13.9	2.15
UACC-62		65.8	11.1	1.69
IGROV1	Ovarian Cancer	>100	5	2.61
OVCAR-3		>100	**2.31**	2.94
OVCAR-4		46.9	**2.1**	3.51
OVCAR-5		>100	3.69	2.94
OVCAR-8		>100	4.89	2.96
NCI/ADR-RES		>100	9.75	2.54
SK-OV-3		>100	**2.15**	2.29
786–0	Renal Cancer	>100	**2.32**	3.36
A498		7.97	**2.01**	2.26
ACHN		>100	**2.8**	2.80
CAKI-1		50.1	4.32	2.86
RXF 393		>100	**2.29**	3.37
SN12C		>100	3.16	2.36
TK-10		>100	**3.2**	4.40
UO-31		77	**2.13**	2.57
PC-3	P.C.	>100	11.5	2.04
DU-145		>100	4.64	3.34
MCF7	Breast Cancer	>100	3.91	2.80
MDA-MB-231/ ATCC		>100	2.44	1.26
HS 578 T		>100	3.43	2.62
BT-549		69.4	11.1	3.28
T-47D		>100	3.05	1.75
MDA-MB-468		54.8	10.1	2.01

[a]**Bold** values indicate superior activity than sorafenib **X**.

Table 2
In vitro cytotoxicity towards human normal WI-38 cell line, expressed as mean growth inhibitory concentration (IC_{50}) values.

Compound	[a] IC_{50} (μM)
17	24.9 ± 0.90
22c	23.0 ± 0.83
Sorafenib	14.5 ± 1.16

[a] Data were expressed as mean ± Standard error (S.E.) of three independent experiments.

Likewise, the potent compound **22c** interacted with Gln859 by its purine *N*-9. The 4-tolylacetamide fragment accomplished a H-bond interaction with the key amino acid Val851 in the hinge region, and achieved several hydrophobic interactions with the hydrophobic side chains of the amino acids Val851, Ile932, Phe930, Ile848, Met922 and Ile800 (Fig. 7).

Compound **17** displayed a different binding pattern, in which a H-bond is formed between the uracil ring substitution at C-8 and the key amino acid Gln859. Moreover, bi-dentate H-bond interactions of both the NH at C-8 and uracil ring NH with the key amino acid Val851 in the hinge region. In addition, different molecule fragments are accommodated in hydrophobic regions lining each of the purine ring (Il800, Ile932 and Ile848), the uracil ring (Val851, Trp780), and the terminal phenyl ring (Met772) (Fig. 8).

Generally, molecular docking simulations in B-Raf_{V600E} indicated resemblance to the binding patterns toward B-Raf_{WT}. Purine C-8 substitution of the *N*-7 benzyl derivatives is responsible for the binding interaction in the gate area as H-bond donor or H-bond acceptor with Glu501 and Asp594, respectively. Compounds **14** and **17** maintained both interactions, while compounds **19a** and **16** displayed H-bonding interaction with Glu501 or Asp594, respectively. Compounds containing an acetamide fragment at *N*-7 displayed the same interactions with Glu501 and Asp594 (**30**) or with Glu501 only (**22c**). Fig. 9 represents these patterns of binding interactions for **17** and **22c**.

The 4-tolyl and naphthyl moieties in compounds **22c** and **30**, respectively, are fitted in the vicinity of the hydrophobic back pocket amino acids Leu505, Val504 and Ile572, and involved in hydrophobic interactions with the hydrophobic side chains of these amino acids. Furthermore, compound **22c** achieves a cation-π interaction with the positively charged Lys483 by its purine scaffold, in addition to a hydrophobic interaction which is maintained by the majority of compounds in the gate area with Leu514, Phe595, Val471, Ala481, Ile527 and Val482 amino acids. The high activity of compound **16** could be attributed to its preferential binding in active site of B-Raf_{V600E} as reflected in its binding free energy (–16.27 kcal/mol). It exhibited further H-bonding with Lys483 residue and additional hydrophobic interactions with the gate area amino acids Leu505, leu597 and Ala481 through its terminal pyrimidine ring. Moreover, the terminal phenyl ring showed a hydrophobic interaction with Phe583 in the gate area (Fig. 10). It is noteworthy that compounds displayed only Lys483 interaction without achieving interaction with DFG-loop (compounds **29b** and **29c)** exhibited the lowest enzyme inhibitory activity (B-Raf_{V600E} IC_{50} of 444 and 609 nM, respectively) compared to their 4-fluoro congener **29a** (B-Raf_{V600E} IC_{50} of 147 nM).

3.4.3. Modeling of 17 and 22c on EGFR and VEGFR-2

Molecular docking study was carried out to predict the possible binding mode that could be responsible for the multi-kinase activity of compounds **17** and **22c** against EGFR and VEGFR-2. This was achieved using EGFR (PDB ID: 1XKK) and VEGFR-2 (PDB ID: 1YWN) in complex with lapatinib (GW572016) and 4-amino-furo[2,3-*d*]pyrimidine derivative (LIF), respectively [82,83]. Initially, the self-docking validation step reproduced all the binding interactions of the co-crystallized ligands on EGFR and VEGFR-2 active site optimally with energy scores of − 15.12 and − 12.09 kcal/mol, respectively, and with RMSD of 1.631 and 0.826 Å, respectively. Docking poses reproduced all the key interactions that were accomplished by the co-crystallized ligands with the hot spots in the active sites of EGFR (Met793) and VEGFR-2 (Asp1044, Glu883, Glu915 and Cys917) [84]. (For further details see

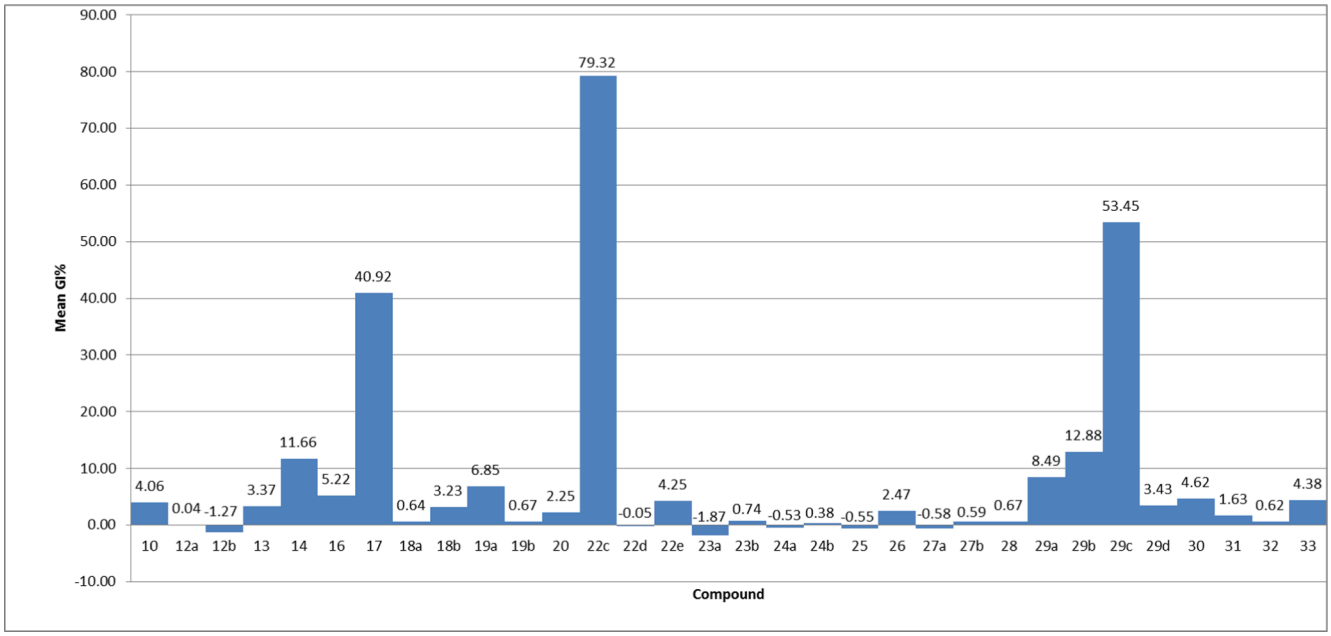

Fig. 5. Mean growth inhibition percent (Mean GI%) of the tested compounds over NCI-60 cell line panel.

Supplementary Materials)

Hisham *et al* [37], reported some C-8 substituted xanthine derivatives with potent inhibitory activity against EGFR. Moreover, purine-based compounds revealed potent activity toward EGFR and considerable inhibitory activity against some other related kinases, including VEGFR-2 [85]. Binding of these purine derivatives depends on a clamp like hydrophobic interaction through *N*-9 hydrophobic side chain with the hydrophobic side chains of Leu844, Leu718 and Val726 residues [85].

Substitutions at *N*-7 and C-8 of compounds **17** and **22c** fitted the purine ring itself into the hydrophobic clamp when they were docked into EGFR crystal structure. Furthermore, the uracil ring at C-8 in compound **17** participated in three H-bonding interactions through its carbonyl groups with Arg841, Lys745 and Phe723 residues. On the other hand, compound **22c** formed H-bond interaction with Thr854 through the acetamide oxygen at *N*-7. Moreover, its terminal 4-tolyl ring involved in hydrophobic interactions with the hydrophobic side chains of Phe856 and Leu777 residues. (For further details see Supplementary Materials, Figures 88, 89)

The reported VEGFR-2 inhibitory activity of xanthine congeners [34], along with the broad and potent *in vitro* anticancer activity of compounds **17** and **22c** encouraged us to explore their experimental enzyme activity, as well as, their binding to VEGFR-2 active site. Compounds **17** and **22c** formed H-bond interactions with the key amino acid Asp1044 through NH of uracil side chain at C-8 and oxygen of acetamide fragment at *N*-7, respectively. Both compounds are fitted properly by hydrophobic interactions with Leu887, Leu1017, Ile890, Ile1042 and Ile886. Additionally, compound **17** showed two H-bond interactions (donor and acceptor) by its uracil ring and purine C-2 carbonyl with Ile1023 and Lys866, respectively. Moreover, compound **22c** showed further H-bond interaction between NH of acetamide fragment and the αC helix Glu883 residue. Also, a hydrophobic interaction was exhibited between terminal phenyl ring and the hydrophobic side chains of Val914, Leu1033, Val846, and Val896 residues. (For further details see Supplementary Materials, Figures 91, 92)

4. Conclusion

The molecular hybridization approach was applied between both of vemurafenib (selective B-Raf$_{V600E}$ inhibitor) and the methylxanthine derivative compound **XV** (PI3Kα inhibitor) cores, through the replacement of 1*H*-pyrrolo[2,3-*b*]pyridine scaffold in vemurafenib with the 1,3-dimethyl-1*H*-purine-2,6(3*H*,7*H*)-dione scaffold in **XV**. This was followed by diverse molecular structure modifications including purine ring *N*-7 methylene replacement with acetamide and further, *N*-7 terminal phenyl substitutions increasing bulkiness of this arm. Furthermore, substitution at C-8 with diverse privileged moieties, such as integration with *N*-7 phenylacetamide in elaboration of novel tricyclic molecules based on the purine ring. In other words, several lead identification and optimization strategies such as hybridization, bio-isosteric replacement, ring fusion and extension were adopted. Finally, a fruitful small library was compiled and subjected to refinement processes based on the crystal structures of PI3Kγ and B-Raf$_{WT}$ binding sites. Essence of this effort was demonstrated by a distinct and broad anti-proliferative activity of several compounds of the designed library and a potent multi-kinase targeting efficacy. Particularly, the effect of compounds **17** and **22c** on B-Raf$_{WT}$ phenotypic melanoma SK-MEL-2 and B-Raf$_{V600E}$ phenotypic colon carcinoma HT-29 cell lines. Compound **17** Showed GI of 103% and 104% at 10 μM, respectively, whereas compound **22c** exhibited GI$_{50}$ of 13.4 μM and 13.8 μM, respectively. Moreover, PI3Kα and B-Raf$_{V600E}$ inhibitory activities of compound **17** (IC$_{50}$ = 12.2 and 199.6 nM, respectively) and compound **22c** (IC$_{50}$ = 10.3 and 129.8 nM, respectively) are augmented by their binding characteristics in the active sites of both targets. Furthermore, *in silico* and *in vitro* biological studies revealed the extension of both compounds' activities toward two kinases, EGFR (**17** and **22c**; IC$_{50}$ = 124 and 277 nM, respectively) and VEGFR-2 (**17** and **22c**; IC$_{50}$ = 152 and 301 nM, respectively). Interestingly, compound **22c** showed renal MG-MID of 2.78 μM vs 3.00 μM of sorafenib. Compound **22c** surpassed sorafenib regarding growth inhibition, cytostatic effect, and cytotoxicity on several NCI-60 panel cell lines. The most sensitive cell lines to compound **17** are NSCLC (HOP-92; GI$_{50}$ = 7.51 μM), CNS (SNB-75; GI$_{50}$ = 12.5 μM) and renal (A498; GI$_{50}$ = 7.97 μM) cancers. Whereas the most sensitive cell lines to compound **22c** are NSCLC (HOP-92; GI$_{50}$ = 1.90 μM), CNS (SNB-75; GI$_{50}$ = 1.43 μM, SF-539; GI$_{50}$ = 1.94 μM), ovarian (OVCAR-4; GI$_{50}$ = 2.10 μM, SK-OV-3; GI$_{50}$ = 2.15 μM) and renal (A498; GI$_{50}$ = 2.01 μM, UO-31; GI$_{50}$ = 2.13 μM) cancers. Both compounds **17** and **22c** exhibited a non-significant *in vitro* cytotoxicity toward normal WI-38 cell line. Finally, it can be concluded that the 1,3-dimethylxanthine scaffold is open for manipulation to afford compounds with promising physicochemical and

Table 3
PI3Kα and B-Raf$_{V600E}$ inhibitory activities of the selected compounds and the reference compounds ($IC_{50,}$ nM).

Compound	PI3Kα IC_{50} (nM)[a]	B-Raf$_{V600E}$ IC_{50} (nM)[a]
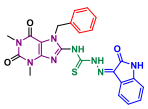 14	**8.46 ± 0.3**	403.8 ± 13
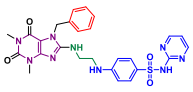 16	44.8 ± 1.5	**99.61 ± 3.3**
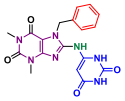 17	12.2 ± 0.4	**199.6 ± 6.6**
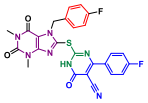 19a	19.1 ± 0.6	401.1 ± 13
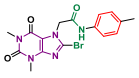 22c	**10.3 ± 0.3**	**129.8 ± 4.3**
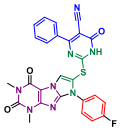 29a	25.7 ± 0.8	**147 ± 4.8**
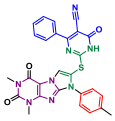 29b	10.8 ± 0.4	444.1 ± 15
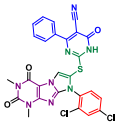 29c	15.9 ± 0.5	609.4 ± 20
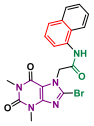 30	**9.76 ± 0.3**	**156.5 ± 5.1**
LY294002	10.6 ± 0.3	–
Sorafenib	–	244.5 ± 8

Bold values indicate superior activity on PI3Kα or BRAF$_{V600E}$ than LY294002 or sorafenib, respectively.

[a] Data were expressed as Mean ± Standard error (S.E.) of three independent experiments.

Table 4
B-Raf$_{WT}$, EGFR and VEGFR-2 *in vitro* inhibitory activity (IC_{50}, nM).

Compound	**IC_{50} (nM)** [a]		
	B-Raf$_{WT}$	EGFR	VEGFR-2
17	**170.6 ± 5.6**	124 ± 2.6	152 ± 4.53
22c	**115.1 ± 3.8**	277 ± 5.8	301 ± 8.98
Sorafenib X	186.5 ± 6.1	78.4 ± 1.6	65.7 ± 1.96

Bold values indicate higher activity than sorafenib.

[a] Data were expressed as mean ± Standard error (S.E.) of three independent experiments.

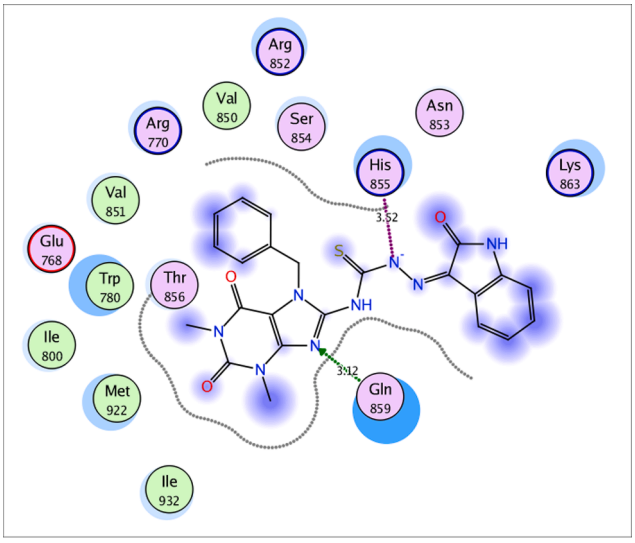

Fig. 6. 2D representation of molecular docking of compound **14** on PI3Kα crystal structure (PDB ID: 4JPS) (Distances in Å).

pharmacokinetic properties such as **22c**, in addition to their potent anticancer activity.

5. Experimental

5.1. Chemistry

Starting materials, reagents and solvents were obtained from commercial suppliers and used without further purification. Melting points were carried out by the open capillary tube method using a Stuart (Stone Staffordshire ST/50SA UK) apparatus and they were uncorrected. Infrared Spectra were performed on Schimadzu FT-IR 8400 S spectrometer Affinity A1 using potassium bromide discs, and expressed in wave number (cm^{-1}). NMR spectra were recorded on a Bruker Ascend 400/R (^{1}H: 400 MHz, ^{13}C and DEPT-135: 100 MHz) spectrophotometer. Chemical shift values (δ) were given in parts per million (ppm) downfield from tetramethylsilane (TMS) as an internal reference. Elemental analyses were carried out using FLASH 2000 CHNS/O analyzer, Thermo Scientific at the Regional Centre for Mycology and Biotechnology (RCMB), Al-Azhar University, Nasr City, Cairo.Mass spectra were carried out on Direct Inlet part to mass analyzer in Thermo Scientific GCMS model ISQ at the Regional Centre for Mycology and Biotechnology (RCMB), Al-Azhar University, Nasr City, Cairo. All the reactions were monitored by thin layer chromatography silica gel F 254, Aluminium sheets 20 × 20 cm (Sigma-Aldrich) were used. Dichlomethane: methanol (1: 0.1) was the adopted elution system. Compounds **1, 2** [46,47], **3a-f** [48–53], **5** [54], **6** [55], **7** [56], **8a-c** [57,58], **9a,b** [86,87], **21** [67], and **22a,b,f** [60,66] were synthesized according to reported procedures.

5.1.1. 4-(2-Aminothiazol-5-ylamino)benzenesulfonamide (4).

A mixture of 2-chloro-*N*-(4-sulfamoylphenyl)acetamide **3f** (2.71 g, 10.90 mmol) and thiourea (0.83 g, 10.90 mmol) in absolute ethanol (25 ml) was refluxed for 12 h. The reaction mixture was poured into ice water, the formed precipitate was filtered, washed with water, dried and recrystallization from methanol to give dark green solid, yield 38%, mp 179–182 °C, ^{1}H NMR (DMSO-d_6) δ: 7.11 (s, 1H, Ar-H), 7.22 (s, 2H, NH_2 exchanged with D_2O), 7.35 (s, 2H, NH_2 exchanged with D_2O), 7.47,7.49 (d, 2H, J = 7.32 Hz, Ar-H), 7.81, 7.83 (d, 2H, J = 7.8 Hz, Ar-H), 11.89 (s, 1H, NH exchanged with D_2O), ^{13}C NMR (DMSO-d_6) δ: 113.7, 120.4, 121.8, 127.5 (Ar-C), 127.9, 131.4, 140.1 (thiazole-C). MS, m/z (%): 270.30 (M^+, 8.87), 271.38 (M^+ + 1, 19.36); Anal. Calcd for $C_9H_{10}N_4O_2S_2$: C, 39.99; H, 3.73; N, 20.73; found C, 39.51; H, 3.42; N,

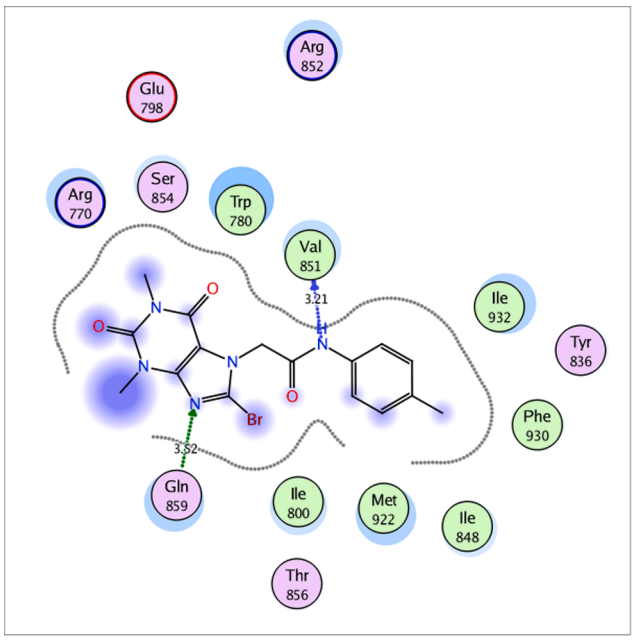

(A)

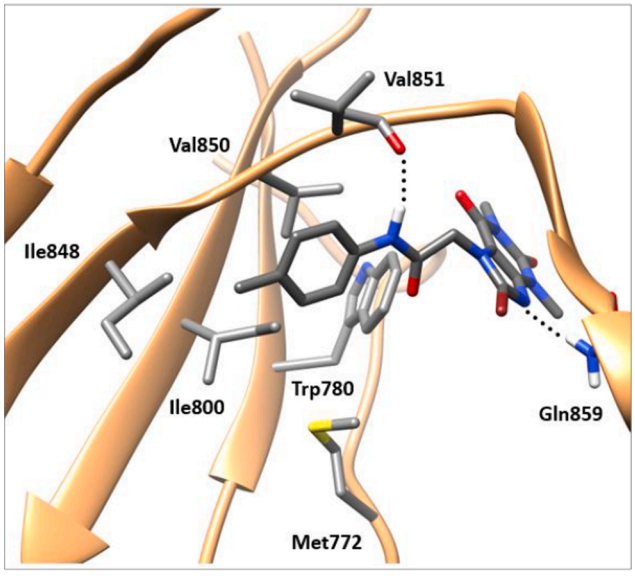

(B)

Fig. 7. 2D diagram (**A**) and 3D representation (**B**) of molecular docking of compound **22c** on PI3Kα crystal structure (PDB ID: 4JPS) (Distances in Å).

20.43.

5.1.2. 2-(4-[(1,3-Dimethyl-2,6-dioxo-2,3-dihydro-1H-purin-7(6H)-yl) methyl]phenylthio)-4-(4-fluorophenyl)-6-oxo-1,6-dihydropyrimidine-5-carbonitrile (10).

Sodium hydride 60% (0.28 g, 6.94 mmol) was added to a mixture of 7-(4-fluorobenzyl)-1,3-dimethyl-1*H*-purine-2,6(3*H*,7*H*)-dione **9b** (0.5 g, 1.73 mmol) and 6-(4-fluorophenyl)-4-oxo-2-thioxo-1,2,3,4-tetrahydropyrimidine-5-carbonitrile **8b** (0.47 g, 1.91 mmol) in DMF (6 ml) and stirred at 120 °C for 24 h. The reaction mixture was cooled to room temperature then poured onto ice water and adjusted at pH 4–5 with hydrochloric acid (1 N). The produced precipitate was filtered, washed with water, dried and recrystallized from ethanol/DMF to give yellow

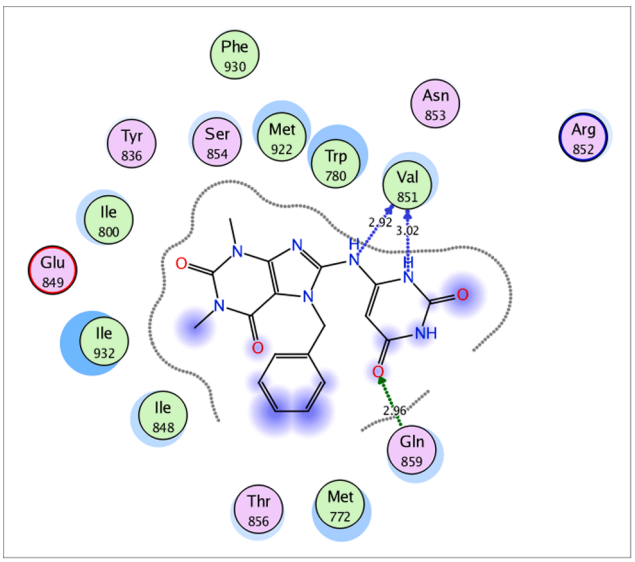

(A)

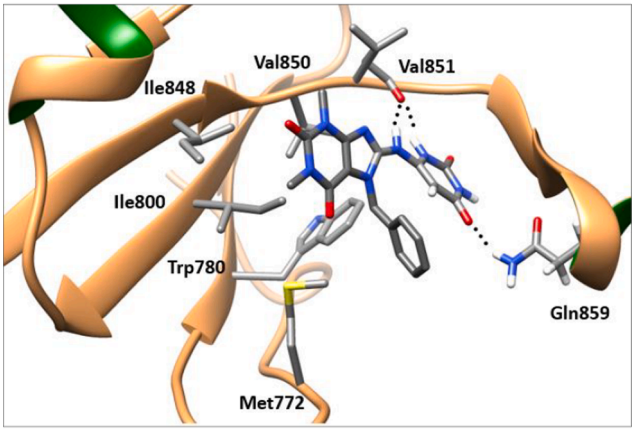

(B)

Fig. 8. 2D diagram (**A**) and 3D representation (**B**) of molecular docking of compound **17** on PI3Kα crystal structure (PDB ID: 4JPS) (Distances in Å).

solid, yield 39%, mp 257–258 °C, IR (KBr) ν (cm^{-1}): 3148 (N—H), 3090 (C—H aromatic), 2955 (C—H aliphatic), 2207 (C≡N), 1700–1650 (3C = O), 1612, 1601 (N—H bending), 1539–1505 (C=C aromatic), ^{1}H NMR (DMSO-d_6) δ: 3.22 (s, 3H, CH_3), 3.42 (s, 3H, CH_3), 5.47 (s, 2H, CH_2), 7.18 (t, 2H, J = 8.86 Hz, Ar-H), 7.35–7.44 (m, 2H, Ar-H), 7.94–7.97 (m, 4H, Ar-H), 8.28 (s, 1H, Ar-H), 11.85 (s, 1H, NH exchanged with D_2O), ^{13}C NMR (DMSO-d_6) δ: 28.0 (CH_3), 29.9 (CH_3), 38.1 (CH_2), 83.2, 107.5, 115.7 (Ar-C), 115.9 (C≡N), 117.9, 130.3, 130.4, 131.3, 131.4, 133.5, 133.6, 143.2 (Ar-C) 151.5 (C=O), 155.0 (C=O), 162.9, 163.6, 165.3 (Ar-C), 168.6 (C=O) . MS, *m/z* (%): 515.47 (M^+, 14.11); Anal. Calcd for $C_{25}H_{18}FN_7O_3S$: C, 58.25; H, 3.52; N, 19.02; found C, 58.61; H, 3.19; N, 19.28.

*5.1.3. General procedure for synthesis of **11a,b***

A mixture of 7-benzyl-1,3-dimethyl-1*H*-purine-2,6(3*H*,7*H*)-dione derivative **9a,b** (14.81 mmol) and NBS (3.95 g, 22.20 mmol) in DMF (35 ml) was refluxed at 90 °C for 8 h. Then the reaction mixture was cooled down to room temperature and poured onto ice water. The formed precipitate was filtered, washed with water, dried and recrystallized from ethanol 95%.

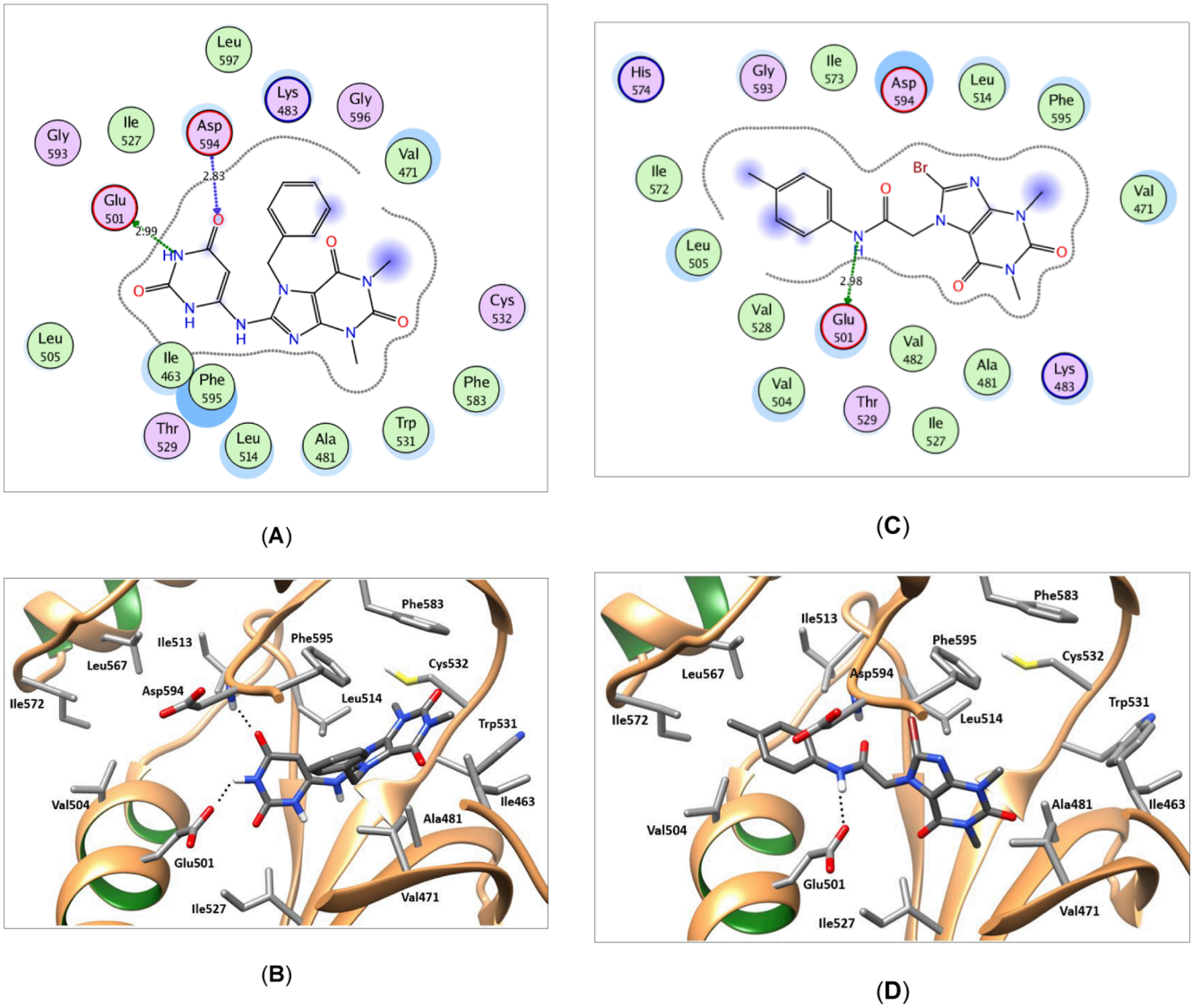

Fig. 9. 2D diagram and 3D representation of molecular docking of compound **17** (**A** and **B,** respectively) and compound **22c** (**C** and **D,** respectively) on B-Raf$_{V600E}$ crystal structure (PDB ID: 3IDP) (Distances in Å).

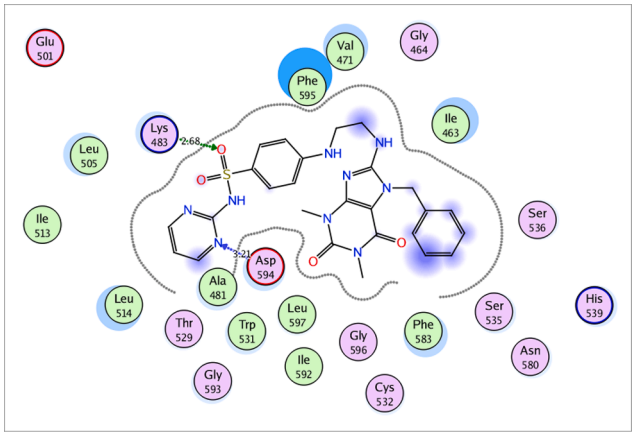

Fig. 10. 2D representation of molecular docking of compound **16** on B-Raf$_{V600E}$ crystal structure (PDB ID: 3IDP) (Distances in Å).

*5.1.3.1. 7-Benzyl-8-bromo-1,3-dimethyl-1H-purine-2,6(3H,7H)-dione (**11a**).*. The titled compound was synthesized using compound **9a** (4.00 g), yield 85%, mp 141–143 °C, IR (KBr) ν (cm^{-1}): 3179 (N—H), 3032–3009 (C—H aromatic), 2951 (C—H aliphatic), 1709, 1667 (2C = O), 1539 (C=C aromatic),^{1}H NMR ($CDCl_3$) δ: 3.41 (s, 3H, CH_3), 3.48 (s, 3H, CH_3), 5.70 (s, 2H, CH_2), 7.24–7.29 (m, 5H, Ar-H), ^{13}C NMR (DMSO-d_6) δ: 28.1 (CH_3), 29.9 (CH_3), 49.7 (CH_2), 109.5, 127.5, 128.2, 128.8, 135.2, 141.2, 148.1 (Ar-C), 151.2 (C=O), 154.6 (C=O).

*5.1.3.2. 8-Bromo-7-(4-fluorobenzyl)-1,3-dimethyl-1H-purine-2,6 (3H,7H)-dione (**11b**).*. The titled compound was synthesized using compound **9b** (4.27 g), yield 83%, mp 168–171 °C, ^{1}H NMR ($CDCl_3$) δ: 3.22 (s, 3H, CH_3), 3.32 (s, 3H, CH_3), 5.59 (s, 2H, CH_2), 7.08 (t, 2H, J = 8.80 Hz, Ar-H), 7.22 (dd, 2H, J = 5.44, 8.24 Hz, Ar-H).

*5.1.4. General procedure for synthesis of **12a,b***

7-Benzyl-8-bromo-1,3-dimethyl-1*H*-purine-2,6(3*H*,7*H*)-dione derivative **11a,b** (1.08 mmol) was added to a mixture of potassium carbonate (0.30 g, 2.16 mmol), DMAP (0.03 g, 0.22 mmol) and (1,1-dioxo-1,2-benzothiazol-3-yl)amine **2** (0.24 g, 1.31 mmol) in DMF (6 ml). The reaction mixture was stirred at 100 °C for 16 h then was cooled to room

temperature and poured onto ice water, medium was neutralized with acetic acid (1 N). The resulted precipitate was filtered, washed with water, dried and recrystallized from ethanol/DMF.

*5.1.4.1. 7-Benzyl-8-[(1,1-dioxo-1,2-benzothiazol-3-yl)amino]-1,3-dimethyl-purine-2,6-dione (**12a**).*. The titled compound was synthesized using compound **11a** (0.38 g) to give yellow solid, yield 46%, mp 242–245 °C, IR (KBr) ν (cm^{-1}): 3179 (N—H), 3086–3032 (C—H aromatic), 2920 (C—H aliphatic), 1701, 1667 (2C = O), 1636 (N—H bending), 1600–1543 (C=C aromatic), 1335, 1157 (SO_2). ^{1}H NMR (DMSO-d_6) *δ:* 3.26 (s, 3H, CH_3), 3.49 (s, 3H, CH_3), 5.58 (s, 2H, CH_2), 7.25 (s, 6H, Ar-H, N—H), 7.88 (t, 2H, *J* = 5.56 Hz, Ar-H), 8.09 (d, 1H, *J* = 6.68 Hz, Ar-H), 8.16 (d, 1H, *J* = 6.64 Hz, Ar-H), ^{13}C NMR (DMSO-d_6) *δ:* 27.9 (CH_3), 30.1 (CH_3), 41.5 (CH_2), 109.2, 120.7, 123.7, 126.5, 127.9, 127.9, 128.1, 128.9, 129.1, 133.0, 138.0 (Ar-C), 151.5 (C=O), 154.2 (C=O). MS, *m/z* (%): 450.92 (M^+, 26.01), 451.48 ($M^+ + 1$, 9.69); Anal. Calcd for $C_{21}H_{18}N_6O_4S$: C, 55.99; H, 4.03; N, 18.66; found C, 55.87; H, 3.84; N, 18.53.

*5.1.4.2. 8-[(1,1-Dioxo-1,2-benzothiazol-3-yl)amino]-7-[(4-fluorophenyl) methyl]-1,3-dimethyl-purine-2,6-dione (**12b**).*. The titled compound was synthesized using compound **11b** (0.4 g) to give yellow solid, yield 42%, mp > 300 °C, IR (KBr) ν (cm^{-1}): 3179 (N—H), 3086 (C—H aromatic), 2928 (C—H aliphatic), 1697, 1667 (2C = O), 1636 (N—H bending), 1601–1543 (C=C aromatic), 1335, 1157 (SO_2). ^{1}H NMR (DMSO-d_6) *δ:* 3.26 (s, 3H, CH_3), 3.49 (s, 3H, CH_3), 5.57 (s, 2H, CH_2), 7.09 (t, 2H, *J* = 8.56 Hz, Ar-H), 7.31 (br.s, 2H, Ar-H), 7.91–7.93 (m, 3H, Ar-H, N—H), 8.12 (d, 1H, *J* = 6.36 Hz, Ar-H), 8.21 (d, 1H, *J* = 5.36 Hz, Ar-H), ^{13}C NMR (DMSO-d_6) *δ:* 27.7 (CH_3), 29.9 (CH_3), 46.1 (CH_2), 102.8, 115.4, 115.6, 120.3, 130.5, 130.6, 131.7, 132.4, 134.8, 134.9, 143.0, 148.6 (Ar-C), 151.5 (C=O), 154.0 (C=O), 158.7, 160.7, 163.1 (Ar-C). MS, *m/z* (%): 468.91 (M^+, 24.65), 471.86 ($M^+ + 2$, 14.11); Anal. Calcd for $C_{21}H_{17}FN_6O_4S$: C, 53.84; H, 3.66; N, 17.94; found C, 54.11; H, 3.94; N, 18.17.

5.1.5. 4-[2-(7-Benzyl-1,3-dimethyl-2,6-dioxo-2,3,6,7-tetrahydro-1H-purin-8-ylamino)thiazol-5-ylamino]benzenesulfonamide (13).

A mixture of 7-benzyl-8-bromo-1,3-dimethyl-1*H*-purine-2,6(3*H*,7*H*)-dione **11a** (0.5 g, 1.43 mmol), 4-(2-aminothiazol-5-ylamino)benzenesulfonamide **4** (0.43 g, 1.58 mmol) and DMAP (0.175 g, 1.43 mmol) in DMF (6 ml) was stirred at 80–90 °C for 6 h. The reaction mixture was cooled to room temperature, poured onto ice water and adjusted at pH 4–5 using hydrochloric acid (1 N). The formed precipitate was filtered, washed with water and recrystallized from ethanol/DMF to give dark grey solid, yield 39%, mp 265–267 °C, IR (KBr) ν (cm^{-1}): 3352 (N—H amine), 3256, 3210 (NH_2), 3063–3009 (C—H aromatic), 2951 (C—H aliphatic), 1709, 1670 (2C = O), 1605 (N—H bending), 1539–1501 (C=C aromatic), 1350, 1157 (SO_2), ^{1}H NMR (DMSO-d_6) *δ:* 3.22 (s, 3H, CH_3), 3.32 (s, 3H, CH_3), 5.60 (s, 2H, CH_2), 7.12–7.26 (m, 7H, Ar-H), 7.35 (br.s, 3H, NH, NH_2 exchanged with D_2O), 7.85–7.87 (m, 3H, Ar-H), 7.96 (br.s, 1H, NH exchanged with D_2O), ^{13}C, DEPT-135 NMR, (DMSO-d_6) *δ:* 28.1 (CH_3), 30.0 (CH_3), 49.4 (CH_2), 109.3 (Ar-C), 127.1, 127.5, 127.9, 128.8 (Ar-CH), 135.9, 141.2, 147.9 (Ar-C), 151.0 (C=O), 154.4 (C=O). MS, *m/z* (%): 538.06 (M^+, 32.79), 541.36 ($M^+ + 3$, 49.28); Anal. Calcd for $C_{23}H_{22}N_8O_4S_2$: C, 51.29; H, 4.12; N, 20.80; found C, 51.52; H, 3.96; N, 20.59.

5.1.6. (Z)-N-(7-Benzyl-1,3-dimethyl-2,6-dioxo-2,3,6,7-tetrahydro-1H-purin-8-yl)-2-(2-oxoindolin-3-ylidene)hydrazinecarbothioamide (14).

A mixture of 7-benzyl-8-bromo-1,3-dimethyl-1*H*-purine-2,6(3*H*,7*H*)-dione **11a** (0.50 g, 1.43 mmol), (Z)-2-(2-oxoindolin-3-ylidene)hydrazinecarbothioamide **7** (0.35 g, 1.58 mmol) and potassium carbonate (0.4 g, 2.86 mmol) in DMF (6 ml) was stirred at 70 °C for 10 h. The reaction mixture was cooled to room temperature then was poured onto ice water. Medium was neutralized with acetic acid (1 N) and the resulted precipitate was filtered, washed with water, dried and recrystallized from ethanol/DMF to give red solid, yield 42%, mp 185–186 °C, IR (KBr) ν (cm^{-1}): 3399 (N—H amine), 3275 (N—H amide), 3090–3071 (C—H aromatic), 2951 (C—H aliphatic), 1701, 1651 (3C = O), 1612 (N—H bending), 1539–1497 (C=C aromatic), 1180 (C=S), ^{1}H NMR (DMSO-d_6) *δ:* 3.18, 3.26 (2 s, 3H, CH_3), 3.41, 3.48 (2 s, 3H, CH_3), 5.46, 5.64 (2 s, 2H, CH_2), 6.84–6.97 (m, 2H, Ar-H), 7.24–7.39 (m, 5H, Ar-H), 7.97(d, 1H, *J* = 7.04 Hz, Ar-H), 8.30 (d, 1H, *J* = 7.28 Hz, 1H, Ar-H), 10.43 (s, 1H, NH exchanged with D_2O), 10.57 (2 s, 2H, 2NH exchanged with D_2O), ^{13}C NMR (DMSO-d_6) *δ:* 28.2 (CH_3), 30.2 (CH_3), 49.4 (CH_2), 109.3, 110.1, 110.5, 111.3, 120.7, 122.8, 127.1, 127.4, 127.9, 128.3, 131.0, 137.0, 141.9, 148.8 (Ar-C), 151.2 (C=O), 154.6 (C=O), 155.7, 163.2 (Ar-C), 165.9 (C=O), 167.6 (C=S). MS, *m/z* (%): 488.19 (M^+, 14.87), 488.83 ($M^+ + 1$, 9.03), 491.01, ($M^+ + 3$, 10.69); Anal. Calcd for $C_{23}H_{20}N_8O_3S$: C, 56.55; H, 4.13; N, 22.94; found C, 56.91; H, 4.38; N, 22.63.

*5.1.7. 7-Benzyl-8-(2-chloroethylamino)-1,3-dimethyl-1H-purine-2,6 (3H,7H)-dione (**15**).*

Triethylamine (0.42 ml, 5.73 mmol) was added to a mixture of 7-benzyl-8-bromo-1,3-dimethyl-1*H*-purine-2,6(3*H*,7*H*)-dione **11a** (2 g, 5.73 mmol) and 2-chloroethylamine HCl (1.33 g, 11.47 mmol) in DMF (20 ml). The resulted mixture was stirred at 50–60 °C for 2 h then potassium carbonate (0.4 g, 2.86 mmol) was added, stirring was then continued for 8 h at 70 °C. The reaction mixture was cooled to room temperature and poured onto ice water, the formed precipitate was filtered, washed with water, petroleum ether and dried to give pale yellow solid, yield 49%, mp 161–162 °C IR (KBr) ν (cm^{-1}): 3345 (N—H), 3067–3032 (C—H aromatic), 2994–2947 (C—H aliphatic), 1697–1667 (2C = O), 1612 (N—H bending), 1535 (C=C aromatic), ^{1}H NMR ($CDCl_3$) *δ:* 3.42 (s, 5H, CH_3, CH_2), 3.57 (s, 2H, CH_2), 3.58 (s, 3H, CH_3), 5.57 (s, 2H, CH_2), 7.29 (s, 1H, 1NH exchanged with D_2O), 7.34–7.39 (m, 5H, Ar-H), ^{13}C NMR ($CDCl_3$) *δ:* 28.1 (CH_3, CH_2), 29.9 (CH_3, CH_2), 50.3 (CH_2), 108.9, 127.9, 128.5, 128.9, 134.9, 148.4 (Ar-C), 151.3 (C=O), 154.3 (C=O). MS, *m/z* (%): 347.73 (M^+, 36.92), 349.21 ($M^+ + 1$, 46.39); Anal. Calcd for $C_{16}H_{18}ClN_5O_2$: C, 55.25; H, 5.22; N, 20.14; found C, 55.28; H, 4.85; N, 20.07.

*5.1.8. 4-[2-(7-Benzyl-1,3-dimethyl-2,6-dioxo-2,3,6,7-tetrahydro-1H-purin-8-ylamino)ethylamino]-N-(pyrimidin-2-yl)benzenesulfonamide (**16**).*

A mixture of 7-benzyl-8-(2-chloroethylamino)-1,3-dimethyl-1*H*-purine-2,6(3*H*,7*H*)-dione **15** (0.5 g, 1.44 mmol), sulfadiazine (0.4 g, 1.59 mmol) and sodium hydride 60% (0.17 g, 4.31 mmol) in DMF (5 ml) was stirred at 80 °C for 12 h. The reaction mixture was cooled to room temperature then poured onto ice water and adjusted at pH 4–5 with hydrochloric acid (1 N). The produced precipitate was filtered, washed with water, dried and recrystallized from ethanol/DMF to give yellow solid, yield 44%, mp 188–190 °C, IR (KBr) ν (cm^{-1}): 3426, 3356, 3260 (*N*-Hs), 3102–3036 (C—H aromatic), 2940 (C—H aliphatic), 1697–1651 (2C = O), 1605 (N—H bending), 1582–1528 (C=C aromatic), 1323–1153 (SO_2), ^{1}H NMR (DMSO-d_6) *δ:* 2.91 (s, 4H, $2CH_2$), 3.18 (s, 3H, CH_3), 3.40 (s, 3H, CH_3), 5.46 (s, 2H, CH_2), 6.00 (s, 2H, 2NH exchanged with D_2O), 6.57 (d, 2H, *J* = 8.72 Hz, Ar-H), 7.01 (t, 1H, *J* = 4.82 Ar-H), 7.11–7.35 (m, 5H, Ar-H), 7.62 (d, 2H, *J* = 8.68, Ar-H), 8.48 (d, 2H, *J* = 4.84, Ar-H), 11.28 (s, 1H, NH exchanged with D_2O), ^{13}C NMR (DMSO-d_6) *δ:* 27.8 (CH_3), 29.9 (CH_3), 41.5 ($2CH_2$), 48.5 (CH_2), 104.1, 112.7, 116.0, 125.3, 126.5, 127.3, 127.4, 127.8, 128.0, 128.7, 129.0, 130.3, 138.0, 148.2 (Ar-C), 151.5 (C=O), 153.5 (Ar-C), 153.9 (C=O), 157.7, 158.7 (Ar-C). MS, *m/z* (%): 561.15 (M^+, 17.69); Anal. Calcd for $C_{26}H_{27}N_9O_4S$: C, 55.60; H, 4.85; N, 22.45; found C, 55.49; H, 4.59; N, 23.13.

*5.1.9. 7-Benzyl-8-(2,6-dioxo-1,2,3,6-tetrahydropyrimidin-4-ylamino)-1,3-dimethyl-1H-purine-2,6(3H,7H)-dione (**17**).*

A mixture of 7-benzyl-8-bromo-1,3-dimethyl-1*H*-purine-2,6(3*H*,7*H*)-dione **11a** (0.42 g, 1.06 mmol), 6-aminouracil (0.15 g, 1.16 mmol) and

sodium acetate (0.13 g, 2.07 mmol) in glacial acetic acid (8 ml) was stirred at 90 °C for 16 h. The reaction mixture was cooled to room temperature then poured onto ice water. The formed precipitate was filtered, washed with water, dried and recrystallized from ethanol/DMF to give grey solid, yield 51%, mp 176–177 °C, IR (KBr) ν (cm^{-1}): 3345, 3171 (*N*-Hs), 3067–3032 (C—H aromatic), 2951 (C—H aliphatic), 1697–1667 (4C = O), 1612 (N—H bending), 1535–1443 (C=C aromatic), ^{1}H NMR (DMSO-d_6) *δ:* 3.23 (s, 3H, CH_3), 3.41 (s, 3H, CH_3), 5.53 (s, 2H, CH_2), 6.67 (s, 1H, NH exchanged with D_2O), 7.25–7.38 (m, 6H, Ar-H, pyrimidine-H), 9.89 (s, 1H, NH exchanged with D_2O), 12.80 (s, 1H, NH exchanged with D_2O), ^{13}C NMR (DMSO-d_6) *δ:* 28.1 (CH_3), 30.0 (CH_3), 49.8 (CH_2), 89.5, 108.8, 127.5, 128.0, 128.4, 128.6, 128.7, 128.9, 129.2, 136.0, 148.3 (Ar-C), 151.2 (C=O), 154.2 (C=O), 165.8 (C=O), 165.9 (C=O). MS, *m/z* (%): 394.80 (M^+, 15.21), 396.55 (M+ + 1, 15.25); Anal. Calcd for $C_{18}H_{17}N_7O_4$: C, 54.68; H, 4.33; N, 24.80; found C, 54.76; H, 4.78; N, 25.17.

5.1.10. General procedure for synthesis of **18a,b**

A mixture of 7-benzyl-8-bromo-1,3-dimethyl-1*H*-purine-2,6(3*H*,7*H*)-dione derivative **11a,b** (1.15 mmol), 6-aminothiouracil (0.18 g, 1.26 mmol) and DMAP (0.14 g, 1.15 mmol) in DMF (6 ml) was stirred at 80–90 °C for 8 h. The reaction mixture was cooled to room temperature, poured onto ice water and adjusted at pH 4–5 using hydrochloric acid (1 N). The formed precipitate was filtered, washed with water and recrystallized from ethanol/DMF to give the product.

5.1.10.1. *8-(4-Amino-6-oxo-1,6-dihydropyrimidin-2-ylthio)-7-benzyl-1,3-dimethyl-1H-purine-2,6(3H,7H)-dione (**18a**)*.

The titled compound was synthesized using compound **11a** (0.4 g) to give white solid, yield 42%, mp 271–274 °C, IR (KBr) ν (cm^{-1}): 3360, 3194 (*N*-Hs), 3090–3009(C—H aromatic), 2951 (C—H aliphatic), 1709, 1667, 1651 (3C = O), 1605 (N—H bending), 1539–1443 (C=C aromatic), ^{1}H NMR (DMSO-d_6) *δ:* 3.22 (s, 3H, CH_3), 3.42 (s, 3H, CH_3), 5.60 (s, 2H, CH_2), 7.06–7.35 (m, 7H, Ar-H, NH_2 exchanged with D_2O), 9.02 (d, 1H, J = 9.40 Hz, pyrimidine-H), 11.88 (s, 1H, NH exchanged with D_2O), ^{13}C, DEPT-135 NMR, (DMSO-d_6) *δ:* 28.1 (CH_3), 30.0 (CH_3), 49.4 (CH_2), 109.3 (Ar-C), 127.1, 127.3, 127.9, 128.9, 129.4 (Ar-CH), 136.0, 141.2, 147.9 (Ar-C), 151.0 (C=O), 154.4 (C=O), 159.9 (C=O). MS, *m/z* (%): 411.12 (M^+, 9.33), 413.64 (M^+ + 2, 12.42); Anal. Calcd for $C_{18}H_{17}N_7O_3S$: C, 52.55; H, 4.16; N, 23.83; found C, 53.03; H, 4.13; N, 24.05.

5.1.10.2. *8-(4-Amino-6-oxo-1,6-dihydropyrimidin-2-ylthio)-7-(4-fluorobenzyl)-1,3-dimethyl-1H-purine-2,6(3H,7H)-dione (**18b**)*.

The titled compound was synthesized using compound **11b** (0.42 g) to give buff solid, yield 46%, mp 287–288 °C, IR (KBr) ν (cm^{-1}): 3352, 3321, 3190 (*N*-Hs), 3082–3017 (C—H aromatic), 2955 (C—H aliphatic), 1705–1656 (3C = O), 1605 (N—H bending), 1539–1443 (C=C aromatic), 1H NMR (DMSO-d_6) *δ:* 3.21 (s, 3H, CH_3), 3.40 (s, 3H, CH_3), 5.57 (s, 2H, CH_2), 7.05–7.35 (m, 6H, Ar-H, NH_2 exchanged with D_2O), 9.02 (t, 1H, J = 7.42 Hz, pyrimidine-H), 11.88 (s, 1H, NH exchanged with D_2O), ^{13}C NMR (DMSO-d_6) *δ:* 28.1 (CH_3), 30.0 (CH_3), 48.7 (CH_2), 107.3, 107.5, 109.2, 115.5, 115.8, 129.5, 129.5, 132.1, 136.9, 141.2, 147.9 (Ar-C), 151.0 (C=O), 154.4 (C=O), 160.7 (C=O), 163.2, 166.9 (Ar-C). MS, *m/z* (%): 429.99 (M^+, 6.24); Anal. Calcd for $C_{18}H_{16}FN_7O_3S$: C, 50.34; H, 3.76; N, 22.83; found C, 50.59; H, 4.02; N, 22.68.

5.1.11. General procedure for synthesis of **19a,b**

Sodium hydride 60% (0.17 g, 4.3 mmol) was added to a mixture of 8-bromo-7-(4-fluorobenzyl)-1,3-dimethyl-1*H*-purine-2,6(3*H*,7*H*)-dione **11b** (0.53 g, 1.43 mmol) and the appropriate 4-oxo-6-phenyl-2-thioxo-1,2,3,4-tetrahydropyrimidine-5-carbonitrile derivative **8b,c** (1.61 mmol) in DMF (6 ml). The mixture was stirred at 0–5 °C for 1 h then stirred at room temperature for 24 h and at 80 °C for 10 h. The reaction mixture was cooled to room temperature then poured onto ice water and adjusted at pH 4–5 with hydrochloric acid (1 N). The produced precipitate was filtered, washed with water, dried and recrystallized from ethanol/water.

5.1.11.1. *2-[7-(4-Fluorobenzyl)-1,3-dimethyl-2,6-dioxo-2,3,6,7-tetrahydro-1H-purin-8-ylthio]-4-(4-fluorophenyl)-6-oxo-1,6-dihydropyrimidine-5-carbonitrile (**19a**)*.

The titled compound was synthesized using compound **8b** (0.40 g) to give dark green solid, yield 40%, mp, IR (KBr) ν (cm^{-1}): 3287 (N—H), 3075–3009 (C—H aromatic), 2924 (C—H aliphatic), 2222 (C≡N), 1700–1663 (3C = O), 1605 (N—H bending), 1539–1512 (C=C aromatic), ^{1}H NMR (DMSO-d_6) *δ:* 3.29 (s, 3H, CH_3), 3.32 (s, 3H, CH_3), 4.54 (s, 2H, CH_2), 7.13–7.47 (m, 7H, Ar-H, NH exchanged with D_2O), 8.04 (dd, 2H, J = 4.75, 8.72 Hz, Ar-H), ^{13}C NMR (DMSO-d_6) *δ:* 28.1 (CH_3), 30.0 (CH_3), 41.6 (CH_2), 93.5 (C≡N), 109.2, 109.7, 115.4, 115.9, 116.3, 122.3, 129.3, 130.7, 131.3, 131.5, 131.9, 132.1, 133.1, 141.2, 147.9 (Ar-C), 151.4 (C=O), 154.8 (C=O), 160.7, 161.5, 163.2, 163.3, 165.8, 166.1(Ar-C), 166.6 (C=O). MS, *m/z* (%): 533.75 (M^+, 9.84); Anal. Calcd for $C_{25}H_{17}F_2N_7O_3S$: C, 56.28; H, 3.21; N, 18.38; found C, 56.73; H, 3.53; N, 18.26.

5.1.11.2. *2-[7-(4-Fluorobenzyl)-1,3-dimethyl-2,6-dioxo-2,3,6,7-tetrahydro-1H-purin-8-ylthio]-4-(4-methoxyphenyl)-6-oxo-1,6-dihydropyrimidine-5-carbonitrile (**19b**)*.

The titled compound was synthesized using compound **8c** (0.42 g) to give yellow solid, yield 39%, mp 268–269 °C, IR (KBr) ν (cm^{-1}): 3151 (N—H), 3094–3028 (C—H aromatic), 2951, 2913 (C—H aliphatic), 2218 (C≡N), 1694–1636 (C=O), 1605 (N—H bending), 1539–1512 (C=C aromatic), ^{1}H NMR (DMSO-d_6) *δ:* 3.30 (s, 3H, CH_3), 3.46 (s, 3H, CH_3), 3.83 (s, 3H, OCH_3), 5.64 (s, 2H, CH_2), 6.95–7.02 (m, 5H, Ar-H, NH exchanged with D_2O), 7.30 (t, 2H, J = 6.8 Hz, Ar-H), 7.64 (d, 2H, J = 8.76 Hz, Ar-H), ^{13}C NMR (DMSO-d_6) *δ:* 28.3 (CH_3), 30.1 (CH_3), 48.9 (CH_2), 56.0 (OCH_3), 91.4 (C≡N), 109.8, 114.5, 115.5, 115.7, 116.4, 127.0, 130.2, 130.3, 130.9, 132.4, 139.0, 148.2 (Ar-C), 151.1 (C=O), 154.8 (C=O), 160.8, 162.7, 163.2, 164.4, 164.6 (Ar-C), 166.8 (C=O). MS, *m/z* (%): 545.02 (M^+, 29.01), 547.54 (M^+ + 2, 51.68); Anal. Calcd for $C_{26}H_{20}FN_7O_4S$: C, 57.24; H, 3.70; N, 17.97; found C, 57.68; H, 3.53; N, 17.68.

5.1.12. *2-[1,3-Dimethyl-2,6-dioxo-2,3-dihydro-1H-purin-7(6H)-yl]-N-p-tolylacetamide. (**20**)*.

Theophylline (0.5 g, 2.78 mmol) was added to a suspension of potassium carbonate (0.96 g, 6.93 mmol) in DMF (8 ml) and stirred at 100 °C for 2 h. A mixture of 2-chloro-*N*-*p*-tolylacetamide **3c** (1.02 g, 5.55 mmol) and potassium iodide (0.23 g, 1.38 mmol) in DMF (4 ml) was added to the previous mixture, and was stirred at 80 °C for 8 h. The reaction mixture was cooled to room temperature, poured onto ice water and adjusted at pH 6 by hydrochloric acid (1 N). The formed precipitate was filtered, washed with water, dried and recrystallized from ethanol/water to give brown solid, yield 46%, mp 120 °C , IR (KBr) ν (cm^{-1}): 3264 (N—H amide), 3075 (C—H aromatic), 2951, 2920 (C—H aliphatic), 1701–1655 (3C = O), 1609 (N—H bending), 1547–1512 (C=C aromatic), ^{1}H NMR (DMSO-d_6) *δ:* 2.14 (s, 3H, CH_3), 2.26 (s, 3H, CH_3), 2.52 (s, 3H, CH_3), 3.22 (s, 2H, CH_2), 7.31–7.77 (m, 5H, Ar-H), 10.73 (s, 1H, NH exchanged with D_2O), ^{13}C NMR (DMSO-d_6) *δ:* 20.9 ($2CH_3$), 21.0 (CH_2, CH_3), 118.6, 119.6, 120.8, 129.6, 129.7, 134.2, 135.6 (Ar-C), 159.0 (C=O), 159.8 (2C = O). MS, *m/z* (%): 327.14 (M^+, 41.00), 328.97 (M^+ + 1, 16.79); Anal. Calcd for $C_{16}H_{17}N_5O_3$: C, 58.71; H, 5.23; N, 21.39; found C, 59.02; H, 5.50; N, 21.65.

5.1.12.1. *General procedure for synthesis of **22a-f**.*

8-Bromotheophylline **21** (1 g, 3.86 mmol) was added to a suspension of potassium carbonate (1.34 g, 9.70 mmol) in DMF (10 ml) and the mixture was stirred at 100 °C for 2 h. The appropriate 2-chloro-*N*-(substituted phenyl)acetamide derivative **3a-f** (5.80 mmol) was dissolved in DMF (4 ml) and then added to the previous mixture. The resulted mixture was stirred at room temperature for 24 h. The reaction mixture was poured onto ice water and adjusted at pH 6 by hydrochloric acid (1 N). The formed precipitate

was filtered, washed with water, dried and recrystallized from ethanol/water to give the product.

*5.1.12.2. 2-[8-Bromo-1,3-dimethyl-2,6-dioxo-2,3-dihydro-1H-purin-7(6H)-yl]-N-p-tolylacetamide (**22c**).*. The titled compound was synthesized using compound **3c** (1.07 g) to give white solid, yield 62%, mp 290–293 °C, IR (KBr) ν (cm^{-1}): 3310 (N—H), 3078–3032 (C—H aromatic), 2920 (C—H aliphatic), 1701–1643 (3C = O), 1601 (N—H bending), 1558–1501 (C=C aromatic). ^{1}H NMR (DMSO-d_6) *δ:* 2.27 (s, 3H, CH_3), 3.19 (s, 3H, CH_3), 3.42 (s, 3H, CH_3), 5.03 (s, 2H, CH_2), 7.13 (d, 2H, *J* = 8.36 Hz, Ar-H), 7.56 (d, 2H *J* = 8.44 Hz, Ar-H), 9.17 (s, 1H, NH exchanged with D_2O). ^{13}C NMR ($CDCl_3$) *δ:* 25.6 (CH_3), 32.3 (CH_3), 34.5 (CH_3), 51.4 (CH_2), 107.2, 123.6, 124.1, 134.1, 134.2, 135.9, 137.5, 141.3, 142.4 (Ar-C), 152.9 (C=O), 155.8 (C=O), 156.2, 158.5 (Ar-C), 170.1 (C=O). MS, *m/z* (%): 406.60 (M^+, 7.87); Anal. Calcd for $C_{16}H_{16}BrN_5O_3$: C, 47.31; H, 3.97; N, 17.24; found C, 47.66; H, 3.83; N, 17.49.

*5.1.12.3. 2-[8-Bromo-1,3-dimethyl-2,6-dioxo-2,3-dihydro-1H-purin-7(6H)-yl]-N-(2,4-dichlorophenyl)acetamide (**22d**).*. The titled compound was synthesized using compound **3d** (0.78 g) to give white solid, yield 70%, mp 141–142 °C, IR (KBr) ν (cm^{-1}): 3256 (N—H amide), 3075–3021 (C—H aromatic), 2970, 2951 (C—H aliphatic), 1697–1659 (3C = O), 1624 (N—H bending), 1589–1520 (C=C aromatic). ^{1}H NMR ($CDCl_3$) *δ:* 3.46 (s, 3H, CH_3), 3.61 (s, 3H, CH_3), 5.09 (s, 2H, CH_2), 7.44 (dd, 1H, *J* = 2.04 Hz, *J* = 8.96 Hz, Ar-H), 8.23–8.38 (m, 2H, Ar-H), 9.11 (s, 1H, NH exchanged with D_2O). ^{13}C NMR (DMSO-d_6) *δ:* 27.9 (CH_3), 30.1 (CH_3), 49.2 (CH_2), 106.2, 119.5, 123.3, 127.6, 127.9, 129.0, 129.2, 135.4, 148.7 (Ar-C), 151.1 (C=O), 154.2 (C=O), 165.6 (C=O). MS, *m/z* (%): 460.20 (M^+, 5.27), 461.50 (M^+ + 1, 14.53), 462.18 (M^+ + 2, 30.51), 462.72 (M^+ + 3, 9.89); Anal. Calcd for $C_{15}H_{12}BrCl_2N_5O_3$: C, 39.07; H, 2.62; N, 15.19; found C, 39.25; H, 2.93; N, 15.64.

*5.1.12.4. N-(4-Acetylphenyl)-2-[8-bromo-1,3-dimethyl-2,6-dioxo-2,3-dihydro-1H-purin-7(6H)-yl]acetamide (**22e**).*. The titled compound was synthesized using compound **3e** (1.23 g) to give white solid, yield 57%, mp 244–245 °C, IR (KBr) ν (cm^{-1}): 3217 (N—H), 3063–3001 (C—H aromatic), 2978 (C—H aliphatic), 1713–1651 (3C = O), 1601 (N—H bending), 1555–1504 (C=C aromatic). ^{1}H NMR (DMSO-d_6) *δ:* 2.52 (s, 3H, CH_3), 3.19 (s, 3H, CH_3), 3.49 (s, 3H, CH_3), 5.27 (s, 2H, CH_2), 7.72–7.96 (m, 4H, Ar-H), 9.67 (s, 1H, NH exchanged with D_2O). ^{13}C NMR ($CDCl_3$) *δ:* 26.8 ($\underline{C}H_3$-C=O), 28.1 (CH_3), 30.5 (CH_3), 50.1 (CH_2), 102.7, 117.4, 118.8, 123.4, 129.7, 130.1, 132.4, 143.4, 144.7 (Ar-C), 151.3 (C=O), 166.1 (C=O), 170.8 (C=O), 197.8 (C=O). MS, *m/z* (%): 434.19 (M^+, 55.26); Anal. Calcd for $C_{17}H_{16}BrN_5O_4$: C, 47.02; H, 3.71; N, 16.13; found C, 47.34; H, 3.72; N, 16.82.

*5.1.12.5. General procedure for synthesis of **23a,b**.* The appropriate 2-(8-bromo-1,3-dimethyl-2,6-dioxo-2,3-dihydro-1*H*-purin-7(6*H*)-yl)-*N*-substituted phenylacetamide derivative **22e,f** (1.06 mmol) was added to a mixture of (1,1-dioxo-1,2-benzothiazol-3-yl)amine **2** (0.21 g, 1.16 mmol) and sodium hydride 60% (0.12 g, 3.18 mmol) in DMF (6 ml). The resulted mixture was stirred at 70 °C for 12 h. The reaction mixture was cooled to room temperature then poured onto ice water and neutralized with acetic acid (1 N). The produced precipitate was filtered, washed with water, dried and recrystallized from ethanol/DMF.

*5.1.12.6. 2-(8-[(1,1-Dioxo-1,2-benzothiazol-3-yl)amino]-1,3-dimethyl-2,6-dioxo-purin-7-yl)-~(N)-(4-acetylphenyl)acetamide (**23a**).*. The titled compound was synthesized using compound **22e** (0.46 g) to give brown solid, yield 42%, mp , IR (KBr) ν (cm^{-1}): 3441, 3287 (*N*-Hs), 3086–3001 (C—H aromatic), 2959 (C—H aliphatic), 1697–1651 (4C = O), 1605 (N—H bending), 1597–1497 (C=C aromatic), 1366–1161 (SO_2), ^{1}H NMR (DMSO-d_6) *δ:* 2.51 (s, 3H, CH_3), 3.20 (s, 3H, CH_3), 3.46 (s, 3H, CH_3), 4.97 (s, 2H, CH_2), 7.68–7.94 (m, 9H, Ar-H, NH exchanged with D_2O), 10.13 (s, 1H, NH exchanged with D_2O). ^{13}C NMR (DMSO-d_6) *δ:* 26.0 ($\underline{C}H_3$-C=O), 26.8 (CH_3), 27.8 (CH_3), 30.0 (CH_2), 102.8, 116.5, 117.3, 127.5, 128.4, 129.3, 130.0, 130.2, 130.5, 133.9, 135.5, 136.7, 142.9, 147.0, 147.6, 149.1, 150.6 (Ar-C), 151.5 (C=O), 154.0 (C=O), 170.5 (C=O), 197.5 (CH_3-$\underline{C}$=O). MS, *m/z* (%): 535.46 (M^+, 13.76); Anal. Calcd for $C_{24}H_{21}N_7O_6S$: C, 53.83; H, 3.95; N, 18.31; found C, 53.62; H, 4.02; N, 18.52.

*5.1.12.7. 2-(8-[(1,1-Dioxo-1,2-benzothiazol-3-yl)amino]-1,3-dimethyl-2,6-dioxo-purin-7-yl)-~(N)-(4-sulfamoylphenyl)acetamide (**23b**).*. The titled compound was synthesized using compound **22f** (0.5 g) to give brown solid, yield 43%, mp, IR (KBr) ν (cm^{-1}): 3441, 3333, 3291, 3198 (NH_2, N—H), 3067–3028 (C—H aromatic), 2990–2909 (C—H aliphatic), 1697–1650 (3C = O), 1601 (N—H bending), 1555–1489 (C=C aromatic), 1339, 1161 (SO_2), ^{1}H NMR (DMSO-d_6) *δ:* 3.24 (s, 3H, CH_3), 3.37 (s, 3H, CH_3), 4.85 (s, 1H, NH exchanged with D_2O), 4.98 (s, 2H, CH_2), 7.17 (s, 1H, NH exchanged with D_2O), 7.49 (s, 2H, NH_2 exchanged with D_2O), 7.65, (d, 1H, *J* = 8.48 Hz, Ar-H), 7.75 (dd, 2H, *J* = 8.52, 12.12 Hz, Ar-H), 7.84 (d, 1H, *J* = 8.48 Hz, Ar-H), 7.96–8.04 (m, 4H, Ar-H), ^{13}C NMR (DMSO-d_6) *δ:* 28.1 (CH_3), 29.9 (CH_3), 50.2 (CH_2), 104.0, 117.6, 123.3, 124.1, 125.4, 127.3, 128.0, 133.8, 135.5, 136.6, 143.2, 143.7, 147.4, 149.3 (Ar-C), 151.3 (C=O), 152.7 (Ar-C), 153.6 (C=O), 162.8 (Ar-C), 170.8 (C=O). MS, *m/z* (%): 572.72 (M^+, 23.33); Anal. Calcd for $C_{22}H_{20}N_8O_7S_2$: C, 46.15; H, 3.52; N, 19.57; found C, 46.49; H, 3.52; N, 19.63.

*5.1.12.8. General procedure for synthesis of **24a,b**.* To a mixture of sodium hydride 60% (0.14 g, 3.45 mmol) and aniline derivative (sulfanilamide, 4-fluoroaniline) in DMF (7 ml), 2-(8-bromo-1,3-dimethyl-2,6-dioxo-2,3-dihydro-1*H*-purin-7(6*H*)-yl)-*N*-substituted phenylacetamide derivative **22e,f** was added. The resulted mixture was stirred at 70 °C for 8 h then at room temperature for 24 h. The reaction mixture was poured onto ice water and neutralized with acetic acid (1 N). The formed precipitate was filtered, washed with hot ethanol several times to remove the excess aniline derivative and dried. The crude was recrystallized from ethanol/DMF to give the product.

*5.1.12.9. N-(4-Acetylphenyl)-2-[1,3-dimethyl-2,6-dioxo-8-(4-sulfamoylphenylamino)-2,3-dihydro-1H-purin-7(6H)-yl]acetamide (**24a**).*. The titled compound was synthesized by reaction of compound **22e** (0.50 g, 1.15 mmol) with sulfanilamide (0.40 g, 2.32 mmol) to give brown solid, yield 43%, mp 243–245 °C, IR (KBr) ν (cm^{-1}): 3441, 3418, 3318, 3217 (NH_2, N—H), 3078–3001 (C—H aromatic), 2959 (C—H aliphatic), 1697–1651 (4C = O), 1601 (N—H bending), 1555–1447 (C=C aromatic), 1362, 1184 (SO_2), ^{1}H NMR (DMSO-d_6) *δ:* 2.63 (s, 3H, CH_3), 3.24 (s, 3H, CH_3), 3.45 (s, 3H, CH_3), 4.97 (s, 2H, CH_2), 6.89 (s, 1H, NH exchanged with D_2O), 7.55 (s, 2H, NH_2 exchanged with D_2O), 7.71 (d, 2H, *J* = 8.6 Hz, Ar-H), 7.78–8.00 (m, 2H, Ar-H), 7.98 (d, 2H, *J* = 8.60 Hz, Ar-H), 8.16 (d, 2H, *J* = 8.60 Hz, Ar-H), 10.71 (s, 1H, NH exchanged with D_2O), ^{13}C NMR (DMSO-d_6) *δ:* 26.7 ($\underline{C}H_3$-C=O), 27.2 (CH_3), 28.1 (CH_2), 30.3 (CH_3), 95.0, 103.2, 104.4, 113.2, 116.5, 117.3, 123.2, 129.8, 130.0, 130.2, 137.0, 145.5, 149.3, 151.4 (Ar-C), 151.6 (C=O), 153.8 (C=O), 156.2 (Ar-C), 171.1 (C=O), 197.4 (CH_3-$\underline{C}$=O). MS, *m/z* (%): 525.06 (M^+, 16.92), 527.57 (M^+ + 2, 18.91); Anal. Calcd for $C_{23}H_{23}N_7O_6S$: C, 52.56; H, 4.41; N, 18.66; found C, 52.88; H, 4.55; N, 18.35.

*5.1.12.10. 2-[8-(4-Fluorophenylamino)-1,3-dimethyl-2,6-dioxo-2,3-dihydro-1H-purin-7(6H)-yl]-N-(4-sulfamoylphenyl)acetamide (**24b**).*. The titled compound was synthesized by reaction of compound **22f** (0.50 g, 1.06 mmol) with 4-fluoroaniline (1 ml, 10.56 mmol) to give dark brown solid, yield 42%, mp 265–267 °C, IR (KBr) ν (cm^{-1}): 3441, 3395, 3333, 3271 (NH_2, N—H), 3090 (C—H aromatic), 2909 (C—H aliphatic), 1697–1650 (3C = O), 1601 (N—H bending), 1555–1493 (C=C aromatic), 1327, 1157 (SO_2), ^{1}H NMR (DMSO-d_6) *δ:* 3.24 (s, 3H, CH_3), 3.46

(s, 3H, CH_3), 4.98 (s, 2H, CH_2), 7.20 (s, 2H, NH_2 exchanged with D_2O), 7.45–8.02 (m, 8H, Ar-H), 9.97 (s, 1H, NH exchanged with D_2O), 12.29 (s, 1H, NH exchanged with D_2O), ^{13}C NMR (DMSO-d_6) *δ:* 28.1 (CH_3), 28.7 (CH_2), 30.3 (CH_3), 102.6, 117.1, 119.6, 124.2, 126.8, 127.3, 127.4, 128.0, 136.6, 143.6, 148.5, 149.1, 151.3 (Ar-C), 151.6 (C═O), 153.6 (C═O), 162.0 (Ar-C), 163.0 (C═O). MS, *m/z* (%): 501.07 (M^+, 27.15), 502.57 ($M^+ + 1$, 1.95); Anal. Calcd for $C_{21}H_{20}FN_7O_5S$: C, 50.29; H, 4.02; N, 19.55; found C, 50.66; H, 4.19; N, 19.89.

*5.1.12.11. 2-[8-(2,6-Dioxo-1,2,3,6-tetrahydropyrimidin-4-ylamino)-1,3-dimethyl-2,6-dioxo-2,3-dihydro-1H-purin-7(6H)-yl]-N-(4-sulfamoylphenyl)acetamide (**25**)..* A mixture of 2-[8-bromo-1,3-dimethyl-2,6-dioxo-2,3-dihydro-1*H*-purin-7(6*H*)-yl]-*N*-(4-sulfamoylphenylphenyl) acetamide **22f** (0.50 g, 1.06 mmol), 6-aminouracil (0.15 g, 1.16 mmol) and sodium acetate (0.13 g, 2.07 mmol) in glacial acetic acid (8 ml) was stirred at 80 °C for 10 h. The reaction mixture was cooled to room temperature then poured onto ice water. The formed precipitate was filtered, washed with water, dried and recrystallized from ethanol/DMF to give red solid, yield 41%, mp 272–273 °C, IR (KBr) ν (cm^{-1}): 3414, 3391, 3333, 3175 (NH_2, N—H), 3067–3032 (C—H aromatic), 2990, 2909 (C—H aliphatic), 1712–1667 (5C = O), 1601 (N—H bending), 1555–1485 (C═C aromatic), 1339, 1161 (SO_2), ^1H NMR (DMSO-d_6) *δ:* 3.25 (s, 3H, CH_3), 3.44 (s, 3H, CH_3), 4.42 (s, 1H, NH exchanged with D_2O), 4.98 (s, 2H, CH_2), 6.22 (s, 1H, NH exchanged with D_2O), 7.17–7.20 (br.s, 1H, NH exchanged with D_2O), 7.49 (s, 2H, NH_2 exchanged with D_2O), 7.64–7.85 (m, 3H, 2Ar-H, pyrimidine-H), 8.01 (dd, 2H, *J* = 4.72, 8.73 Hz, Ar-H), 10.08, 10.11 (2 s, 1H, NH/OH exchanged with D_2O), ^{13}C, DEPT-135 NMR (DMSO-d_6) *δ:* 28.1 (CH_3), 30.5 (CH_3), 50.2 (CH_2), 74.6 (CH = C), 104.0, 117.8 (Ar-C), 124.1, 127.3 (Ar-CH), 135.5, 143.2, 149.3, 151.3 (Ar-C), 151.5 (C═O), 152.7, 153.6 (C═O), 155.7 (C═O), 164.8 (C═O), 170.8 (C═O). MS, *m/z* (%): 516.69 (M^+, 37.05), 518.52 ($M^+ + 1$, 24.51), 519.71 ($M^+ + 2$, 13.95), 520.65 ($M^+ + 3$, 11.09); Anal. Calcd for $C_{19}H_{19}N_9O_7S$: C, 44.10; H, 3.70; N, 24.36; found C, 43.84; H, 4.12; N, 23.57.

*5.1.12.12. 2-[8-(4-Amino-6-oxo-1,6-dihydropyrimidin-2-ylthio)-1,3-dimethyl-2,6-dioxo-2,3-dihydro-1H-purin-7(6H)-yl]-N-(4-sulfamoylphenyl)acetamide (**26**)..* A mixture of 2-(8-bromo-1,3-dimethyl-2,6-dioxo-2,3-dihydro-1*H*-purin-7(6*H*)-yl)-*N*-(4-sulfamoylphenyl)acetamide **22f** (0.5 g, 1.06 mmol), 6-aminothiouracil (0.15 g, 1.16 mmol) and DMAP (0.13 g, 1.06 mmol) in DMF (8 ml) was stirred at 70 °C for 8 h. The reaction mixture was cooled to room temperature, poured onto ice water and adjusted at pH 4–5 using hydrochloric acid (1 N). The formed precipitate was filtered, washed with water and recrystallized from ethanol/DMF to give reddish brown solid, yield 56%, mp 283–285 °C, IR (KBr) ν (cm^{-1}): 3329, 3194, 3140, 3109 (NH_2, N—H), 3090 (C—H aromatic), 2913 (C—H aliphatic), 1697–1667 (4C = O), 1605 (N—H bending), 1556–1457 (C═C aromatic), 1327, 1157 (SO_2), ^1H NMR (DMSO-d_6) *δ:* 3.24 (s, 3H, CH_3), 3.45 (s, 3H, CH_3), 4.89 (s, 1H, NH exchanged with D_2O), 4.98 (s, 2H, CH_2), 7.20 (s, 2H, NH_2 exchanged with D_2O), 7.48 (s, 1H, NH exchanged with D_2O), 7.68–7.89 (m, 3H, Ar-H, pyrimidine-H), 7.97–8.04 (m, 2H, Ar-H), 10.08, 10.11 (2 s, 2H, NH_2 exchanged with D_2O), ^{13}C NMR (DMSO-d_6) *δ:* 28.1 (CH_3), 30.3 (CH_3), 50.2 (CH_2), 82.0 (CH = C), 104.0, 117.1, 124.2, 127.3, 128.1, 135.5, 136.6, 143.2, 147.4, 149.1 (Ar-C), 151.3 (C═O), 152.7 (Ar-C), 153.6 (C═O), 163.8 (C═O), 170.8 (C═O). MS, *m/z* (%): 533.26 (M^+, 24.55); Anal. Calcd. for $C_{19}H_{19}N_9O_6S_2$: C, 42.77; H, 3.59; N, 23.63; found C, 42.46; H, 3.39; N, 23.54.

*5.1.12.13. General procedure for synthesis of **27a,b**.* Sodium hydride 60% (0.14 g, 3.45 mmol) was added to a mixture of appropriate 2-(8-bromo-1,3-dimethyl-2,6-dioxo-2,3-dihydro-1*H*-purin-7(6*H*)-yl)-*N*-substituted phenylacetamide derivative **22e,f** (1.15 mmol) and 4-oxo-6-phenyl-2-thioxo-1,2,3,4-tetrahydropyrimidine-5-carbonitrile **8a** (0.29 g, 1.27 mmol) in DMF (6 ml). The mixture was stirred at 0–5 °C for 1 h, and then stirred at room temperature for 24 h and at 80 °C for 10 h. The reaction mixture was cooled to room temperature then poured onto ice water and adjusted at pH 4–5 with hydrochloric acid (1 N). The produced precipitate was filtered, washed with water, dried and recrystallized from ethanol/water.

*5.1.12.14. N-(4-Acetylphenyl)-2-[8-(5-cyano-6-oxo-4-phenyl-1,6-dihydropyrimidin-2-ylthio)-1,3-dimethyl-2,6-dioxo-2,3-dihydro-1H-purin-7(6H)-yl]acetamide (**27a**)..* The titled compound was synthesized using compound **22e** (0.50 g) to give brown solid, yield 46%, mp 267–268 °C, IR (KBr) ν (cm^{-1}): 3329, 3202 (*N*-Hs), 3063 (C—H aromatic), 2994–2955 (C—H aliphatic), 2214 (C≡N), 1697–1655 (5C = O), 1601 (N—H bending), 1555–1493 (C═C aromatic), ^1H NMR (DMSO-d_6) *δ:* 2.52 (s, 3H, CH_3), 3.19 (s, 3H, CH_3), 3.44 (s, 3H, CH_3), 5.05 (s, 2H, CH_2), 7.53 (s, 2H, Ar-H, NH exchanged with D_2O), 7.73–8.03 (m, 8H, Ar-H), 9.73, 11.73 (2 s, 1H, NH/OH exchanged with D_2O), ^{13}C, DEPT-135 NMR (DMSO-d_6) *δ:* 26.8 (CH_3-C═O), 27.7 (CH_3), 28.7 (CH_3), 45.6 (CH_2), 102.6 (C≡N), 117.4, 118.0, 128.7, 129.1, 130.0, 130.2, 130.7, 131.5 (Ar-CH), 144.7, 147.5, 148.8, 150.2 (Ar-C), 151.3 (C═O), 154.0 (C═O), 166.9 (C═O), 169.5 (C═O), 196.6 (CH_3-C═O). MS, *m/z* (%): 582.28 (M^+, 17.45); Anal. Calcd for $C_{28}H_{22}N_8O_5S$: C, 57.72; H, 3.81; N, 19.23; found C, 57.81; H, 4.21; N, 19.18.

*5.1.12.15. 2-[8-(5-Cyano-6-oxo-4-phenyl-1,6-dihydropyrimidin-2-ylthio)-1,3-dimethyl-2,6-dioxo-2,3-dihydro-1H-purin-7(6H)-yl]-N-(4-sulfamoylphenyl)acetamide (**27b**)..* The titled compound was synthesized using compound **22f** (0.54 g) to give brown solid, yield 62%, mp 251–253 °C, IR (KBr) ν (cm^{-1}): 3476, 3441, 3325 (NH_2, N—H), 3090 (C—H aromatic), 2955, 2928 (C—H aliphatic), 2226 (C≡N), 1697–1650 (4C = O), 1632 (N—H bending), 1555–1489 (C═C aromatic), 1335, 1157 (SO_2), ^1H NMR (DMSO-d_6) *δ:* 3.18 (s, 3H, CH_3), 3.24 (s, 3H, CH_3), 5.06 (s, 2H, CH_2), 7.22 (s, 2H, NH_2 exchanged with D_2O), 7.52–7.95 (m, 9H, Ar-H), 9.62 (s, 1H, NH exchanged with D_2O), 10.66, 12.34 (2 s, 1H, NH/OH exchanged with D_2O), ^{13}C NMR (DMSO-d_6) *δ:* 27.8 (CH_3), 30.0 (CH_2), 31.2 (CH_3), 97.5 (C≡N), 117.1, 117.9, 126.2, 127.1, 127.3, 127.7, 128.5, 128.7, 128.8, 128.9, 129.6, 131.5, 132.7, 141.0 (Ar-C), 151.5 (C═O), 154.3 (C═O), 162.9 (2C = O). MS, *m/z* (%): 619.01 (M^+, 12.31); Anal. Calcd for $C_{26}H_{21}N_9O_6S_2$: C, 50.87; H, 3.63; N, 20.34; found C, 50.82; H, 3.68; N, 20.26.

*5.1.12.16. 7-Hydroxy-1,3-dimethyl-8-phenyl-1H-imidazo[1,2-f]purine-2,4(3H,8H)-dione (**28**)..* 2-[8-bromo-1,3-dimethyl-2,6-dioxo-2,3-dihydro-1*H*-purin-7(6*H*)-yl]-*N*-phenylacetamide **22a** (0.42 g, 1.06 mmol) was added to sodium hydride 60% (0.12 g, 3.18 mmol) in DMF (6 ml). The resulted mixture was stirred at gradually increased temperature 70–90 °C for 3 h. The reaction mixture was cooled to room temperature then poured onto ice water and neutralized with acetic acid (1 N). The produced precipitate was filtered, washed with water, dried and recrystallized from ethanol/DMF to give brownish green solid, yield 42%, mp 281–282 °C, IR (KBr) ν (cm^{-1}): 3383 (O—H), 3094, 3055 (C—H aromatic), 2995 (C—H aliphatic), 1694–1660 (2C = O), 1566–1497 (C═C aromatic), ^1H NMR (DMSO-d_6) *δ:* 3.23 (s, 3H, CH_3), 3.44 (s, 3H, CH_3), 6.96 (t, 1H, *J* = 7.32 Hz, Ar-H), 7.30 (t, 2H, *J* = 7.86 Hz, Ar-H), 7.57 (d, 2H, *J* = 7.88 Hz, Ar-H), 9.43 (s, 1H, imidazole-H), 11.90 (s, 1H, OH exchanged with D_2O), ^{13}C NMR (DMSO-d_6) *δ:* 28.0 (CH_3), 30.2 (CH_3), 102.2, 118.0, 121.9, 129.3, 140.5, 148.8, 150.2 (Ar-C), 151.7 (C═O), 153.4 (Ar-C). MS, *m/z* (%): 311.27 (M^+, 13.53); Anal. Calcd for $C_{15}H_{13}N_5O_3$: C, 57.87; H, 4.21; N, 22.50; found C, 57.63; H, 4.01; N, 22.91.

*5.1.12.17. General procedure for synthesis of **29a-d**.* 2-(8-Bromo-1,3-dimethyl-2,6-dioxo-2,3-dihydro-1*H*-purin-7(6*H*)-yl)-*N*-substituted phenylacetamide derivative **22b-e** (1.22 mmol) was added to sodium hydride 60% (0.15 g, 3.67 mmol) in DMF (6 ml). The resulted mixture was stirred at gradually increased temperature 70–90 °C for 3 h. 4-Oxo-6-

phenyl-2-thioxo-1,2,3,4-tetrahydropyrimidine-5-carbonitrile **8a** (0.31 g, 1.34 mmol) was dissolved in DMF (2 ml) and was added to previous mixture. The resulted reaction mixture was stirred for 12 h at 90 °C, then cooled to room temperature, poured onto ice water and neutralized with acetic acid (1 N). The produced precipitate was filtered, washed with water, dried and recrystallized from ethanol/DMF

*5.1.12.18. 2-(8-(4-Fluorophenyl)-1,3-dimethyl-2,4-dioxo-2,3,4,8-tetrahydro-1H-imidazo[1,2-f]purin-7-ylthio)-6-oxo-4-phenyl-1,6-dihydropyrimidine-5-carbonitrile (**29a**).*. The titled compound was synthesized using compound **22b** (0.50 g) to give white solid, yield 38%, mp 296 °C, IR (KBr) ν (cm^{-1}): 3225 (N—H), 3063, 3005 (C—H aromatic), 2959–2928 (C—H aliphatic), 2218 (C≡N), 1709, 1653 (3C = O), 1601 (N—H bending), 1566–1493 (C=C aromatic), ^{1}H NMR (DMSO-d_6) *δ:* 3.26 (s, 3H, CH_3), 3.47 (s, 3H, CH_3), 7.22 (t, 2H, *J* = 8.80 Hz, Ar-H), 7.51–7.53 (m, 4H, 3Ar-H, imidazole-H), 7.66–7.69 (m, 2H, Ar-H), 8.02 (dd, 2H, *J* = 2.86, 17.40 Hz, Ar-H), 11.45 (s, 1H, NH exchanged with D_2O), ^{13}C NMR (DMSO-d_6) *δ:* 28.6 (CH_3), 30.2 (CH_3), 91.3, 101.3 (Ar-C), 116.0 (C≡N), 116.3, 119.5, 120.7, 128.7, 129.1, 130.8, 135.1, 137.5, 150.5, 151.0 (Ar-H), 151.5 (C=O), 152.9 (Ar-H), 156.5 (C=O), 157.1 (Ar-C), 168.6 (C=O), 171.5 (Ar-C). MS, *m/z* (%): 539.66 (M^+, 34.88), 540.85 (M^+ + 1, 26.72); Anal. Calcd for $C_{26}H_{17}FN_8O_3S$: C, 57.77; H, 3.17; N, 20.73; found C, 57.86; H, 3.19; N, 21.36.

*5.1.12.19. 2-(1,3-Dimethyl-2,4-dioxo-8-p-tolyl-2,3,4,8-tetrahydro-1H-imidazo[1,2-f]purin-7-ylthio)-6-oxo-4-phenyl-1,6-dihydropyrimidine-5-carbonitrile (**29b**).*. The titled compound was synthesized using compound **22c** (0.50 g) to give white solid, yield 39%, mp > 300 °C, IR (KBr) ν (cm^{-1}): 3271, 3194 (N—H), 3028 (C—H aromatic), 2955–2924 (C—H aliphatic), 2214 (C≡N), 1709–1662 (3C = O), 1635 (N—H bending), 1553–1489 (C=C aromatic), ^{1}H NMR (DMSO-d_6) *δ:* 2.29 (s, 3H, CH_3), 3.26 (s, 3H, CH_3), 3.49 (s, 3H, CH_3), 7.20 (d, 2H, *J* = 8.32 Hz, Ar-H), 7.50–7.56 (m, 6H, Ar-H, imidazole-H), 8.02 (dd, 2H, *J* = 4.40, 7.32 Hz, Ar-H), 11.41 (s, 1H, NH exchanged with D_2O), ^{13}C, DEPT-135 NMR (DMSO-d_6) *δ:* 20.9 (CH_3), 28.5 (CH_3), 30.3 (CH_3), 91.1, 101.2 (Ar-C), 119.2 (CH = C), 119.7 (C≡N), 128.6, 129.1, 130.0, 130.7 (Ar-CH), 132.3, 136.2, 137.7, 150.7, 151.1 (Ar-C), 151.7 (C=O), 152.8 (Ar-C), 156.8 (C=O), 168.7 (C=O), 171.3 (Ar-C). MS, *m/z* (%): 536.86 (M^+, 17.62); Anal. Calcd for $C_{27}H_{20}N_8O_3S$: C, 60.44; H, 3.76; N, 20.88; found C, 59.98; H, 3.55; N, 20.97.

*5.1.12.20. 2-[8-(2,4-Dichlorophenyl)-1,3-dimethyl-2,4-dioxo-2,3,4,8-tetrahydro-1H-imidazo[1,2-f]purin-7-ylthio]-6-oxo-4-phenyl-1,6-dihydropyrimidine-5-carbonitrile (**29c**).*. The titled compound was synthesized using compound **22d** (0.56 g) to give greyish white solid, yield 36%, mp > 300 °C, ^{1}H NMR (DMSO-d_6) *δ:* 3.22 (s, 3H, CH_3), 3.42 (s, 3H, CH_3), 7.41–7.65 (m, 5H, Ar-H, imidazole-H), 7.86 (d, 1H, *J* = 6.88 Hz, Ar-H), 8.21 (d, 2H, *J* = 8.84 Hz, Ar-H), 8.81 (s, 1H, Ar-H), 11.80 (s, 1H, NH exchanged with D_2O), ^{13}C NMR (DMSO-d_6) *δ:* 28.0 (CH_3), 30.3 (CH_3), 92.5, 98.8, 102.3 (Ar-C), 115.8 (C≡N), 122.0, 123.9, 126.9, 128.5, 128.9, 129.1, 129.3, 135.7, 141.8, 147.3, 148.3, 149.5 (Ar-C), 151.6 (C=O), 153.5 (C=O), 156.0 (C=O). MS, *m/z* (%): 591.04 (M^+, 31.86); Anal. Calcd for $C_{26}H_{16}Cl_2N_8O_3S$: C, 52.80; H, 2.73; N, 18.95; found C, 52.67; H, 3.22; N, 18.93.

*5.1.12.21. 2-(8-(4-Acetylphenyl)-1,3-dimethyl-2,4-dioxo-2,3,4,8-tetrahydro-1H-imidazo[1,2-f]purin-7-ylthio)-6-oxo-4-phenyl-1,6-dihydropyrimidine-5-carbonitrile (**29d**).*. The titled compound was synthesized using compound **22e** (0.53 g) to give red solid, yield 42%, mp 297–298 °C, IR (KBr) ν (cm^{-1}): 3321 (N—H), 3063 (C—H aromatic), 2951 (C—H aliphatic), 2214 (C≡N), 1694–1650 (3C = O), 1632 (N—H bending), 1555–1504 (C=C aromatic), ^{1}H NMR (DMSO-d_6) *δ:* 2.11 (s, 3H, CH_3), 3.24 (s, 3H, CH_3), 3.46 (s, 3H, CH_3), 7.54–7.58 (m, 4H, Ar-H, imidazole-H), 7.69 (d, 2H, *J* = 8.20 Hz, Ar-H), 7.91 (d, 4H, *J* = 8.28 Hz, Ar-H), 10.00, 12.31 (2 s, 1H, NH/OH exchanged with D_2O), ^{13}C NMR (DMSO-d_6) *δ:* 26.8 (CH$_3$-C=O), 28.1 (CH_3), 30.3 (CH_3), 102.7 (Ar-C), 116.7 (C≡N), 128.9, 130.2, 145.0, 148.4, 148.9, 151.6 (Ar-C), 151.7 (C=O), 153.6 (C=O), 166.8 (C=O), 196.5 (C=O). MS, *m/z* (%): 564.05 (M^+, 40.32); Anal. Calcd for $C_{28}H_{20}N_8O_4S$: C, 59.57; H, 3.57; N, 19.85; found C, 59.34; H, 3.63; N, 19.92.

*5.1.12.22. 2-(8-Bromo-1,3-dimethyl-2,6-dioxo-2,3-dihydro-1H-purin-7(6H)-yl)-N-(naphthalen-1-yl)acetamide (**30**).*. The titled compound was synthesized according to general procedure for synthesis of compounds **22a-f** using 8-bromotheophylline **21** (1.00 g, 3.86 mmol) and 2-chloro-*N*-(naphthalen-1-yl)acetamide **5** (1.27 g, 5.80 mmol) to give brown solid, yield 49%, mp 199–202 °C, IR (KBr) ν (cm^{-1}): 3271 (N—H), 3055–3013 (C—H aromatic), 2947 (C—H aliphatic), 1701–1651 (3C = O), 1559 (N—H bending), 1550–1443 (C=C aromatic). ^{1}H NMR ($CDCl_3$) *δ:* 3.22 (s, 3H, CH_3), 3.36 (s, 2H, CH_2), 3.44 (s, 3H, CH_3), 7.48–7.56 (m, 3H, Ar-H), 7.65 (d, 1H, *J* = 8.12 Hz, Ar-H), 7.94 (t, 1H, *J* = 4.52 Hz, Ar-H), 8.03 (d, 1H, *J* = 7.44 Hz, Ar-H), 8.30 (t, 1H, *J* = 4.22 Hz, Ar-H), 9.85 (s, 1H, NH exchanged with D_2O). ^{13}C NMR (DMSO-d_6) *δ:* 28.0 (CH_3), 30.2 (CH_3, CH_2), 102.1, 116.7, 122.5, 123.5, 126.2, 126.5, 126.6, 128.7, 134.4, 135.5, 148.7 (Ar-C), 151.7 (C=O), 151.8 (C=O), 153.3 (C=O). MS, *m/z* (%): 442.63 (M^+, 30.76), 443.13 (M^+ + 1, 35.17); Anal. Calcd for $C_{19}H_{16}BrN_5O_3$: C, C, 51.60; H, 3.65; N, 15.84; found C, 51.73; H, 3.71; N, 15.72.

*5.1.12.23. 8-Bromo-7-[2-(indolin-1-yl)-2-oxoethyl]-1,3-dimethyl-1H-purine-2,6(3H,7H)-dione (**31**).*. The titled compound was synthesized according to general procedure for synthesis of compounds **22a-f** using 8-bromotheophylline **21** (1 g, 3.86 mmol) and 2-chloro-1-(indolin-1-yl) ethanone **6** (1.13 g, 5.80 mmol) to give white solid, yield 88%, mp 268–269 °C. IR (KBr) ν (cm^{-1}): 3067 (C—H aromatic), 2936 (C—H aliphatic), 1697–1670 (3C = O), 1597–1485 (C=C aromatic). ^{1}H NMR (DMSO-d_6) *δ:* 3.20 (s, 3H, CH_3), 3.27 (t, 2H, *J* = 8.28 Hz, CH_2), 3.44 (s, 3H, CH_3), 4.30 (t, 2H, *J* = 8.32 Hz, CH_2), 5.36 (s, 2H, CH_2), 7.05 (t, 1H, *J* = 7.32 Hz, Ar-H), 7.16 (t, 1H, *J* = 7.62 Hz, Ar-H), 7.30 (d, 1H, *J* = 7.28 Hz, Ar-H), 7.95 (d, 1H, *J* = 8.00 Hz, Ar-H). ^{13}C NMR (DMSO-d_6) *δ:* 27.8 (CH_3), 28.0 (CH_2), 30.0 (CH_3), 47.1 (CH_2), 49.4 (CH_2), 109.0, 116.3, 124.5, 125.5, 127.6, 130.1, 132.3, 142.7, 147.9 (Ar-C), 151.1 (C=O), 154.2 (C=O), 163.6 (C=O). MS, *m/z* (%): 418.40 (M^+, 100), 420.18 (M^+ + 2, 20.94); Anal. Calcd for $C_{17}H_{16}BrN_5O_3$: C, 48.82; H, 3.86; N, 16.74; found C, 49.06; H, 3.60; N, 16.69.

*5.1.12.24. 8-[(1,1-Dioxo-1,2-benzothiazol-3-yl)amino]-7-(2-indolin-1-yl-2-oxo-ethyl)-1,3-dimethyl-purine-2,6-dione (**32**).*. The titled compound was synthesized according to general procedure for synthesis of compounds **23a,b** using 8-bromo-7-(2-(indolin-1-yl)-2-oxoethyl)-1,3-dimethyl-1*H*-purine-2,6(3*H*,7*H*)-dione **31** (0.44 g, 1.05 mmol) and (1,1-dioxo-1,2-benzothiazol-3-yl)amine **2** (0.21 g, 1.16 mmol) to give yellow solid, yield 41%, mp > 300 °C, IR (KBr) ν (cm^{-1}): 3244 (N—H), 3067–3028 (C—H aromatic), 2943 (C—H aliphatic), 1705–1660 (C=O), 1628 (N—H bending), 1551–1485 (C=C aromatic), 1331, 1161 (SO_2). ^{1}H NMR (DMSO-d_6) *δ:* 3.21 (br.s, 5H, CH_3, CH_2), 3.51 (s, 3H, CH_3), 4.22 (t, 2H, *J* = 7.96 Hz, CH_2), 5.34 (s, 2H, CH_2), 7.01 (t, 1H, *J* = 7.20 Hz, Ar-H), 7.13 (t, 1H, *J* = 7.46 Hz, Ar-H), 7.26 (d, 1H, *J* = 7.04 Hz, Ar-H), 7.76–7.83 (m, 2H, Ar-H), 7.94 (d, 1H, *J* = 7.92 Hz, Ar-H), 8.00 (d, 1H, *J* = 7.04 Hz, Ar-H), 8.20 (d, 1H, *J* = 6.76 Hz, Ar-H), ^{13}C, DEPT-135 NMR (DMSO-d_6) *δ:* 27.8 (CH_3), 28.0 (CH_2), 30.1 (CH_3), 47.0 (CH_2), 47.1 (CH_2), 104.7 (Ar-C), 116.3, 120.9, 124.1, 125.4, 127.5, 132.1, 132.9, 133.0 (Ar-CH), 142.0, 143.1, 147.4 (Ar-C), 151.5 (C=O), 154.3 (C=O), 158.3 (Ar-C), 165.2 (C=O). MS, *m/z* (%): 519.85 (M^+, 12); Anal. Calcd for $C_{24}H_{21}N_7O_5S$: C, 55.48; H, 4.07; N, 18.87; found C, 55.82; H, 4.53; N, 18.59.

*5.1.12.25. 8-(4-Amino-6-oxo-1,6-dihydropyrimidin-2-ylthio)-7-[2-(indolin-1-yl)-2-oxoethyl]-1,3-dimethyl-1H-purine-2,6(3H,7H)-dione (**33**).*. The titled compound was synthesized according to the adopted

procedure for synthesis of compound **26** using 8-bromo-7-(2-(indolin-1-yl)-2-oxoethyl)-1,3-dimethyl-1*H*-purine-2,6(3*H*,7*H*)-dione **31** (0.5 g, 1.2 mmol), 6-aminothiouracil (0.19 g, 1.32 mmol), and DMAP (0.15 g, 1.2 mmol) to give off white solid, yield 59%, mp 268–270 °C, IR (KBr) ν (cm^{-1}): 3391, 3364, 3194 (NH_2, N—H), 3067–3028 (C—H aromatic), 2951, 2909 (C—H aliphatic), 1701–1657 (4C = O), 1612 (N—H bending), 1539–1485 (C=C aromatic), ^{1}H NMR (DMSO-d_6) *δ:* 3.14–3.26 (m, 5H, CH_2, CH_3), 3.46 (s, 3H, CH_3), 4.26 (t, 2H, *J* = 8.22 Hz, CH_2), 5.45 (s, 2H, CH_2), 7.03–7.30 (m, 5H, 2Ar-H, pyrimidine-H, NH_2 exchanged with D_2O), 7.72 (d, 1H, *J* = 6.36 Hz, Ar-H), 7.92 (d, 1H, *J* = 8.04 Hz, Ar-H), 12.02 (s, 1H, NH exchanged with D_2O), ^{13}C NMR (DMSO-d_6) *δ:* 27.6 (CH_3), 28.1 ($2CH_2$), 30.3 (CH_3), 51.0 (CH_2), 90.0 (CH = C), 102.6, 107.4, 117.1, 127.4, 136.6, 143.6, 148.4, 149.1 (Ar-C), 151.6 (C=O), 153.6 (C=O), 162.3 (Ar-C), 164.1 (C=O), 166.1 (C=O). MS, *m/z* (%): 480.65 (M^+, 32.41); Anal. Calcd for $C_{21}H_{20}N_8O_4S$: C, 52.49; H, 4.20; N, 23.32; found C, 52.33; H, 4.06; N, 22.97.

5.2. In vitro anticancer screening

5.2.1. Anti-proliferative assay

The antitumor assay of the targeted compounds was performed at the Drug Evaluation Branch, NCI, Bethesda (Maryland, USA), using sulforhodamine B (SRB) assay to assess the cell growth and viability [72]. In accordance with Drug Evaluation Branch protocol, the levels of cellular protein were determined after 48 h of drug exposure by using the seven absorbance measurements [time zero (Tz), control growth (C), and test growth in the presence of drug at the five concentration levels (Ti)], the percentage growth was calculated at each of the drug concentration levels. Percentage growth inhibition was calculated as:

[(Ti – Tz) / (C – Tz)] X 100 for concentrations for which Ti ≥ Tz

[(Ti – Tz) / Tz] X 100 for concentrations for which Ti < Tz

Three dose response parameters were calculated for each tested compound (**17** and **22c**): Growth inhibition of 50% (GI_{50}) was calculated when [(Ti – Tz) / (C – Tz)] X 100 = 50. The compound concentration resulting in total growth inhibition (TGI) was calculated when Ti = Tz. The LC_{50} indicating a net loss of cells following treatment was calculated when [(Ti – Tz) / Tz] X 100 = -50.

5.2.2. In vitro cytotoxicity toward human normal WI-38 cell line

Cell culture protocol of normal human diploid fibroblasts (WI-38) which was obtained from American Type Culture Collection, cells were cultured using Dulbecco's modified Eagle medium (DMEM) (Invitrogen/Life Technologies) supplemented with 10% fetal bovine serum (FBS) (Hyclone), 10 mg/ml of insulin (Sigma-Aldrich), and 1% penicillin streptomycin. All of the other chemicals and reagents were purchased from Sigma-Aldrich, or Invitrogen. The culture medium was transferred to a centrifuge tube. In order to remove any traces of serum, the cell layer was washed with 0.25% (w/v) Trypsin 0.53 mM EDTA solution. Trypsin EDTA solution (2.0–3.0 ml) was added and cells were examined under an inverted microscope until cell layer was dispersed (5–15 min). Complete growth medium (6.0–8.0 ml) was added and cells were aspirated by gentle pipetting. The cell suspension in addition to the medium and cells from previous step was centrifuged (5–10 min) at 125 X g. The supernatant was thrown out then fresh growth medium was added to the cell pellet and the cell suspension was transferred to new culture vessels. To induce hypoxia, 25 mM stock solution was prepared in sterile water (prepared immediately before use). Culture was incubated for 24 h at 37 °C. Cells were treated with serial concentrations of the test compounds **17, 22c** and sorafenib then incubated for 48 h at 37 °C, then, proceeded for the MTT assay.

MTT cytotoxic assay protocol; cells were plated in a volume of 100 ml complete growth medium (cells density 1.2–1.8 X 10,000 cells/well) and 100 ml of the tested compound per well in a 96-well plate for 24 h before the MTT assay. Cultures from incubator were removed into laminar flow hood or other sterile work area. Each vial of MTT [M – 5655] to be used was reconstituted with 3 ml of medium or balanced salt solution without phenol red and serum. Reconstituted MTT was added in an amount equal to 10% of the culture medium volume. Cultures were incubated for 2–4 h depending on cell type and maximum cell density. MTT Solubilization Solution [M – 8910] was added to cultures to dissolve the resulting formazan crystals and dissolution was enhanced by mixing in gyratory shaker. Moreover, trituration was helpful for complete dissolution. ROBONIK P2000 was used to measure the color intensity at wavelength of 450 nM. To draw the survival curve for WI-38 cell line after specified time, surviving fraction was plotted versus the drug concentration. The half maximal inhibitory concentration (IC_{50}) was calculated to the test compounds **17, 22c** and the reference drug sorafenib. The surviving fractions were expressed as means ± S.E.

5.3. Multi-kinase inhibitory activity screening

5.3.1. PI3Kα inhibitory activity screening

Assay was carried out using PI3K kit [88], which is used for determination of the degree of (general and isoform-specific) class I PI3 Kinase inhibition. Screening of the selected compounds against PI3Kα was achieved in accordance to instruction manual for PI3 kinase activity/inhibitor assay kit, PI3K, p110α (Part No. CS203304).

5.3.2. B-RafV600E, B-RafWT, EGFR and VEGFR-2 inhibitory assays

These assays were carried out using B-Raf_{V600E}, B-Raf_{WT} [89,90] EGFR [91], and VEGFR-2 [92], (Bioscience) kinase assay kits and employing Kinase-Glo Plus luminescence (Promega) kit as detection reagent in accordance to Data Sheet B-Raf(V600E) Kinase Assay Kit (Catalog # 48688), bpsbioscience.com . A stock solution of the tested compounds and sorafenib in DMSO e.g. 10% was initially prepared. Serial dilutions were carried out and 5 ml of the dilution was added to a 50 ml reaction mixture. After the enzymatic reaction, 50 ml of Kinase-Glo Plus Luminescence kinase assay solution was added to each reaction and the plate was incubated for 15 min at room temperature. Luminescence signal was measured using Promega multimode microplate reader. The difference between luminescence intensities in the absence of Kinase (Lu_t) and in the presence of Kinase (Lu_c) was defined as 100% activity (Lut e Lu_c). Using luminescence signal (Lu) in the presence of the compound, % activity was calculated as: % activity = [(Lu_t - Lu) / (Lu_t - Lu_c)] X 100%, where Lu = the luminescence intensity in the presence of the compound. The luminescence data were analyzed using Graphpad Prism and IC50 values were calculated as the average value from two independent experiments.

5.4. Modeling studies

All molecular docking studies were performed using Molecular Operating Environment (MOE 2010.10) software package. The X-ray crystal structures of the target kinases were obtained from RSCB protein data bank [93]. Namely; the molecular docking study of the compiled library (selection stage) in the binding sites of PI3Kγ (PDB ID: 4 GB9) and B-Raf_{WT} (PDB ID: 1UWH), and the newly synthesized compounds in the binding sites of PI3Kα (PDB ID: 4JPS), B-Raf_{V600E} (PDB ID: 3IDP), EGFR (PDB ID: 1XKK) and VEGFR-2 (PDB ID: 1YWN).

For the preparation of the crystal structures for the intended molecular docking studies, water molecules and ligands that are not involved in binding were removed from each protein. In B-Raf_{WT}, chain B was removed. All proteins were prepared for the docking study using *Protonate 3D* protocol with default options. For docking protocol validation, the prepared PDB crystal structures were validated by self-docking of each co-crystallized ligand, then evaluation of the reproduced binding pattern. All molecular docking protocols proved suitability in the validation step with produced RMSD values of 1.112 and 0.754 Å in PI3Kγ and B-Raf_{WT}, respectively, in the selection stage and 1.473, 0.310, 1.631 and 0.826 Å in PI3Kα, B-Raf_{V600E}, EGFR and VEGFR-2, respectively. (For further details see Supplementary Materials)

Chemical structures of the compiled library compounds were

subjected to energy minimization until an RMSD gradient of 0.05 kcal·mol^{-1}Å^{-1} with MMFF94x forcefield and the partial charges were automatically calculated followed by a systematic conformational search using MMFF94x force field and the default MOE settings then the lowest energy conformer of each molecule was used as an initial conformer for the intended molecular docking simulation. Triangle Matcher placement method and London dG scoring function were used in the docking simulation. The obtained poses were subjected to force field refinement using the same scoring function. 3D diagrams were generated by UCSF Chimera software.

Declaration of Competing Interest

None.

Acknowledgement

Our sincere thanks to the National Cancer Institute (NCI), Bethesda (Maryland, USA), for carrying out the *in vitro* anti-proliferative analysis of compounds described in this paper.

Appendix A. Supplementary material

Supplementary data to this article can be found online at https://doi.org/10.1016/j.bioorg.2020.104569.

References

[1] World Health Organization, Cancer, https://www.who.int/news-room/fact-sheets/detail/cancer, (accessed March 1, 2020).
[2] B.A. Chabner, T.G. Roberts, Chemotherapy and the war on cancer, Nat. Rev. Cancer 5 (2005) 65–72.
[3] G. Krauss, N. Schönbrunner, J. Cooper, Biochemistry of signal transduction and regulation, Wiley Online Library, Weinheim, 2003.
[4] K.-S.-H. Nguyen, S. Kobayashi, D.B. Costa, Acquired resistance to epidermal growth factor receptor tyrosine kinase inhibitors in non–small-cell lung cancers dependent on the epidermal growth factor receptor pathway, Clin. Lung Cancer 10 (2009) 281–289.
[5] C. Morais, Sunitinib resistance in renal cell carcinoma, J. Kidney Cancer VHL 1 (2014) 1.
[6] T.W. Miller, J.M. Balko, C.L. Arteaga, Phosphatidylinositol 3-kinase and antiestrogen resistance in breast cancer, J. Clin. Oncol. 29 (2011) 4452.
[7] T.M. Bauer, M.R. Patel, J.R. Infante, Targeting PI3 kinase in cancer, Pharmacol. Ther. 146 (2015) 53–60.
[8] V. Asati, D.K. Mahapatra, S.K. Bharti, PI3K/Akt/mTOR and Ras/Raf/MEK/ERK signaling pathways inhibitors as anticancer agents: Structural and pharmacological perspectives, Eur. J. Med. Chem. 109 (2016) 314–341.
[9] K. Stemke-Hale, A.M. Gonzalez-Angulo, A. Lluch, R.M. Neve, W.-L. Kuo, M. Davies, M. Carey, Z. Hu, Y. Guan, A. Sahin, An integrative genomic and proteomic analysis of PIK3CA, PTEN, and AKT mutations in breast cancer, Cancer Res. 68 (2008) 6084–6091.
[10] A.J. Folkes, K. Ahmadi, W.K. Alderton, S. Alix, S.J. Baker, G. Box, I.S. Chuckowree, P.A. Clarke, P. Depledge, S.A. Eccles, The identification of 2-(1 H-indazol-4-yl)-6-(4-methanesulfonyl-piperazin-1-ylmethyl)-4-morpholin-4-yl-thieno [3, 2-d] pyrimidine (GDC-0941) as a potent, selective, orally bioavailable inhibitor of class I PI3 kinase for the treatment of cancer, J. Med. Chem. 51 (2008) 5522–5532.
[11] S.-M. Maira, S. Pecchi, A. Huang, M. Burger, M. Knapp, D. Sterker, C. Schnell, D. Guthy, T. Nagel, M. Wiesmann, Identification and characterization of NVP-BKM120, an orally available pan-class I PI3-kinase inhibitor, Mol. Cancer Ther. 11 (2012) 317–328.
[12] D.P. Sutherlin, L. Bao, M. Berry, G. Castanedo, I. Chuckowree, J. Dotson, A. Folks, L. Friedman, R. Goldsmith, J. Gunzner, Discovery of a Potent, Selective, and Orally Available Class I Phosphatidylinositol 3-Kinase (PI3K)/Mammalian Target of Rapamycin (mTOR) Kinase Inhibitor (GDC-0980) for the Treatment of Cancer, J. Med. Chem. 54 (2011) 7579–7587.
[13] S.D. Knight, N.D. Adams, J.L. Burgess, A.M. Chaudhari, M.G. Darcy, C.A. Donatelli, J.I. Luengo, K.A. Newlander, C.A. Parrish, L.H. Ridgers, Discovery of GSK2126458, a highly potent inhibitor of PI3K and the mammalian target of rapamycin, ACS Med. Chem. Lett. 1 (2010) 39–43.
[14] W.J. Scott, M.F. Hentemann, R.B. Rowley, C.O. Bull, S. Jenkins, A.M. Bullion, J. Johnson, A. Redman, A.H. Robbins, W. Esler, Discovery and SAR of novel 2, 3-dihydroimidazo [1, 2-c] quinazoline PI3K inhibitors: identification of copanlisib (BAY 80–6946), ChemMedChem 11 (2016) 1517–1530.
[15] A. Poulsen, H. Nagaraj, A. Lee, S.p. Blanchard, C.K. Soh, D. Chen, H. Wang, S. Hart, K.C. Goh, B. Dymock, Structure and ligand-based design of mTOR and PI3-kinase inhibitors leading to the clinical candidates VS-5584 (SB2343) and SB2602, J. Chem. Inf. Model., 54 (2014) 3238-3250.
[16] A. Markham, Idelalisib: first global approval, Drugs 74 (2014) 1701–1707.
[17] H.A. Blair, Duvelisib: first global approval, Drugs 78 (2018) 1847–1853.
[18] A. Markham, Alpelisib: first global approval, Drugs 79 (2019) 1249–1253.
[19] I.B. Greenwell, A. Ip, J.B. Cohen, PI3K inhibitors: understanding toxicity mechanisms and management, Oncology 31 (2017) 821–828.
[20] L.M. Thorpe, H. Yuzugullu, J.J. Zhao, PI3K in cancer: divergent roles of isoforms, modes of activation and therapeutic targeting, Nat. Rev. Cancer 15 (2015) 7–24.
[21] I. Sánchez-Hernández, P. Baquero, L. Calleros, A. Chiloeches, Dual inhibition of (V600E)BRAF and the PI3K/AKT/mTOR pathway cooperates to induce apoptosis in melanoma cells through a MEK-independent mechanism, Cancer Lett. 314 (2012) 244–255.
[22] J. Avruch, X.F. Zhang, J.M. Kyriakis, Raf meets Ras: completing the framework of a signal transduction pathway, Trends Biochem. Sci. 19 (1994) 279–283.
[23] D. Vigil, J. Cherfils, K.L. Rossman, C.J. Der, Ras superfamily GEFs and GAPs: validated and tractable targets for cancer therapy? Nat. Rev. Cancer. 10 (2010) 842–857.
[24] J. Hasskarl, Sorafenib: targeting multiple tyrosine kinases in cancer, in: U. M. Martens (Ed.), Small Molecules in Oncology, Springer, Berlin Heidelberg, Berlin, Heidelberg, 2014, pp. 145–164.
[25] J.-H. Pan, H. Zhou, S.-B. Zhu, J.-L. Huang, X.-X. Zhao, H. Ding, Y.-L. Pan, Development of small-molecule therapeutics and strategies for targeting RAF kinase in BRAF-mutant colorectal cancer, Cancer Manag. Res. 10 (2018) 2289.
[26] N.M. Raghavendra, D. Pingili, S. Kadasi, A. Mettu, S.V.U.M. Prasad, Dual or multi-targeting inhibitors: The next generation anticancer agents, Eur. J Med. Chem. 143 (2018) 1277–1300.
[27] G. Bollag, J. Tsai, J. Zhang, C. Zhang, P. Ibrahim, K. Nolop, P. Hirth, Vemurafenib: the first drug approved for BRAF-mutant cancer, Nat. Rev. Drug Discov. 11 (2012) 873–886.
[28] A.D. Ballantyne, K.P. Garnock-Jones, Dabrafenib: first global approval, Drugs 73 (2013) 1367–1376.
[29] P.I. Poulikakos, C. Zhang, G. Bollag, K.M. Shokat, N. Rosen, RAF inhibitors transactivate RAF dimers and ERK signalling in cells with wild-type BRAF, Nature 464 (2010) 427–430.
[30] M. Sabisz, A. Skladanowski, Modulation of cellular response to anticancer treatment by caffeine: inhibition of cell cycle checkpoints, DNA repair and more, Curr. Pharm. Biotechnol. 9 (2008) 325–336.
[31] A. Tenzer, M. Pruschy, Potentiation of DNA-damage-induced cytotoxicity by G2checkpoint abrogators, Anti-Cancer Agents Med. Chem. 3 (2003) 35–46.
[32] D. Makower, U. Malik, Y. Novik, P.H. Wiernik, Therapeutic efficacy of theophylline in chronic lymphocytic leukemia, Med. Oncol. 16 (1999) 69–71.
[33] A. Lentini, H. Kleinman, P. Mattioli, V. Autuori-Pezzoli, L. Nicolini, A. Pietrini, A. Abbruzzese, M. Cardinali, S. Beninati, Inhibition of melanoma pulmonary metastasis by methylxanthines due to decreased invasion and proliferation, Melanoma Res. 8 (1998) 131–137.
[34] K. Lee, K.-W. Jeong, Y. Lee, J.Y. Song, M.S. Kim, G.S. Lee, Y. Kim, Pharmacophore modeling and virtual screening studies for new VEGFR-2 kinase inhibitors, Eur. J Med. Chem. 45 (2010) 5420–5427.
[35] D. Kim, H. Lee, H. Jun, S.-S. Hong, S. Hong, Fluorescent phosphoinositide 3-kinase inhibitors suitable for monitoring of intracellular distribution, Bioorg. Med. Chem. 19 (2011) 2508–2516.
[36] R.R. Ruddarraju, A.C. Murugulla, R. Kotla, M.C.B. Tirumalasetty, R. Wudayagiri, S. Donthabakthuni, R. Maroju, K. Baburao, L.S. Parasa, Design, synthesis, anticancer, antimicrobial activities and molecular docking studies of theophylline containing acetylenes and theophylline containing 1, 2, 3-triazoles with variant nucleoside derivatives, Eur. J Med. Chem. 123 (2016) 379–396.
[37] M. Hisham, B.G. Youssif, E.E.A. Osman, A.M. Hayallah, M. Abdel-Aziz, Synthesis and biological evaluation of novel xanthine derivatives as potential apoptotic antitumor agents, Eur. J. Med. Chem. 176 (2019) 117–128.
[38] A.L. Smith, F.F. DeMorin, N.A. Paras, Q. Huang, J.K. Petkus, E.M. Doherty, T. Nixey, J.L. Kim, D.A. Whittington, L.F. Epstein, Selective inhibitors of the mutant B-Raf pathway: discovery of a potent and orally bioavailable aminoisoquinoline, J. Med. Chem. 52 (2009) 6189–6192.
[39] S.P. Hong, S.K. Ahn, Discovery of a novel pan-RAF inhibitor with potent anti-tumor activity in preclinical models of BRAFV600E mutant cancer, Life Sci. 183 (2017) 37–44.
[40] G.L. Card, L. Blasdel, B.P. England, C. Zhang, Y. Suzuki, S. Gillette, D. Fong, P. N. Ibrahim, D.R. Artis, G. Bollag, A family of phosphodiesterase inhibitors discovered by cocrystallography and scaffold-based drug design, Nat. Biotechnol. 23 (2005) 201–207.
[41] J. Tsai, J.T. Lee, W. Wang, J. Zhang, H. Cho, S. Mamo, R. Bremer, S. Gillette, J. Kong, N.K. Haass, Discovery of a selective inhibitor of oncogenic B-Raf kinase with potent antimelanoma activity, PNAS 105 (2008) 3041–3046.
[42] G. Bollag, P. Hirth, J. Tsai, J. Zhang, P.N. Ibrahim, H. Cho, W. Spevak, C. Zhang, Y. Zhang, G. Habets, Clinical efficacy of a RAF inhibitor needs broad target blockade in BRAF-mutant melanoma, Nature 467 (2010) 596–599.
[43] D.A. Horton, G.T. Bourne, M.L. Smythe, The Combinatorial Synthesis of Bicyclic Privileged Structures or Privileged Substructures, Chem. Rev. 103 (2003) 893–930.
[44] J.M. Murray, Z.K. Sweeney, B.K. Chan, M. Balazs, E. Bradley, G. Castanedo, C. Chabot, D. Chantry, M. Flagella, D.M. Goldstein, Potent and Highly Selective Benzimidazole Inhibitors of PI3-Kinase Delta, J. Med. Chem. 55 (2012) 7686–7695.
[45] J. Dietrich, C. Hulme, L.H. Hurley, The design, synthesis, and evaluation of 8 hybrid DFG-out allosteric kinase inhibitors: A structural analysis of the binding interactions of Gleevec®, Nexavar®, and BIRB-796, Bioorg. Med. Chem. 18 (2010) 5738–5748.

[46] H. Rode, T. Sprang, A. Besch, J. Loose, H.-H. Otto, Pseudosaccharin amine derivatives: synthesis and elastase inhibitory activity, Pharmazie 60 (2005) 723–731.

[47] C.B. Schapira, I.A. Perillo, S. Lamdan, 3-Oxo-1, 2-benzoisothiazoline-2-acetic acid 1, 1-dioxide derivatives. I. Reaction of esters with alkoxides, J Heterocycl. Chem., 17 (1980) 1281-1288.

[48] M.A. Matulenko, A.A. Hakeem, T. Kolasa, M. Nakane, M.A. Terranova, M.E. Uchic, L.N. Miller, R. Chang, D.L. Donnelly-Roberts, M.T. Namovic, Synthesis and functional activity of (2-aryl-1-piperazinyl)-N-(3-methylphenyl) acetamides: selective dopamine D4 receptor agonists, Bioorg. Med. Chem. 12 (2004) 3471–3483.

[49] Z. Ashraf, D. Kim, S.-Y. Seo, S.K. Kang, Synthesis and crystal structures of the potential tyrosinase inhibitors N-(4-acetylphenyl)-2-chloroacetamide and 2-(4-acetylanilino)-2-oxoethyl cinnamate, Acta Crystallogr. C Struct. Chem. 72 (2016) 94–98.

[50] B.T. Gowda, S. Foro, H. Terao, H. Fuess, 2-Chloro-N-(2, 4-dichlorophenyl) acetamide, Acta Crystallogr. E Struct. Chem. 65 (2009) o1367.

[51] S.-S. Kang, H.-S. Zeng, H.-L. Li, H.-B. Wang, 2-Chloro-N-(4-fluorophenyl) acetamide, Acta Crystallogr. E Struct. Chem. 64 (2008) o1194.

[52] H.G. Shaaban, Synthesis of some Heterocyclic Compounds Derived from 2-Chloro-Np-Tolylacetamide, MJS 27 (2016).

[53] M. Akkurt, Ş.P. Yalçın, H. Türkmen, O. Büyükgüngör, 2-Chloro-N-(4-sulfamoylphenyl) acetamide, Acta Crystallogr. E Struct. Chem. 66 (2010) o1596.

[54] B. Li, X. Lin, Y. Zhang, D. Zhang, Y. Xiao, F. Lin, Synthesis and characterization of novel N-phenylacetamide bearing 1, 2, 4-triazole derivatives as potential antimicrobial agents, Chem. Res. Chin. Univ. 33 (2017) 70–73.

[55] I. Jablonkai, Alkylating reactivity and herbicidal activity of chloroacetamides, Pest Manag. Sci. 59 (2003) 443–450.

[56] M.T. Gabr, N.S. El-Gohary, E.R. El-Bendary, M.M. El-Kerdawy, N. Ni, Isatin-β-thiocarbohydrazones: Microwave-assisted synthesis, antitumor activity and structure-activity relationship, Eur. J Med. Chem. 128 (2017) 36–44.

[57] M. Mohamed, S. Awad, N. Ahmed, Synthesis and antimicrobial evaluation of some 6-aryl-5-cyano-2-thiouracil derivatives, Acta Pharm. 61 (2011) 171–185.

[58] H. Basavaraja, K. Jayadevaiah, M.M. Hussain, V. Kumar, P. Basavaraj, Synthesis of novel piperazine and morpholine linked substituted pyrimidine derivatives as antimicrobial agents, J. Pharm. Sci. 2 (2010) 5–12.

[59] U. Onn, Synthesis of some derivatives of 4-phenyl-1, 3-dihydro-2H-imidazole-2-thion using ionic liquid as catalyst and evaluation of their antimicrobial activity, Int. J. Chem. 9 (2017).

[60] A.R. Mohamed, H.H. Georgey, R.F. George, W.I. El-Eraky, D.O. Saleh, N.M. Abdel Gawad, Identification of some novel xanthine-based derivatives with bronchodilator activity, Future Med. Chem., 9 (2017) 1731-1747.

[61] SpectraBase, 6-amino-2-thiouracil, https://spectrabase.com/spectrum/7lqprL4wKD5?a=SPECTRUM_7lqprL4wKD5, (accessed Aprile 19, 2020).

[62] G. Li, Y. Huan, B. Yuan, J. Wang, Q. Jiang, Z. Lin, Z. Shen, H. Huang, Discovery of novel xanthine compounds targeting DPP-IV and GPR119 as anti-diabetic agents, Eur. J Med. Chem. 124 (2016) 103–116.

[63] Y. Wang, S. Chackalamannil, Z. Hu, C.D. Boyle, C.M. Lankin, Y. Xia, R. Xu, T. Asberom, D. Pissarnitski, A.W. Stamford, Design and synthesis of xanthine analogues as potent and selective PDE5 inhibitors, Bioorg. Med. Chem. Lett. 12 (2002) 3149–3152.

[64] J. Liang, J.C. Ruble, G.C. Fu, Dynamic kinetic resolutions catalyzed by a planar-chiral derivative of DMAP: Enantioselective synthesis of protected α-amino acids from racemic azlactones, J. Org. Chem. 63 (1998) 3154–3155.

[65] H.-T. Yang, M.-L. Xing, X.-W. Lu, J.-X. Li, J. Cheng, X.-Q. Sun, C.-B. Miao, BF3·Et2O-or DMAP-Catalyzed Double Nucleophilic Substitution Reaction of Aziridinofullerenes with Sulfamides or Amidines, J. Org. Chem. 79 (2014) 11744–11749.

[66] A.R. Mohamed, Synthesis and antitumor evaluation of some xanthine derivatives, in: CU Theses, Cairo, Cairo university, 2016.

[67] A. Drabczyńska, O. Yuzlenko, M. Köse, M. Paskaleva, A.C. Schiedel, J. Karolak-Wojciechowska, J. Handzlik, T. Karcz, K. Kuder, C.E. Müller, Synthesis and biological activity of tricyclic cycloalkylimidazo-, pyrimido-and diazepinopurinediones, Eur. J Med. Chem. 46 (2011) 3590–3607.

[68] A. Zagórska, M. Kołaczkowski, A. Bucki, A. Siwek, G. Kazek, G. Satała, A. J. Bojarski, A. Partyka, A. Wesołowska, M. Pawłowski, Structure–activity relationships and molecular studies of novel arylpiperazinylalkyl purine-2, 4-diones and purine-2, 4, 8-triones with antidepressant and anxiolytic-like activity, Eur. J Med. Chem. 97 (2015) 142–154.

[69] A. Drabczyńska, C.E. Müller, J. Karolak-Wojciechowska, B. Schumacher, A. Schiedel, O. Yuzlenko, K. Kieć-Kononowicz, N9-Benzyl-substituted 1, 3-dimethyl-and 1, 3-dipropyl-pyrimido [2, 1-f] purinediones: Synthesis and structure–activity relationships at adenosine A1 and A2A receptors, Bioorg. Med. Chem. 15 (2007) 5003–5017.

[70] A. Drabczyńska, C.E. Müller, B. Schumacher, S. Hinz, J. Karolak-Wojciechowska, B. Michalak, E. Pękala, K. Kieć-Kononowicz, Tricyclic oxazolo [2, 3-f] purinediones: potency as adenosine receptor ligands and anticonvulsants, Bioorg. Med. Chem. 12 (2004) 4895–4908.

[71] G.C. Lloyd-Jones, J.D. Moseley, J.S. Renny, Mechanism and application of the Newman-Kwart O→ S rearrangement of O-aryl thiocarbamates, Synthesis-STUTTGART 5 (2008) 661.

[72] B.A. Teicher, Anticancer drug development guide: preclinical screening, clinical trials, and approval, Springer Science & Business Media, Dana-Farber Cancer Institute, Boston, MA, 2013.

[73] DTP Data Search, http://dtp.nci.nih.gov/dtpstandard/dwindex/index.jsp, (accessed February 7, 2020).

[74] E.M. Acton, V.L. Narayanan, P.A. Risbood, R.H. Shoemaker, D.T. Vistica, M. R. Boyd, Anticancer specificity of some ellipticinium salts against human brain tumors in vitro, J. Med. Chem. 37 (1994) 2185–2189.

[75] L. Ding, G. Getz, D.A. Wheeler, E.R. Mardis, M.D. McLellan, K. Cibulskis, C. Sougnez, H. Greulich, D.M. Muzny, M.B. Morgan, Somatic mutations affect key pathways in lung adenocarcinoma, Nature 455 (2008) 1069–1075.

[76] M.S. Brose, P. Volpe, M. Feldman, M. Kumar, I. Rishi, R. Gerrero, E. Einhorn, M. Herlyn, J. Minna, A. Nicholson, BRAF and RAS mutations in human lung cancer and melanoma, Cancer Res. 62 (2002) 6997–7000.

[77] M.C. Alley, D.A. Scudiero, A. Monks, M.L. Hursey, M.J. Czerwinski, D.L. Fine, B. J. Abbott, J.G. Mayo, R.H. Shoemaker, M.R. Boyd, Feasibility of drug screening with panels of human tumor cell lines using a microculture tctrazolium assay, Cancer Res 48 (1988) 589–601.

[78] C.C.G. Inc., Molecular operating environment (MOE), in, Chemical Computing Group Inc 1010 Sherbooke St. West, Suite# 910, Montreal …, 2010.

[79] E.F. Pettersen, T.D. Goddard, C.C. Huang, G.S. Couch, D.M. Greenblatt, E.C. Meng, T.E. Ferrin, UCSF Chimera–a visualization system for exploratory research and analysis, J. Comput. Chem. 25 (2004) 1605–1612.

[80] P.T. Wan, M.J. Garnett, S.M. Roe, S. Lee, D. Niculescu-Duvaz, V.M. Good, C.G. Project, C.M. Jones, C.J. Marshall, C.J. Springer, D. Barford, Mechanism of activation of the RAF-ERK signaling pathway by oncogenic mutations of B-RAF, Cell, 116 (2004) 855-867.

[81] P. Furet, V. Guagnano, R.A. Fairhurst, P. Imbach-Weese, I. Bruce, M. Knapp, C. Fritsch, F. Blasco, J. Blanz, R. Aichholz, Discovery of NVP-BYL719 a potent and selective phosphatidylinositol-3 kinase alpha inhibitor selected for clinical evaluation, Bioorg. Med. Chem. Lett. 23 (2013) 3741–3748.

[82] E.R. Wood, A.T. Truesdale, O.B. McDonald, D. Yuan, A. Hassell, S.H. Dickerson, B. Ellis, C. Pennisi, E. Horne, K. Lackey, A unique structure for epidermal growth factor receptor bound to GW572016 (Lapatinib): relationships among protein conformation, inhibitor off-rate, and receptor activity in tumor cells, Cancer Res. 64 (2004) 6652–6659.

[83] Y. Miyazaki, S. Matsunaga, J. Tang, Y. Maeda, M. Nakano, R.J. Philippe, M. Shibahara, W. Liu, H. Sato, L. Wang, Novel 4-amino-furo [2, 3-d] pyrimidines as Tie-2 and VEGFR2 dual inhibitors, Bioorg. Med. Chem. Lett. 15 (2005) 2203–2207.

[84] R. Roskoski Jr, Classification of small molecule protein kinase inhibitors based upon the structures of their drug-enzyme complexes, Pharmacol. Res. 103 (2016) 26–48.

[85] S.J. Zhu, P. Zhao, J. Yang, R. Ma, X.E. Yan, S.Y. Yang, J.W. Yang, C.H. Yun, Structural insights into drug development strategy targeting EGFR T790M/C797S, Oncotarget, 9 (2018) 13652.

[86] G.P. Hager, J.C. Krantz Jr, J.B. Harmon, Theophylline derivatives. I. Analogs of 2-benzyl-2-imidazoline (priscoline), J. Am. Pharm. Assoc., 42 (1953) 36-39.

[87] M.N.S. Rad, A. Khalafi-Nezhad, S. Behrouz, M.A. Faghihi, A. Zare, A. Parhami, One-pot synthesis of N-alkyl purine and pyrimidine derivatives from alcohols using TsIm: a rapid entry into carboacyclic nucleoside synthesis, Tetrahedron 64 (2008) 1778–1785.

[88] http://www.millipore.com, (accessed March 7, 2020).

[89] E.R. Cantwell-Dorris, J.J. O'Leary, O.M. Sheils, BRAFV600E: implications for carcinogenesis and molecular therapy, Mol. Cancer Ther. 10 (2011) 385–394.

[90] N.M. Obaid, K. Bedard, W.-Y. Huang, Strategies for overcoming resistance in tumours harboring BRAF mutations, Int. J. Mol. Sci. 18 (2017) 585.

[91] J.L. Nakamura, The epidermal growth factor receptor in malignant gliomas: pathogenesis and therapeutic implications, Exp. Opin. Ther. Targets 11 (2007) 463–472.

[92] C. Fontanella, E. Ongaro, S. Bolzonello, M. Guardascione, G. Fasola, G. Aprile, Clinical advances in the development of novel VEGFR2 inhibitors, Ann. Transl. Med. 2 (2014).

[93] H. Berman, K. Henrick, H. Nakamura, J.L. Markley, The worldwide Protein Data Bank (wwPDB): ensuring a single, uniform archive of PDB data, Nucl. Acids Res. 35 (2007) D301–D303.